Project no. 034692

VERTIGO

Versatile Two Micron Light Source

STREP - Specific Target Research Project
IST - Information Society Technologies

Publishable Final Activity Report

Period covered :	from 1.6.2006 to 30.11.2009	Date of preparation:	Feb. 2010
Start date of project :	01.06.2006	Duration:	42 months
Project coordinator name :	Marcel Rattunde	Revision:	2
Project coordinator organization name :	Fraunhofer IAF		

Dissemination level		
PU	Public	**X**
PP	Restricted to other programme participants (including the Commission Service)	
RE	Restricted to a group specified by the consortium (including the Commission Services)	
CO	Confidential, only for members of the consortium (including the Commission Services)	

Contents

1. Project execution

1.1.Project objectives

The VERTIGO project focused on the development of compact, high performance optically pumped semiconductor disk lasers (OPSDLs) emitting in the 2.0-2.5µm wavelength regime.

The OPSDL concept combines the high efficiency and wavelength versatility of more traditional semiconductor lasers, but introduces the circular, high quality beam and resonator versatility more commonly associated with solid-state lasers. In this project, the (AlGaIn)(AsSb) material system was exploited to access the 2.0-2.5µm regime to satisfy the demand of high performance lasers in this range.

The project combined the design and development of the laser sources with the necessary steps for specific applications implementation and eventual exploitation. The multi-partner consortium, originally comprising two non-university government funded research institutes, one university research group, one industrial research laboratory, and two SMEs, had been carefully selected to accommodate all aspects of device development and its potential route to market. One SME (CableFree Solutions Ltd.) stopped all project activities after the 2nd project year. Its participation was terminated with effect of 01/06/2008.

We believe that the novel laser sources realized within the project represent a new and versatile photonic component, suitable to serve a variety of needs expressed in the IST call. The most notable impact areas of VERTIGO technology will be in:

1. Environment: e.g. highly sensitive gas detection and monitoring of enviro-chemical compounds, and precise data collation for global climatic modeling, and natural disaster prediction.
2. Healthcare: e.g. sensitive non-invasive, diagnostic devices and high-throughput medical screening technologies as well as high-power lasers for medical therapy
3. Communication: e.g. high-speed, free space optical communications.
4. Security: e.g. sensitive chemical and explosives sensing as homeland security measures and, stand-off turbulence detection in aviation.

Due to the recent progress within the VERTIGO consortium, we were able to exceed the initial project output power and power efficiency goals of the 2.Xµm Semiconductor disk laser. The results achieved so far are unprecedented in the international community.

1.2.Partners

No.	Participant name *& Activities in the project*	Short name	Country
1	Fraunhofer Institute for Applied Solid State Physics *project coordination; design and epitaxial growth of the required III-antimonide heterostructures; laser characterisation; laser module design*	**IAF**	Germany

2	Thales III-V Labs *processing of OPSDL laser chips; substrate removal technology; mounting technology*	**TL**	France
3	Institute of Photonics, University of Strathclyde *layer structure, resonator and laser module design; thermal modelling; laser characterisation; OPSDL embodiments with advanced functionality*	**IOP**	UK
4	Institute of Electron Technology *optical and thermal characterization of IR- OPSDL; thermal mapping of the OPSDL*	**IET**	Poland
5	CableFree Solutions Ltd. *OPSDL with integrated modulator; realization of a free space optics link operating at 2 µm*	**CFS**	UK
6	LISA Laser Products *stable, single mode, narrow linewidth, tunable 2.Xµm OPSDL*	**LISA**	Germany

1.3.Project coordinator

Marcel Rattunde
Fraunhofer Institute for Applied Solid State Physics (IAF)
Tullastr.72
79104 Freiburg
Germany
marcel.rattunde@iaf.fraunhofer.de

1.4. Work performed and end results

1.4.1. Overview

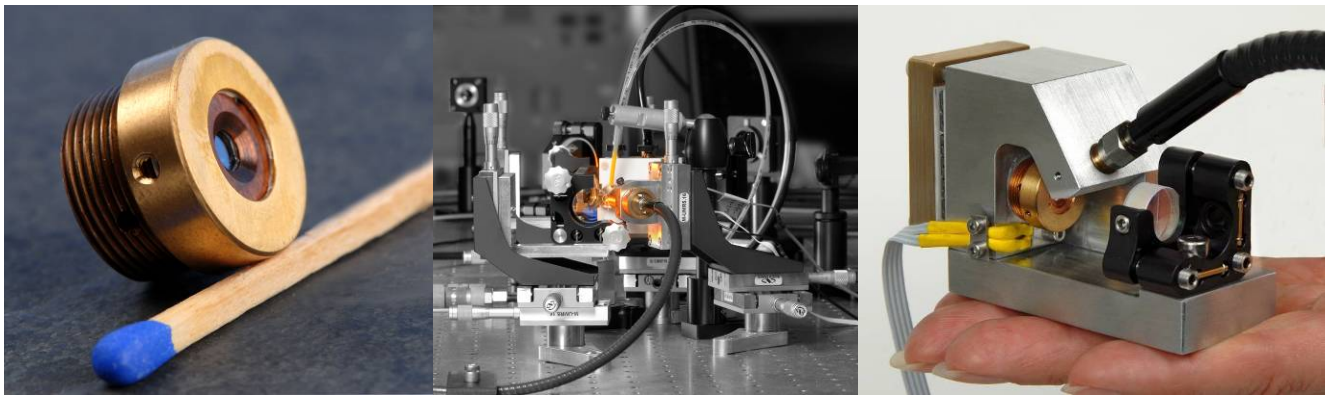

Fig. 1: The VERTIGO project covered all aspects – from device growth to applications-ready OEM laser modules – in order to establish a new, mature long-wavelength 2-3 µm semiconductor disk laser technology.

The VERTIGO project has developed a new, versatile photonic component: Optically pumped semiconductor disk lasers (OPSDLs), emitting in the 1.9 – 2.8 µm wavelength range. The project has mastered all relevant aspects in order to establish a mature long-wavelength GaSb-based disk laser technology: knowledge of the GaSb-based semiconductor materials for the laser design; high-quality semiconductor fabrication using Molecular Beam Epitaxy (MBE), mature chip mounting and thermal management techniques; design of compact and robust laser modules and the demonstration of application specific laser setups.

The semiconductor lasers, developed within VERTIGO represent a new class of high-power, high-brightness, 2.Xµm laser source with many modes of operation and application. Continuous-wave output powers as high as 8W and pulsed outputs above 20W have been demonstrated from a compact and low-cost laser format. This represents a three order of magnitude improvement over the state-of-the-art technology at the time VERTIGO commenced. In addition to world-leading output power performances, wide wavelength accessibility from 1.8 to 2.8µm and individual tunability over 150nm from these lasers demonstrates their inherent flexibility and suitability for many applications. The versatility of the external cavity was then utilised in the demonstration of narrow linewidth and single frequency operation using a volume Bragg grating as an output coupler. In this way a frequency selective low noise prototype seed source for a solid-state amplified LIDAR system has been realised. Finally, the high brightness (good beam quality) available from the OPSDL format has been exploited by using a single-mode external waveguide modulator in concert with a 2.2µm OPSDL to produce an eye-safe modulated source able to carry information further than existing NIR FSO systems. The single frequency operation and modulated outputs of up to 200MHz, compact, high-power pulsed OPSDL embodiments have direct relevance to many applications areas. All this has been achieved using potentially low-cost components due to the flexibility of the OPSDL format. Within the project programme, engineering prototypes were developed in a robust, modular and reconfigurable geometry leading to commercial prototypes which will permit new approaches to address important existing and emerging challenges where flexible, high-power, narrow-line, user-friendly and cost-effective sources are required. Examples of such areas are:

- Airport sensing and security
- Resource assessment and management in the renewable energy industry
- Sensitive detection for environmental monitoring at range for applications health and security

1.4.2. WP1 OPSDL laser device design

Several experiments and studies were performed in order to determine the optical and thermal properties for the GaSb-based material system to the degree of accuracy necessary for the design of the OPSDL semiconductor structure. Based on this data, simulations were performed using a variety electro-optical software packages in order to create a multilayer structural model incorporating: the mirror reflectivity bandwidth, position and quality and the band structure, gain properties and strain requirements for enhanced emission performance.

By using the experimental results from the comprehensive analysis of the fabricated 2.Xµm OPSDL lasers, the design of the semiconductor structures was improved in several loops, leading to the impressive high-power results described below.

In addition, a finite element analysis (FEA) software package was used to develop a thermal model of the OPSDL chips to provide detailed information on the thermal pathways and bottlenecks of the various mounting, and thermal management methods used throughout the project. The figure below shows the comparative heat rise in a GaSb based OPSDL structure using different techniques for chip mounting (and thus different methods of thermal management). One can clearly see, that for the 2.Xµm OPSDLs, the approach of bonding an intracavity thermally conductive, transparent heatspreader results in a much lower temperature rise that the thin disk approach, where the substrate is completely removed. This finding demonstrates, that for these long-wavelength GaSb-based disk lasers, new thermal management technologies must be established, compared to existing GaAs-based semiconductor disk lasers around 1µm emission wavelength.

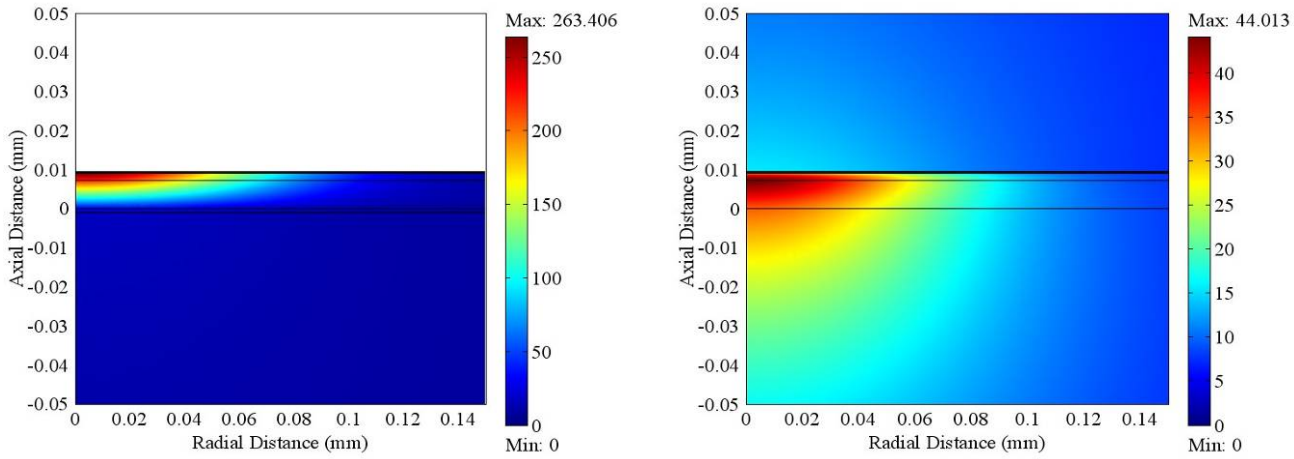

Fig. 1.1: Comparison of temperature rise (in K) for a 2.3µm semiconductor disk laser (a) using a thin device approach (263K) and (b) with an intracavity diamond heatspreader (44K).

For the laser cavity setup, a number of existing software tools were adapted for use with mid-IR OPSDL configurations giving a full analysis suite for the high performance cavity configurations for the air-spaced, multi-element (modulator and frequency tuned) and micro cavities by ensuring optimum pump-cavity mode overlap and therefore threshold and power extraction conditions.

1.4.3. WP2 Material growth and processing

MBE growth of high-quality GaSb-based OPSDL structures

The (AlGaIn)(AsSb)-based OPSDL semiconductor heterostructures to be developed in the VERTIGO project were grown by molecular beam epitaxy (MBE) at Fraunhofer IAF. A picture of an MBE system used at Fraunhofer IAF for the fabrication of group III-Sb structures is shown in Fig. 2.1. The MBE allows the growth of thin, crystalline semiconductor epitaxial layer structures with atomic precision and relies on the reaction of thermal, non-ionised molecular beams with a heated substrate surface. The epitaxy process takes place in ultra high vacuum (UHV) of 10^{-10} mbar.

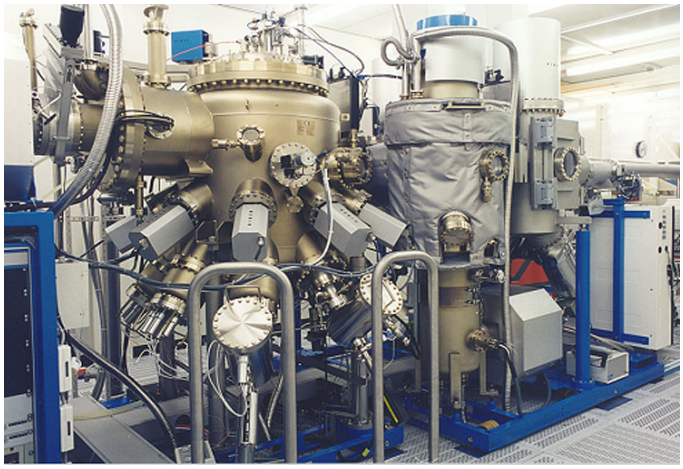

Fig. 2.1. Molecular beam epitaxy (MBE) system at IAF used for the epitaxy of III-V compound semiconductor heterostructures.

The OPSDL heterostructures were grown in a Varian Gen II MBE system on GaSb substrates 2” in diameter. The used chemical elements for the OPSDL structures are Al, Ga, In, As and Sb which are provided by solid-source effusion cells attached to the epitaxy chamber of the MBE system.

The OPSDL structures consist of a GaSb/AlAsSb distributed Bragg reflector (DBR), an active region where GaInAsSb quantum wells (QWs) are embedded between pump-absorbing AlGaAsSb barrier layers, an AlGaAsSb window and a GaSb capping layer. As can be seen, mainly ternary and quaternary compound semiconductor materials have to be grown with precise control of the respective layer thicknesses and strain values. The complete OPSDL structures possess thicknesses in the 10 µm range and for these reasons, the epitaxy process is very challenging. In order to obtain high-epitaxial-quality OPSDL heterostructures, a four-step calibration procedure has been developed: The first step is to grow single epitaxial layers of a specific material composition. The grown layer is then characterized by HRXRD and SIMS analysis techniques (see below) in order to extract the material composition, strain as well as the layer thickness. If all three quantities fulfill the requirements, single layers of another material composition used in OPSDL structures are fabricated and characterized. When all materials can be grown with sufficient precision of thickness and material quality, functional test structures (DBR, QW embedded in barrier layers) are grown and again carefully analyzed.

If the single layers and test structures fabricated in the first three steps, are within an acceptable range of tolerance with respect to the specifications, complete OPSDL structures are then grown. As in the

case of the first three steps, a structure is grown and promptly post-growth characterized. The characterization results are used to give a feedback for the growth of the next OPSDL structure, in order to obtain an optimized structure within a few iterative steps.

In order to obtain semiconductor epitaxial layer structures with a high crystalline quality, with strains and layer thicknesses within the specified range, a thorough post-growth analysis of the structures is required. The available characterization tools for (AlGaIn)(AsSb)-based OPSDL structures at Fraunhofer IAF are high-resolution X-ray diffraction (HRXRD), secondary ion mass spectrometry (SIMS) as well as photoluminescence and reflectivity measurements as optical characterization methods.

With the help of high-resolution x-ray diffraction (HR-XRD) we were able to investigate the crystalline structure of the MBE grown samples. For this purpose, x-ray radiation was directed onto a piece of the grown wafers. Diffracted x-rays could be observed at different angles. The crystalline lattice of the substrate material as well as the lattice of the epitaxially grown layers give rise to specific intensity peaks according to the respective intrinsic lattice parameter. In the HR-XRD measurement shown in fig.2.2 the pronounced intensity maximum is due to the crystalline lattice of the substrate material. In the OPSDL samples fabricated within the scope of this project, all layers except for the quantum wells were grown lattice-matched to the substrate. Thus the intensity peak arising from this layers should be identical to the peak which belongs to the lattice of the substrate. In fig.2.2 we also observe a broad intensity distribution beside the main intensity peak which again splits up into several peaks. This group of side peaks is attributed to the lattice of the quantum well layers. Since the quantum wells are grown compressively strained with respect to the substrate, the position of this group of side peaks is not identical to the position of the intensity peak arising from the substrate. We were able to estimate the amount of strain achieved in the quantum wells from this displacement in the HR-XRD curve. Finally, we were also able to estimate the thickness and the mutual distance of the quantum wells from the HR-XRD measurements. In the case these findings significantly differed from the structural parameters that were theoretically expected from the intended design, the MBE system was recalibrated and a new growth run could be launched if necessary.

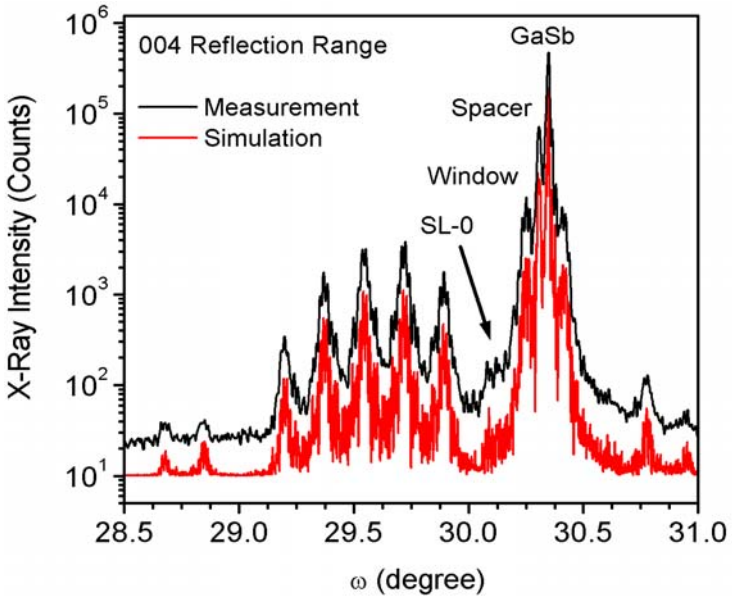

Fig.2.2: Example of an HR-XRD curve (obtained from measurements performed with an OPSDL structure designed for 2.25µm emission wavelength)

Subsequently, the thicknesses of all semiconductor layers were verified by means of SIMS measurements (Secondary Ion Mass Spectroscopy, see fig. 2.3). Here, the laser chip is gradually sputtered while secondary ions removed from each layer are being detected. Particular count rates for different ions are observed according to the composition of each layer. With the help of these measurements it was possible to recognize deviations from the intended layer structure. In particular, the exact length of the micro-cavity given by group of layers between sample surface and the distributed Bragg reflector (DBR) could be verified. The length of the micro-cavity was intended to be a multiple of a half-wavelength since the field intensity in the active region can be resonantly enhanced in this way. Furthermore, SIMS measurements proved that the quantum wells were located precisely at the antinodes of the standing wave pattern. In arranging the quantum well layers in this way, the modal gain could be increased by a factor of approximately two.

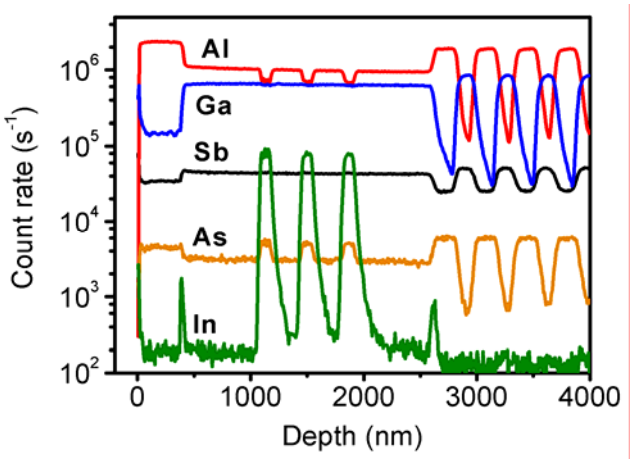

Fig.2.3: Count rates for different kinds of ions as obtained from SIMS measurements. The DBR region was truncated in this graph for simplicity reasons (extends further to the substrate side).

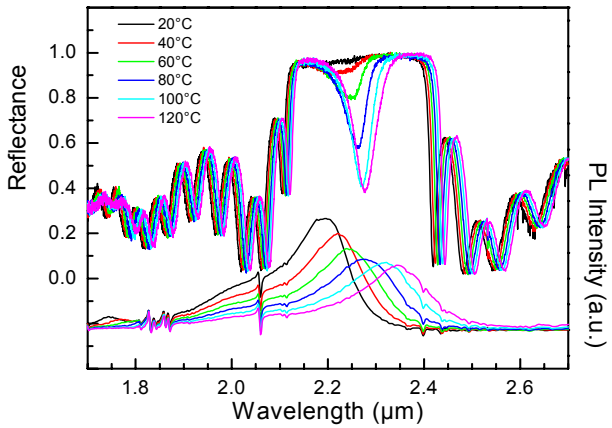

Fig.2.4: PL spectra of an OPSDL chip designed for an emission wavelength of 2.25µm. The wavelength of the PL peak is traced separately

The gain properties of the QWs are investigated by means of photoluminescence (PL) measurements. For this characterization method a low output power Nd:YAG laser is focused on the surface of an OPSDL chip. The light emitted from the OPSDL chip is then collected by a FTIR spectrometer which generates PL spectra. The PL spectra clearly show the spectral distribution of the material gain in the QWs. Measuring PL spectra at different temperatures one observes a red shift of the PL curves. (Fig.2.4).

Reflectance measurements are also performed using a FTIR spectrometer. Here, light from a 'globar' IR source is reflected from the laser structures and collected by a spectrometer which generates reflectance spectra. Using a specially adapted software tool the reflectance spectra of the intended layer structure is simulated and compared to the measured result. Spectra obtained from the laser structure designed for an emission wavelength of 2.25µm are shown in fig.2.4. Here, we observe a good agreement between simulated and experimental data which again proves the accuracy of the epitaxial growth.

Processing & mounting of GaSb-based OPSDL structures

After the successful growth, the GaSb-based OPSDL structures were mounted into the common heatspreader, the VERTIGO consortium designed. Different techniques were used in order to examine different ways for the thermal management and in order to realize special functionalities for the OPSDL lasers:

OPSDL with heatspreaders

2.Xµm OPSDL chips were bonded, using the liquid capillarity bonding technique, to diamond and SiC windows at the IOP and Fraunhofer IAF, respectively. The samples were then mounted in a VERTIGO consortium designed copper/brass compression sub-mount, The best choice for an intracavity heatspreader is diamond, however, SiC may give also adequate device performance for many applications and has a significant cost/convenience advantage over custom diamond windows.

The experimental results, achieved with these devices, shows the tremendous potential of this heatspreader approach, as we were able to achieve output powers above 3W in CW-operation at room-temperature and even above 6W at -15°C heatsink temperature (see below).

In order to push the performances of the devices further, TL developed a specific procedure to fabricate SiC heatspreaders, with stringent specifications. In fact, the SiC heatspreader must be wedged, with a controlled angle of a few degrees. Moreover this side has to be coated with an anti reflection multilayer stack, presenting, simultaneously, minimums of reflectivity (<1%) at 980nm and 2.25µm. The fabrication was carried out with a good level of success confirmed by characterization.

OPSDL with the substrate completely removed

In order to achieve OPSDL samples with the substrate completely removed, special samples were grown by the IAF with the layer sequence in reverse order ("up-side down" OPSDLs). These samples were then processed further by TL: After soldering to the VERTIGO sub-mount, the GaSb substrate is entirely chemically removed in order to permit the optical pumping of the structure. At the end, we get a sample which is only few microns thick.

To prepare the samples before soldering, a dielectric Bragg mirror is deposited, following by metallization.

To properly etch the GaSb substrate, we developed a special wet-etch solution. At the same time, we identified the compatible etch stop layer that could be inserted in the structure growth.
Specific developments have also been performed on the sub-mounts. Their top surface is polished with an optical finish with final roughness below a few hundred nm, ensuring a perfect planarity and contact with the surface. Using 6x6mm by 12µm thick AuSn. Performs a 4µm thick deposition of this alloy was realised directly on the sub-mount surface. Decreasing the thickness further will decrease the stress induced by the solder on the final thin sample.

Fabrication of an electro-absorption (EA) modulator

One strand for the development for a modulated laser module was the realization of an electro-absorption (EA) modulator. After some design studies, the IAF grew appropriate layer structures and TL developed a five step fabrication process, including: optical photolithography; dry etching; a planarization step and then metallization. The following figure represents a cross section schematic of the final device.

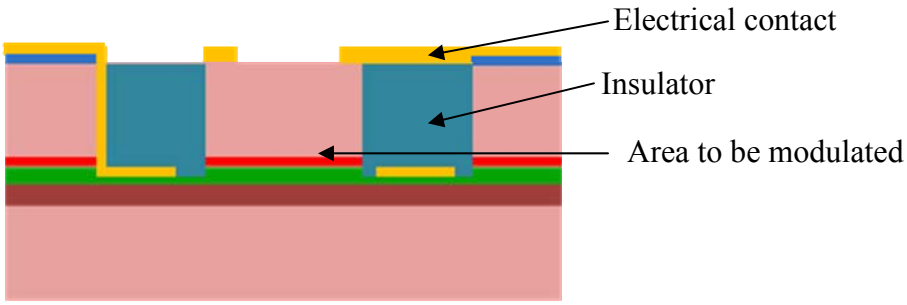

Fig.2.5: Cross sectional schematic of the EA-modulator.

Temperature mapping of OPSDL chips

The major constraints imposed on the performance of OPSDLs are thermal, as in case of majority of diode pumped solid-state lasers, due to the temperature dependence of a number of the material parameters. The optical pumping results in high temperature rises in the active region due to absorption of the pump. The bigger the difference in energy between the pump and the emission, known as the quantum defect, the higher the heat load. In the case of antimonide OPSDLs, examined in this work, the quantum defect is large, since the difference in energies is 0.73 eV (pump 0.98 µm, emission 2.3 µm). The inherently poor thermal conductivity of the antimonide compounds exaggerates the thermal problems. Thus, the thermal roll-over effect becomes more pronounced.

The modal gain in semiconductor laser depends on spatial and spectral overlap of the optical field and the material gain. The central wavelength of the gain spectrum is temperature dependent because the bandgap shrinks with increases in temperature. The active region in OPSDL contains several QWs placed at the anti-nodes of the electric field standing wave. This resonance is red-shifted due to the temperature dependence of the refractive index and thermal expansion. Although for common materials this results in a red-shift with increasing temperature in both cases, typically, the gain and resonance shift at different rates.

Aside from proper external cavity alignment, the stable and efficient operation of the OPSDL requires the careful temperature tuning of cavity resonance and the emission from the quantum wells. The

quantum wells are usually intentionally designed to be detuned to shorter wavelength than desired oscillating wavelength to account for inherent temperature rise in operating device, as the emission from wells shifts faster with temperature than the cavity resonance.

All these temperature effects take place during the optical pumping of the chip. When the temperature of the active region is too high, thermal roll-over is observed, i.e., the emission from quantum wells not only drops, but also shifts beyond the cavity resonance, resulting in the observed decrease of emitted output power. Figure 2.6 presents the scheme of the thermal roll-over process. OPSDLs are designed to operate at certain temperature, beyond which, the spectral features are no longer aligned. Therefore the reliable operation of OPSDL requires efficient heat removal from active region. Also, the knowledge about the temperatures is important in the process of designing and simulating OPSDLs.

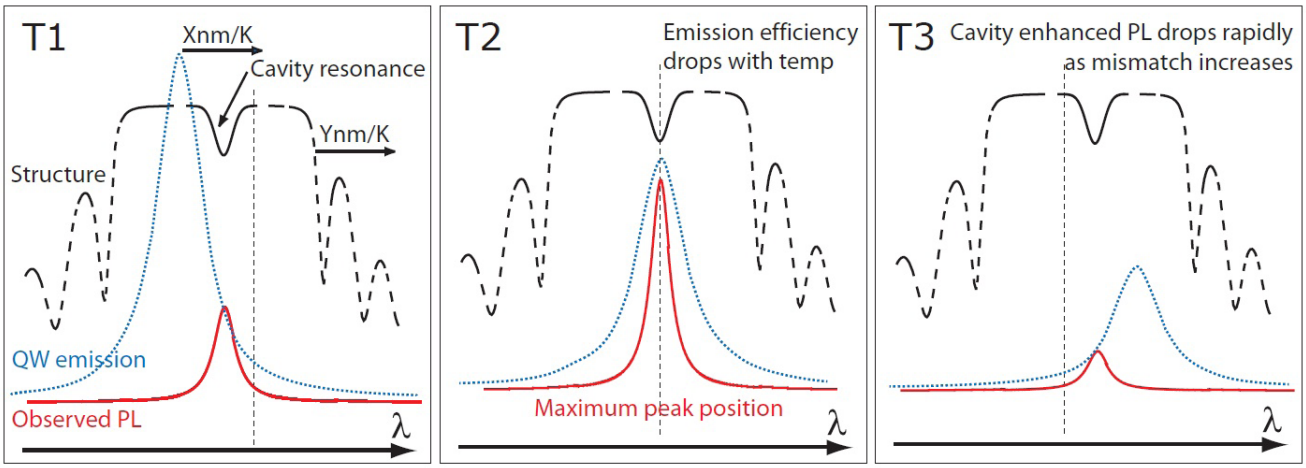

Fig. 2.6: Schematic representation of roll-over process.

The performance of different thermal solutions applied to keep the OPSDL temperature under control was studied experimentally by means of thermoreflectance (TR).

The thermoreflectance spectroscopy is a technique which was developed in Institute of Electron Technology in Department of Physics and Technology of Low Dimensional Structures to study facet heating of semiconductor edge emitting lasers.

Thermoreflectance relies on measuring the relative changes of reflectivity of the sample induced by a periodic variation of the temperature. The sample's temperature can be changed in many ways; direct heating, electrical heating (Joule heating) or optical heating with the laser pulse. The variation of the sample's reflectance is related to the relative changes of temperature by the following equation, reported by Epperlein.

$$\frac{\Delta R}{R} = \frac{1}{R}\frac{\partial R}{\partial T}\Delta T \quad \rightarrow \quad \Delta T = C_{TR}\frac{\Delta R}{R}$$

The relative change of reflectivity per unit temperature is called the thermoreflectance coefficient (C_{TR}). This coefficient varies strongly with the examined material and wavelength of probe beam, therefore it needs to be determined experimentally. Measurement of temperature increase distribution induced by optical pumping of the sample, requires 2D scanning of the surface of the device. In order to measure 2D maps of temperature distribution with high spatial resolution, a new setup had to be constructed. The setup must allow for data collection for the device being constantly illuminated with the pump beam. This required a different approach to the existing TR measurements. In the case of these measurements, reaching the lowest possible resolution was not the most important task, as the

expected diameter of temperature distribution was c.a. 200 µm in diameter, due to the dimensions of the pump beam spot.

The schematic and photograph of the experimental setup is shown in figure 2.7. The probe beam wavelength is chosen to be near the energy for which there will be a high response of the material to the temperature changes. The probe beam is focused on the surface of the device and the reflected beam collected by silicon photodiode and lock-in amplifier. In case of all optical measurements, it is very important to reject the unwanted background from the signal. In the case of TR, it is necessary to use a filter to cut out the pump, which has an intensity many orders of magnitude higher than that of the probe beam at the peak of the silicon detector sensitivity (900-1000 nm). The power of probe beam is kept low at several tens of µW to prevent any additional heating of the sample. The main part of the setup is based on a commercial microscope, which provides proper mechanical stability and optimal beam alignment

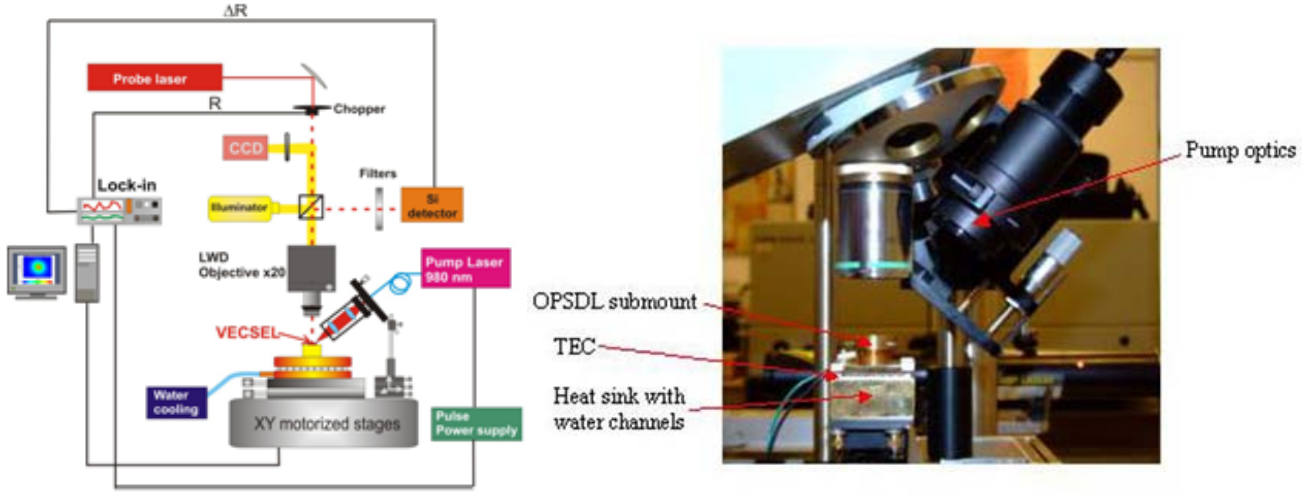

Fig. 2.7: Scheme of the TR setup (left). Photograph of the OPSDL sub-mount and the heat sink placed under the thermoreflectance head. Pump optics is mounted in the tube that can be seen on the right hand side (right).

The device is mounted on the temperature stabilised heatsink, which, in turn, is mounted on motorised stages enabling full 2D surface mapping. In this project, the temperature modulation of the sample is obtained by optical pumping with an external high power laser. Therefore, a long working distance objective lens was used in the microscope to allow access for the pump beam optics. The pump laser was a high-power (25W) commercial 980 nm fibre coupled diode laser. For all measurements, the stabilisation of the sample sub-mount temperature was required. It was achieved by a temperature controller and a water cooled Peltier element. The specifics of the measurement, required the sample to be placed on positioning stages, independent of the pump optics, i.e. the adjustment of the pump spot size and the point of the sample being illuminated is done by placing the sample and pump optics on independent x-y-z stages. This allows the precise adjustment of the sample position, and pump beam in respect to the probe beam, which is fixed in this setup. To allow 2D mapping of the temperature distribution, the sample and the pump optics, together with the stages on which they are mounted, are placed on further motorised XY stages.

Thermoreflectance, as every thermometric technique, requires calibration in order to determine the real temperatures from experimental data. In case of TR, the calibration procedure not only provides the value of thermoreflectance coefficient, which links the relative changes of reflectance with the change of temperature, but also yields the optimal wavelength for which the technique has the highest sensitivity to small temperature changes. For the calibration procedure, several spectra of reflectance

have been recorded at different temperatures. Then, the C_{TR} value is obtained from the slope of linear fit to the experimental data, according to the equation:

$$C_{TR} = \left(\frac{\partial R}{\partial T}\frac{1}{R}\right)^{-1}$$

A He-Ne laser was determined as a suitable probe beam, as the sensitivity was shown not to be greatly reduced for this particular probe beam wavelength.

During the project several types of samples were tested in order to gain a better understanding of the thermal management of OPSDLs. The samples investigated included the plain chips and chips with bonded intracavity heatspreader.

The OPSDL sample without heatspreader was optically pumped in pulsed mode at duty cycle of 25%, with pulse width τ_{pulse}= 0.5 ms and cycle width τ_{cycle}= 2ms. In each case, the temperature of the heat sink was stabilized at 20 °C. The registered temperature distribution is presented in figure 2.8. Such value of duty cycle for OPSDL without HS is caused by the fact that at higher duty cycles heat accumulation effects were observed, resulting in the decrease of the experimental signal intensity. These effect can be investigated experimentally.

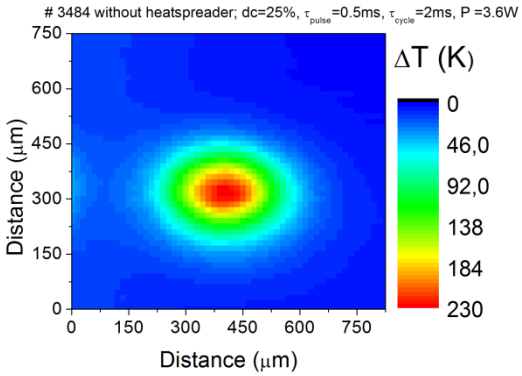

Fig. 2.8 Temperature distribution on the surface of OPSDL chip without heatspreader (experimental). Pump power incident on the sample equals 3.6W.

The next measurements for the OPSDL chip without the heatspreader were done for different duty cycles of pump at constant T_{pulse} as well as at constant T_{cycle}. Resulting maximal temperature increases are shown in figure 2.9 and 2.10, respectively. In the first case we have the same time of "pumping/heating" and different times of "cooling". The latter is similar, though the frequency/total time of the cycle remains the same, but the duration of pulse varies. Thus, more power is delivered to the sample during the pulse, and time to dissipate this heat is also changed. There is a very good agreement between the time of the heating pulse and maximal temperature increase. As it could be expected, the longer the pulse, the higher the temperature rise.

The temperature increases presented in figure 2.9, recorded for T_{pulse} =2.15 ms, are: 170 K for dc=25%, 160 K for dc=50% and 138 K for dc=75%. The incident pump power was 1 W and the temperature of the heatsink was stabilised at 20^{O}C. The highest temperature increase is observed for the lowest filling factor of 25%.

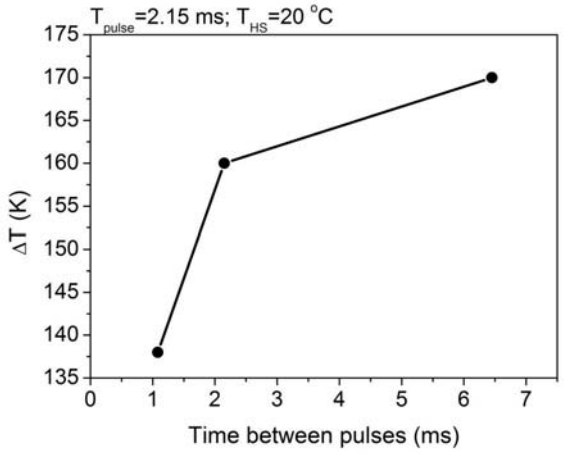

Fig. 2.9: Comparison of maximal temperature increases for different measurement conditions: different duty cycles of pump at constant T_{pulse} = 2.15 ms, 25% (6.5 ms between pulses), 50% (2.15 ms between pulses), 75% (1 ms between pulses).

In figure 2.10 maximal temperature increases are presented for T_{cycle} =8.6 ms. The pump power and the heatsink temperature were the same as previously. The maximal temperature increases presented are as follows: 104 K for dc=15%, 170 K for dc=25%, 240 K for dc=50% and 165 K for dc=75%. The maximal temperature change is higher than in previous measurement series, and occurs for the T_{pulse}=4.3 ms. Again it can be observed, that for some of the conditions, there is the decrease in the observed temperature change. This results from the lack of efficient heat removal from the sample, since the excess heat has to be extracted through DBR stack and substrate, both of low thermal conductivity.

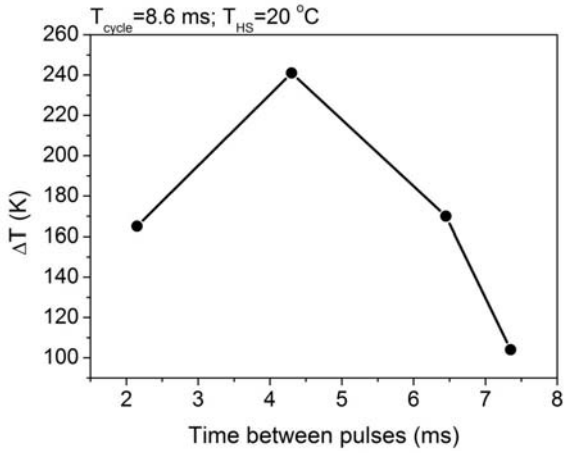

Fig. 2.10: Comparison of maximal temperature rise for OPSDL chip for different filling factors of pump at constant T_{cycle} = 8.6 ms: 15% (a), 25% (b), 50% (c), 75% (d).

The figure 2.11, which presents the temperature horizontal cross sections taken from temperature maps in the centre of the hot spots: for measurement series of T_{pulse}=2.15 ms (left) and T_{cycle}=8.6 ms (right).

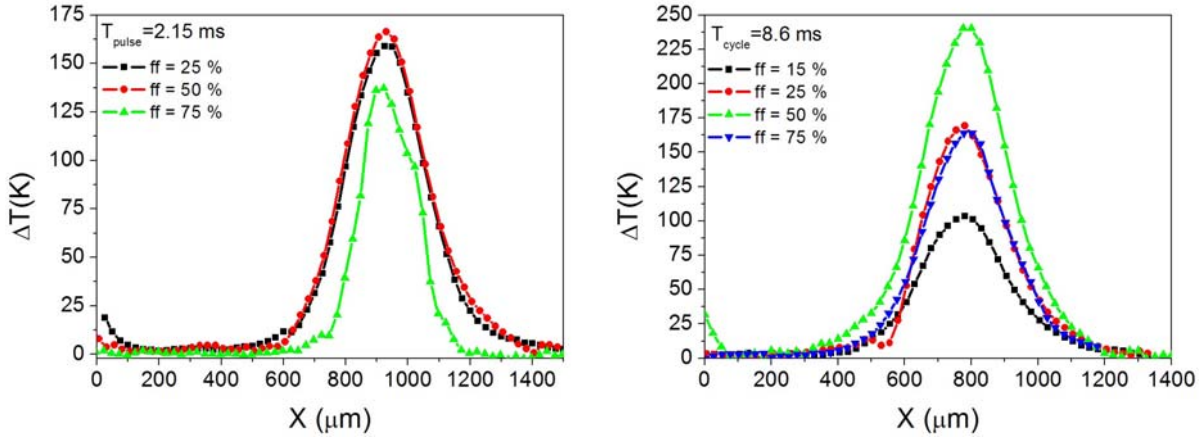

Fig. 2.11: Temperature horizontal cross sections taken from the temperature maps in the centre of the hot spot. Profiles for T_{pulse}=2.15 ms (left) and for T_{cycle}=8.6 ms (right)

Next group of samples investigated included the OPSDL chips with bonded intracavity heatspreader of SiC or diamond material.

OPSDL sample with SiC heatspreader was investigated with good bonding quality on large part of the sample.

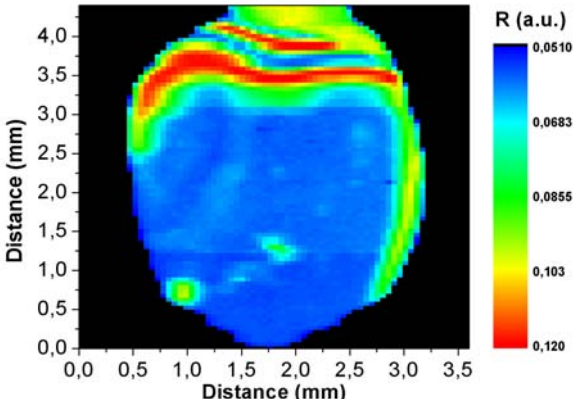

Fig. 2.12: Reflectivity map for OPSDL sample with SiC heatspreader.

Figure 2.12 presents reflectivity map for OPSDL sample measured at 20^0C temperature of the heatsink and HeNe laser as scanning line.

The thermoreflectance measurements were performed for this sample. The measurement was done for the pump power of 3.6 W, 50 % filling factor. The temperature of the heatsink was stabilised at 20^0C. Temperature distribution map recorded for such experimental conditions is presented in figure 2.13.

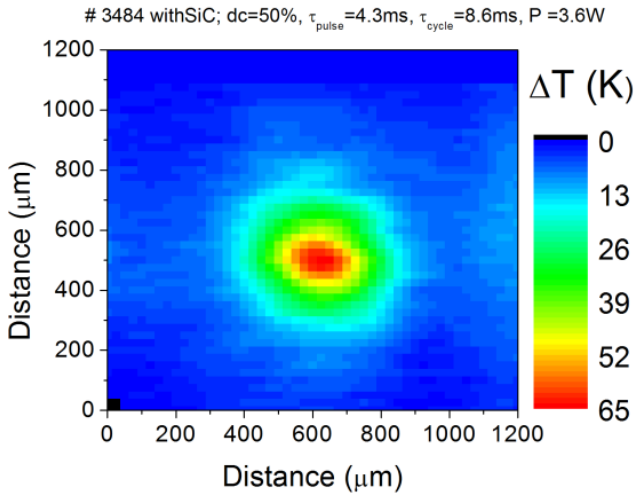

Fig. 2.13: *Temperature distribution on the surface of OPSDL chip with SiC heatspreader (experimental). Pump power incident on the sample equals 3.6W*

Figure 2.14 presents the recorded temperature increases for different pump powers (0.3 W, 0.75 W, 1 W and 3.6 W) at 3 points for the SiC bonded sample (black lines). The dashed line is for the point in the region affected by the air-gap (not perfect bonding).

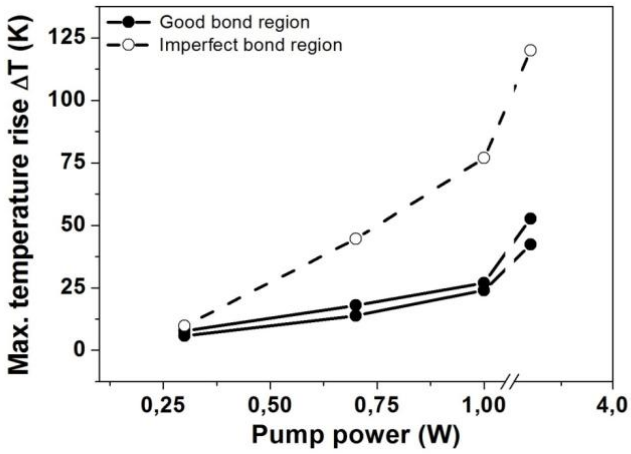

Fig. 2.14: Comparison of temperature increases for different points on SiC bonded sample (black lines). Red line presents results for the sample without the heatspreader

The OPSDL chip with diamond heatspreader was also investigated. Figure 2.15 presents photograph of the sample (left) and exemplary reflectivity map measured at 20^0C temperature of the heatsink and HeNe laser used as scanning beam.

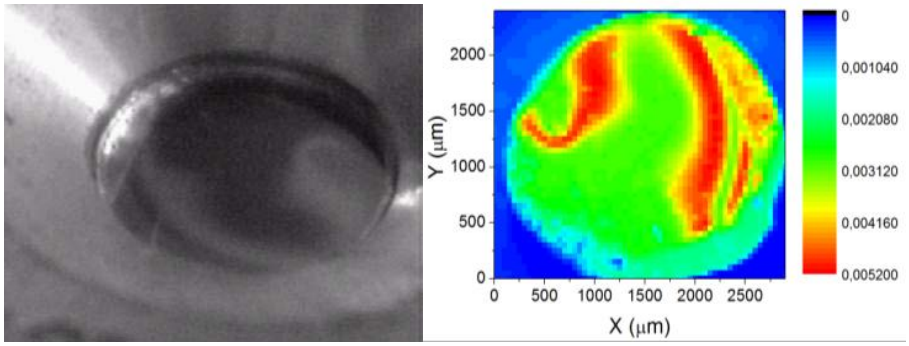

Fig. 2.15: Photograph and reflectivity map for OPSDL chip with diamond heatspreader

Temperature map is shown in figure 2.16. The measurement was done for 3.6 W of incident power at duty cycle of 50 %. Maximal registered temperature increase reaches 4 K.

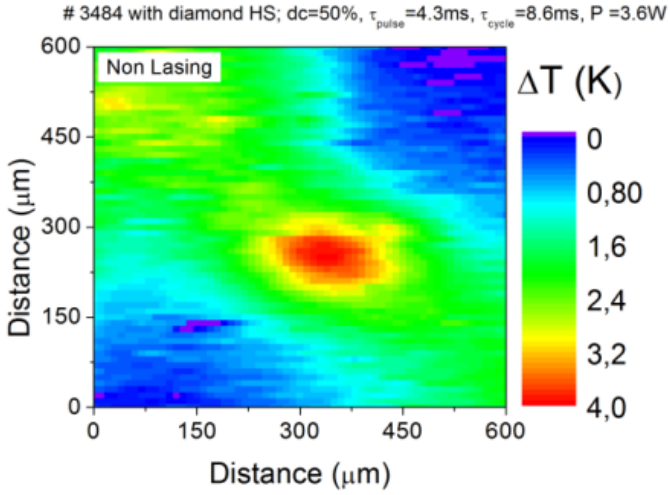

Fig. 2.16: Temperature map for the OPSDL chip with diamond heatspreader

The figure 2.17 presents comparison of temperature line-scans for the sample without heatspreader and with SiC and diamond heatspreaders. For the OPSDL chip without heatspreader and with SiC heatspreader, the temperature line scans were registered at dc=25 %, τ_{pulse}=0.5 ms, τ_{pulse}=2 ms, and incident power of 3.6 W. For OPSDL with diamond heatspreder the dc=50 %, τ_{pulse}=4.3 ms, τ_{pulse}=8.6 ms, and incident power was 3.6 W. In the last case the use of the higher duty cycle (50 % instead of 25 %), is imposed by the very low temperature increases attained for lower duty cycle, below the resolution of the setup. The horizontal temperature line scans for these three samples are collected in the figure 2.18.

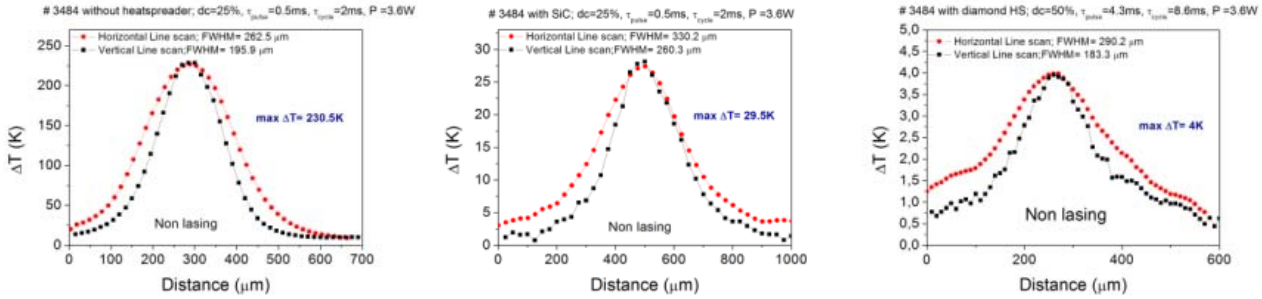

VECSEL w/o HS	
Max ΔT (K)	230.5 K
FWHM_H	262.5μm
FWHM_V	195.9μm

VECSEL SiC HS	
Max ΔT (K)	29.5 K
FWHM_H	330.2 μm
FWHM_V	260.3 μm

VECSEL diamond HS	
Max ΔT (K)	4 K
FWHM_H	290.5μm
FWHM_V	198.2μm

a) b) c)

Fig. 2.17: Comparison of horizontal and vertical temperature line-scans for the sample without heatspreader (a), with SiC heatspreader (b) and with diamond heatspreader (c)

Apart from a significant difference in temperature increase of ΔT=230.5 K for the sample without heatspreader and ΔT=29.5 K for SiC sample, and ΔT=4 K for sample with diamond heatspreader , the broadening of distribution can be observed. This can be attributed to the effect of heat spreading by the SiC and diamond plate. The heat is extracted from pumped region and dissipated in the SiC or diamond material. This is exactly what the heatspreader is designed to do.

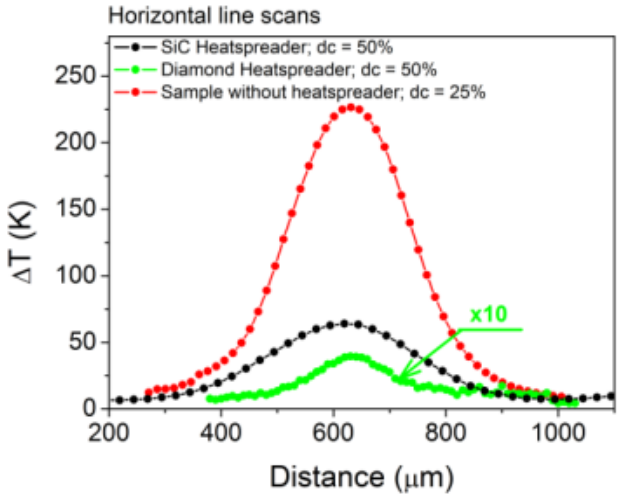

Fig. 2.18: Comparison of the horizontal temperature line-scans for the sample without heatspreader (red), with SiC heatspreader (black) and with diamond heatspreader (green).

Fig. 2.19(left) shows the temperature rise for different pump powers for OPSDLs without heatspreader (red line) and with intracavity SiC and diamond intracavity heatspreaders (black and green lines respectively). As it can be seen, the introduction of heatspreader reduces the temperature significantly by the factor of 6 in case of SiC heatspreader and by the factor of 57 in case of diamond heatspreader, when compared to the sample without heatspreader. The slope of temperature rise versus pump power (ΔT/ΔP) gives insight into thermal behavior of the system. The higher the slope, the less efficient the heat extraction from the device. However, the quality of liquid capillary bonding seriously affects the

ability to decrease the temperature. If the bonding is not perfect (dashed black line), the temperature drop is not as high as expected, though still the temperature is lower than without the heatspreader. The maximum temperature rises for different mounting techniques are compared in figure 2.19(right).

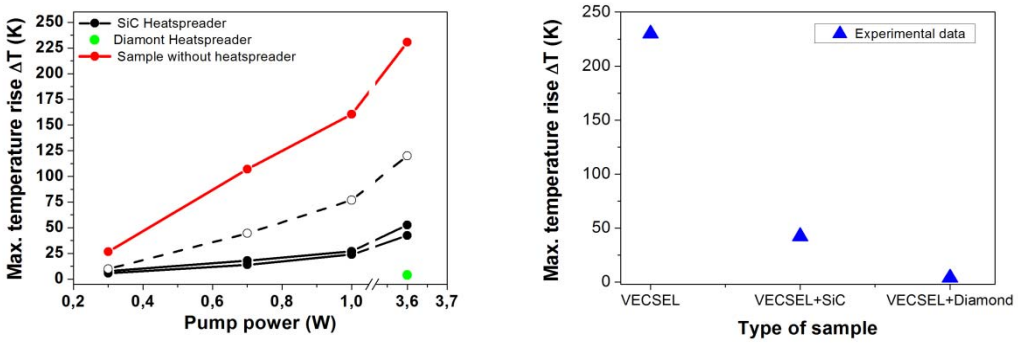

Fig. 2.19: *The OPSDLs temperature rise vs. pump power for different mounting techniques (experimental)(left). Maximum temperature rise for different mounting techniques (experimental). Pump power 1W (right).*

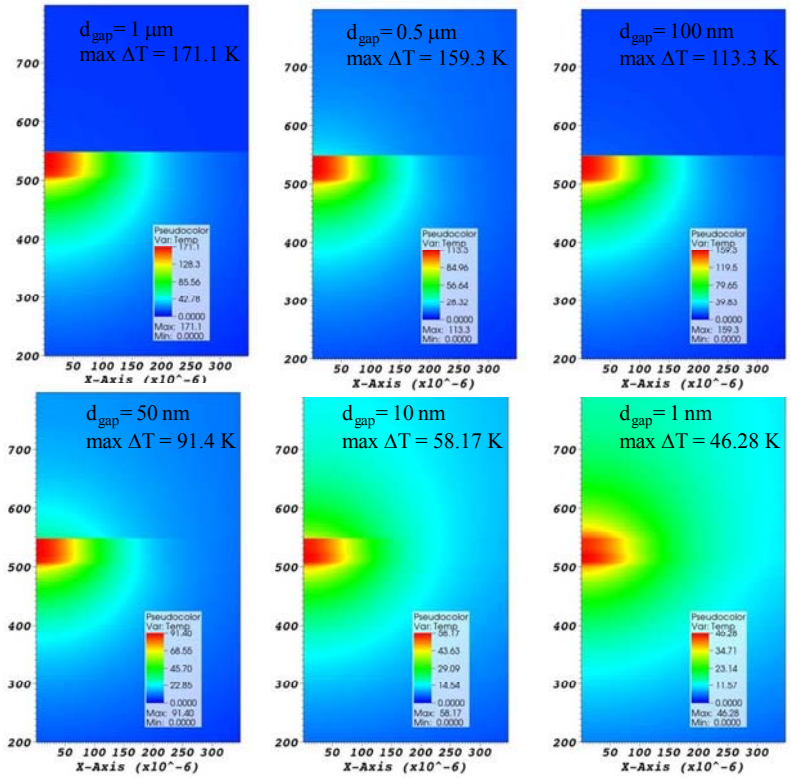

Fig. 2.20: Simulated temperature distribution for air gap of different thickness between the chip and the heatspreader

This effect that bond quality has on the OPSDL temperature has also been confirmed by the numerical modelling. The model that was developed for OPSDL sample with SiC heatspreader, was employed to study the behaviour of a system with a non-ideal bond between the sample and the heatspreader. To

alleviate this an additional layer of variable thickness was introduced, to account for non-uniform bonding.

The resulting temperature maps for different thicknesses of the air gap, ranging from 1 micron to 1 nanometre, are presented in figure 2.20. It can be observed, how the temperature spreads into the heatspreader for small thickness of air gap.

The measurements that were performed together with the numerical calculations allowed to better understand the thermal management in OPSDLs, giving feedback to further development of the structures and devices. The efficient reduction of the device temperature by the intracavity heatspreader was confirmed experimentally and numerically.

1.4.4. WP3 Photonic component

OPSDL characterisation

For the optical characterisations of the OPSDL chips a number of standard laboratory setups were developed generally consisting of 2 or 3-mirror resonator geometries. The main components of these setups included an OPSDL chip in the standard Vertigo sub-mount, pump focussing optics and an output coupling mirror. Figure 3.1 below shows a couple of examples of Vertigo test resonators.

Figure 3.1-left shows a typical 2-mirror test setup: here the temperature of the chip holder, T_h, was varied between –20°C and 100° by a thermo-electric module which was water-cooled from its rear side. To prevent condensation and icing, a weak gaseous nitrogen flux was applied from the front side of the holder. A -50mm radius of curvature (ROC) concave output-coupling mirror formed a linear OPSDL resonator. A 1.064 µm Nd:YAG laser or 980nm diode laser was focussed by a plane-convex lens onto the OPSDL chip yielding pump spot diameters on the chip surface between 50 and 150 µm. Each component could be precisely aligned via three-axis xyz translational stages. Figure 3.1-right shows a typical 3-mirror characterisation setup used: here the chip temperature could be varied between –20°C and 50° with a liquid cooled brass sub-mount, the cavity mirrors typically consisted of a 100mm ROC high-reflector (HR) and a ~10% output coupling mirror. Here each optical element of the resonator could be independently adjusted in the critical dimensions using a number of translation stages and adjusters shown. The 3-mirror configuration permitted greater stable variation of the cavity mode size on the OPSDL chip for a given set of cavity optics and greater flexibility in the insertion of extra optical elements such as birefringent tuning filters (BRF) and other polarising elements.

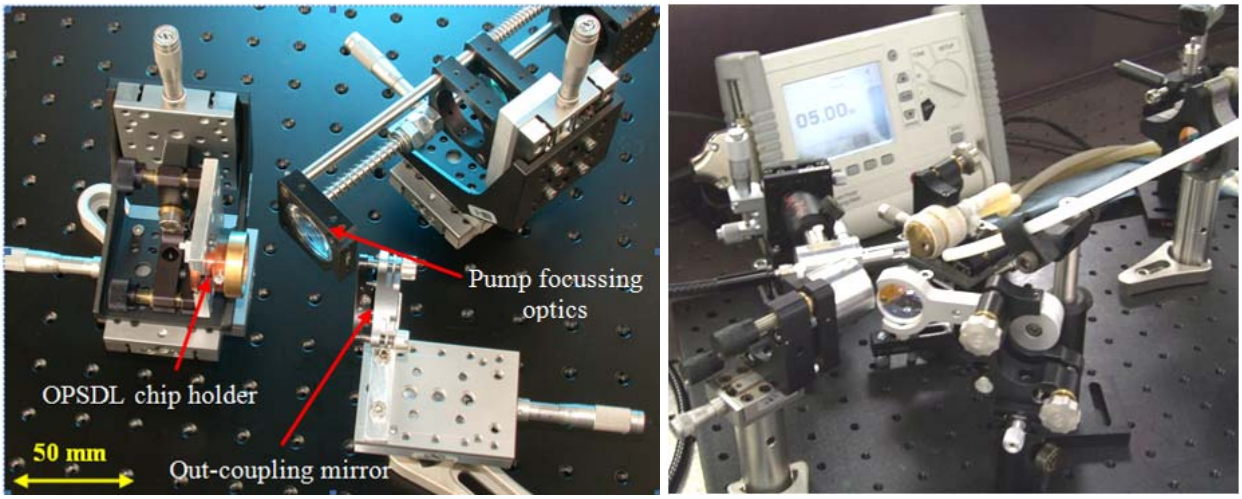

Fig. 3.1 Photographs of two of the typical OPSDL laboratory setups (left – 2-mirror, right – 3-mirror) used for characterisation.

In these standard resonator configurations described above, characterisation measurements were carried out. These measurements included the determination of the OPSDL emission wavelength, λ_{laser}, in cw mode for different heat sink temperatures and pump powers. For advanced characterisations, the OPSDL cw output power, P_{out}, was recorded as a function of the absorbed pump

power, P_{pump}, respectively for different heat sink temperatures, T_h, and reflectivities of the output-coupling mirror, R_{ext}. The absorbed pump power was determined by the difference between the incident pump power and the power that was reflected specularly off the chip. By forming the derivative dP_{out}/dP_{pump} above the laser threshold, the differential power efficiency, η_{diff}, was obtained. By plotting η_{diff} as function of R_{ext} and fitting the relationships of the OPSDL model to the data, the internal efficiency, η_{int}, and the resonator round-trip transmission factor, T_{loss}, could be determined.

Output power and power efficiency

The VERTIGO project over-exceeded by far the initial project goal of 0.5W concerning the CW-output power performance at room temperature. In fact at the project end, more than an order of magnitude increase was achieved with 5.8W CW-output power at -15°C heatsink temperature out of a single OPSDL chip with a power efficiency of 22%. The performance of the different samples is described below:

The best performing sample at 2.02µm was bonded to a diamond heatspreader (4mm diameter, 250µm thick disc) and placed in 3-mirror laser cavity configuration and pumped with a 15W and then 25W 980nm fibre-coupled diode lasers. Initially pump-power limited performance of ~4W (3.7W) was obtained which was improved to ~5W by retro-reflecting the pump lost in reflection at the diamond heatspreader surface. By increasing the available pump power (45W 980nm fibre-coupled diode laser array) output powers over 6W (5.8W shown) were recorded (see figure 3.2 below). The OPSDL samples were able to accommodate a large degree of output coupling (~15%) not normally associated with such lasers without a large degradation in laser threshold performance. This implied very good device design and material quality of the samples.

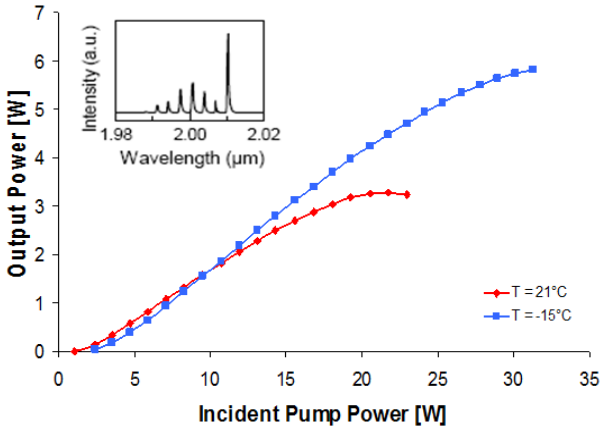

Fig. 3.2: Left-Power transfer of the 2.02µm sample with 9% output coupling at a mount temperature of 21°C (red) and -15°C (blue) – with Corresponding maximum power and efficiencies 3.3 W (η_{pp} ~22%) 5.8 W (η_{pp} ~25%) respectively, Inset: free-running unstabilised spectral output showing the Fabry-Perot modes imposed by the 250µm thick heatspreader. Right-Photograph of the 2µm SDL with cooling below 0°C showing the Nitrogen tube used to reduce icing on the front surface of the SDL mount.

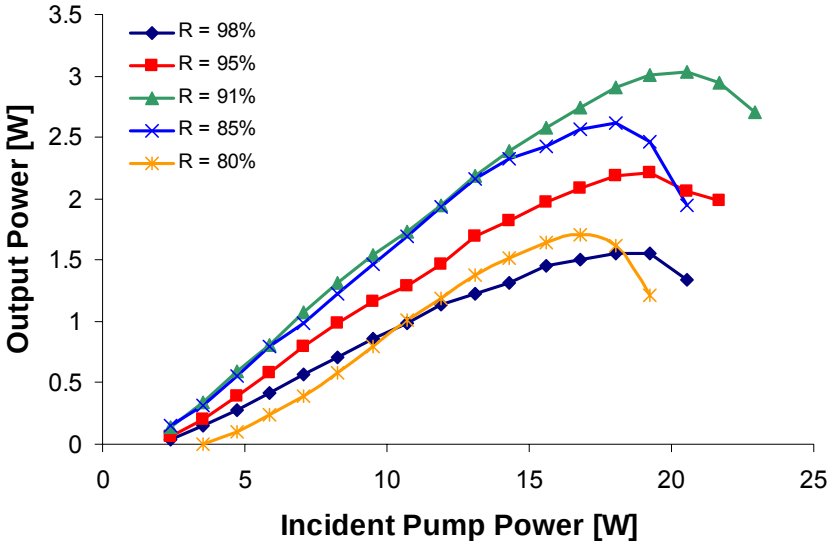

Fig. 3.3.: 1.9µm sample – power transfer @15°C for different output coupling mirrors

The power transfer characteristic of the 1.9µm OPSDL sample is shown in Fig. 3.3 for different output-coupling mirrors. The maximum CW-output power is reached with a mirror reflectivity of 91%, which results in a maximum output power above 3 W at 15°C heatsink temperature.

At longer wavelengths a 2.25µm sample was assessed in a 2-mirror cavity arrangement with a 980-nm fibre coupled diode laser pump source. Power transfer curves for different heatsink temperatures are shown in Fig. 3.4. When using an optimum output coupler reflectivity of 95 %, a maximum output of 3.4 W was measured at -10°C for an absorbed pump power of 21 W. From the linear part of the power transfer curve measured at -10°C, a differential efficiency with respect to the incident pump power of 19.0 % was calculated. Since approximately 20 % of the incident pump power was reflected by the gain medium and the heatspreader, this corresponds to a differential efficiency with respect to the absorbed pump of 24 %. From this value, a differential quantum efficiency of 54.5% can be derived. For higher heat-sink temperatures, the differential efficiency with respect to the incident pump power slightly decreased to ~14 % at 20°C, nevertheless, a maximum output power of >1.6 W at 20°C could still be observed.

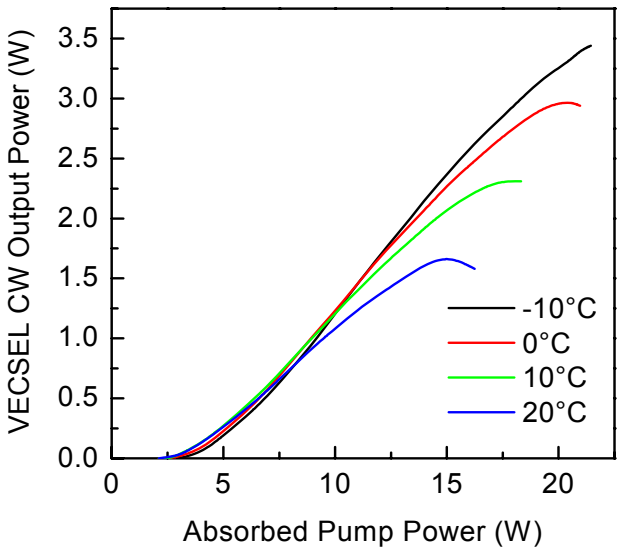

Fig. 3.4: CW output power characteristics of a GaSb-based OPSDL emitting at 2.25µm for several heat-sink temperatures**Fehler! Textmarke nicht definiert.**. The pump wavelength was 980nm.

Longer wavelength OPSDLs at 2.8µm

After the initial success around 2 µm smaples were prepared with target emissions around 2.8 µm. From the post-growth characterization of the grown sample it was concluded that the quality of this first 2.8 µm OPSDL is not as high as the quality of the previous structures at 2.0 µm and 2.25 µm emission wavelength. Both the crystalline quality and also the level of perfection to which the ideal RPG-design (resonant periodic gain) was realized, were inferior to the previous 2.0 - 2.25 µm samples (which is of course due to the higher number of iteration we did so far with the latter structures).

Despite this, it was still possible to operate a 2.8 µm OPSDL cw at room temperature. Fig. 3.5 shows the power transfer characteristics (left side) and the emission spectra (right side) of a SiC-bonded sample, measured at 20°C heatsink temperature. The device emits up to 120 mW of output power right at 2.8 µm wavelength. To our knowledge this is the highest emission wavelength ever realized with an III-V based OPSDL. In pulsed operation (4µs pulse width) over 0.5 W of peak output power were achieved, again at 20°C heatsink temperature.

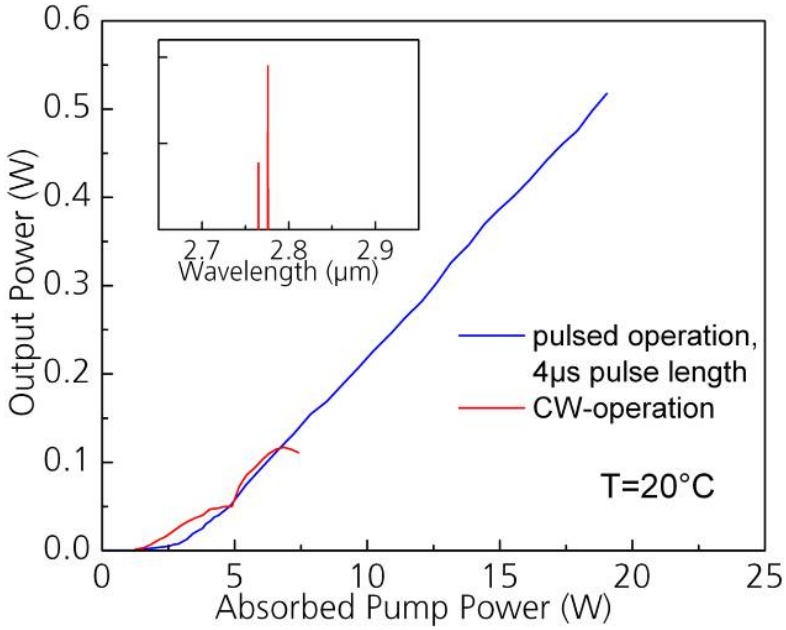

Fig. 3.5: Power transfer characteristics of a SiC-bonded sample of the 2.8 µm OPSDL, measured at 20°C heatsink temperature in CW (red line) and pulsed operation (blue line). The inset shows the emission spectra in pulse mode, revealing a multi mode emission on the etalon-modes of the SiC intra-cavity heat-spreader.

Brightness

By carefully adjusting the cavity mode/pump mode size ration in both resonator schemes the OPSDLs could be aligned for emission in the fundamental TEM_{00} mode. In the case of the 2-mirror resonator this typically involved a slight reduction in the resonator length (compared to the alignment for maximal output power by approximately 1 mm) which leads to an increase in the diameter of the fundamental resonator mode on the OPSDL chip and hence an increased overlap between the pump spot and the fundamental mode. Due to the slight inflexibility of the 2-mirror cavity configuration this typically resulted in the reduction of output power by ~20-30%. The beam propagation constant, M^2, was measured with an automated DATARAY beam-scope beam profiler in both transversal directions at several pump power levels. In the 3-mirror configuration (figure 3.6) the 'long' arm (typically ~250-300mm) of the cavity could be considerably shortened (50-100mm) to improve the cavity/pump mode overlap and therefore the beam quality. M^2 values below 1.3 (approaching the diffraction limit) could be achieved with only a moderate (~10%) loss in output power.

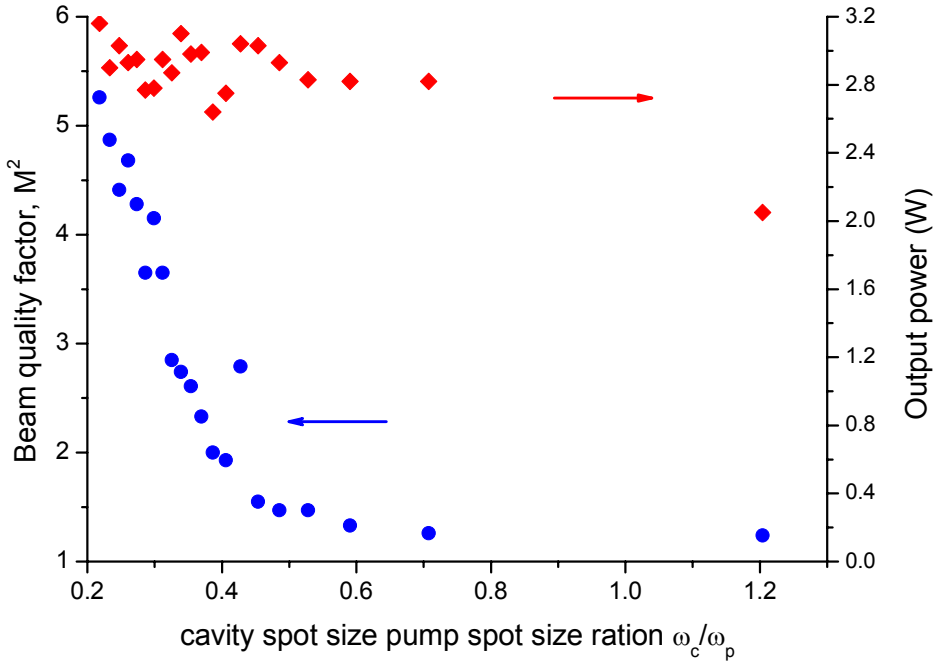

Fig. 3.6: Plots of the cavity length/M^2 relationship of 3-mirror characterization configurations.

Dual chip cavity

The basic power-scaling scheme of a semiconductor disk laser is to increase the pumped area while holding the pump power intensity at a constant level. However, depending on the heat extraction scheme employed for thermal management of the OPSDL, there is an upper limit for the maximum pump spot size. This can be also observed in case of GaSb-based OPSDLs employing intracavity heatspreaders. This behavior was attributed to the fact that an optimum heat transfer is achieved for a certain pump spot diameter. The less efficient heat removal at higher pump spot sizes can be explained as follows: due to the fact that there is still a radial heat-flow component inside the pumped region and not true 1D heat flow, as in the case of a crystalline solid-state disc laser - when increasing the pump spot size further, this heat path is constrained and the relative contribution of the radial heat flux to the total heat removal capability decreases and the temperature in the active region rises more quickly reducing the maximum output power at thermal rollover.

An alternative approach in order to enable even higher output power is the use of several separately pumped gain media in a common laser cavity. Within the scope of this work, we realized a laser cavity consisting of two OPSDL chips emitting at 2.25 µm wavelength and yielding several Watts of output power. For these experiments, we employed two mounted OPSDL chips which were liquid-capillary bonded to SiC heatspreaders. In order to coherently couple the two OPSDL chips we used a cavity in which one OPSDL chip (chip 1) served as an end mirror while the other chip (chip 2) was used as a folding mirror (see Fig. 3.7). We used an output coupler with a radius of curvature (ROC) of 150 mm placed at a distance of ~140 mm with respect to chip 2. An HR coated folding mirror (ROC=50 mm) was placed at a distance of 100 mm with respect to both, chip 1 and chip 2. We thus obtained equal fundamental cavity mode diameters on chip 1 and on chip 2 which could be easily controlled in changing the length of the resonator arm between chip 2 and the output coupler. Due to a small folding angle of 6° negligible astigmatism was introduced to the cavity mode by the employment of the curved

folding mirror. Chip 1 and chip 2 were pumped by fiber-coupled diode laser modules emitting at 980 nm.

Power transfer curves for the dual-chip configuration recorded at 20°C heat sink temperature are shown in Fig. 3.8. Using an output coupler reflectivity of 92 %, we obtained a maximum output power of more than 3.3 W. From the linear part of the power transfer curve a maximum optical-to-optical conversion efficiency of ~15% was calculated. We thus obtained a slightly reduced efficiency when comparing with the results obtained for a single-chip OPSDL. But due to the higher gain in this setup (two gain chips), output couplers with lower reflectivity can be used in order to obtain similar efficiencies as in case of the single-chip VECSEL.

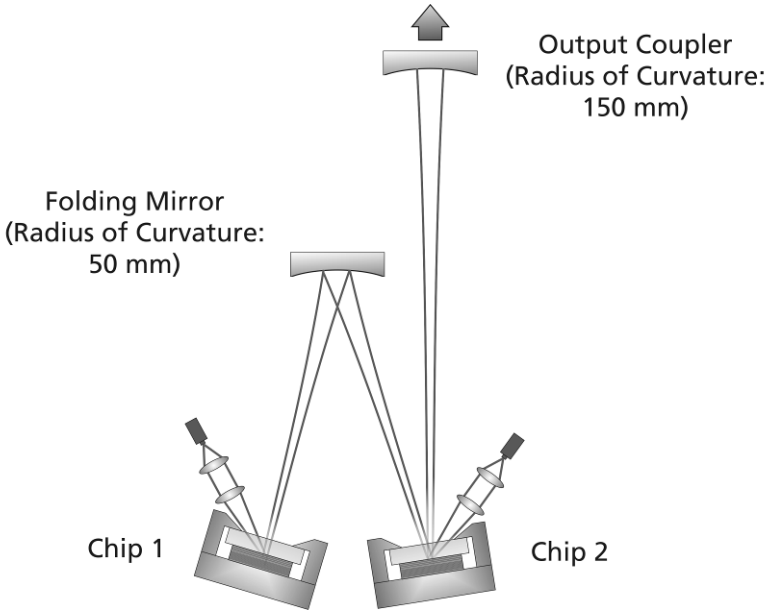

Fig. 3.7: Sketch of the dual-chip VECSEL configuration used for the experiments.

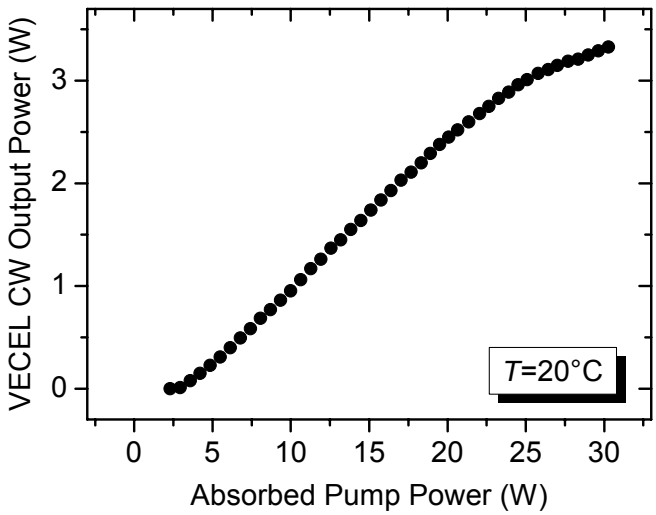

Fig. 3.8: Power transfer characteristic of the present dual-chip VECSEL recorded for an output coupler reflectivity of 92 %. Both chips were run at the same heat sink temperature of 20°C.

For the 2.0µm OPSDL sample, a slightly different two chip cavity was used (see Fig. 3.9). The cavity was essentially two 3-mirror OPSDLs configured back to back. This geometry was not optimised for output as the power is divided across two beams however implementation of a suitable coating on the diamond surface and cavity geometry similar to that described above would yield similar results in a single beam. At a mount temperature of 20°C the individual chips delivered output powers of 2.9 and 3W and a combined output of 6.1W (figure 3.10). At -5°C the chips provided 4.2 and 3.8W separately and the laser operated with an output of 8.1W (figure 3.11).

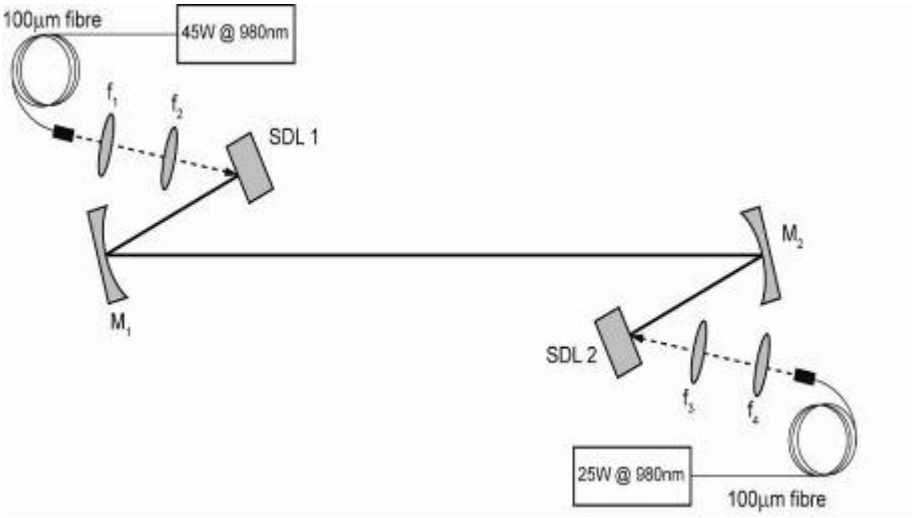

Fig. 3.9: Dual chip cavity configuration used with the 2.0µm sample.

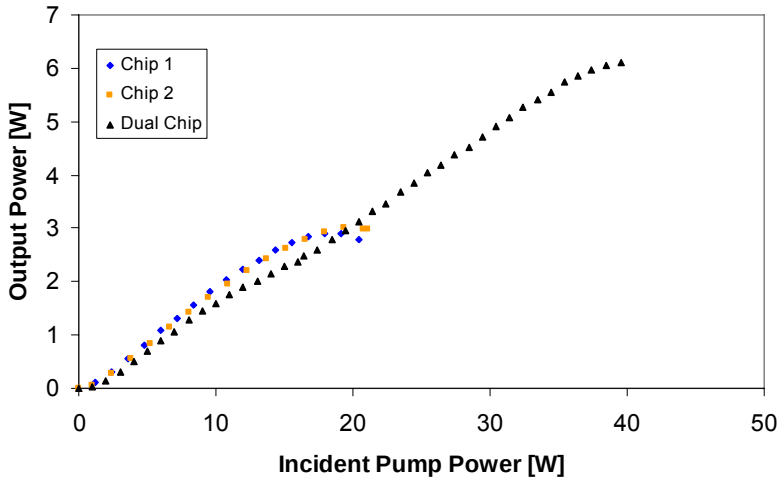

Fig. 3.10: Output power transfer characteristics for the dual chip setup for room temperature (20°C) operation, Chip 1: Pout = 2.9W, Chip 2: Pout = 3W, Maximum slope 19%, Dual Chip: Pout = 6.1W.

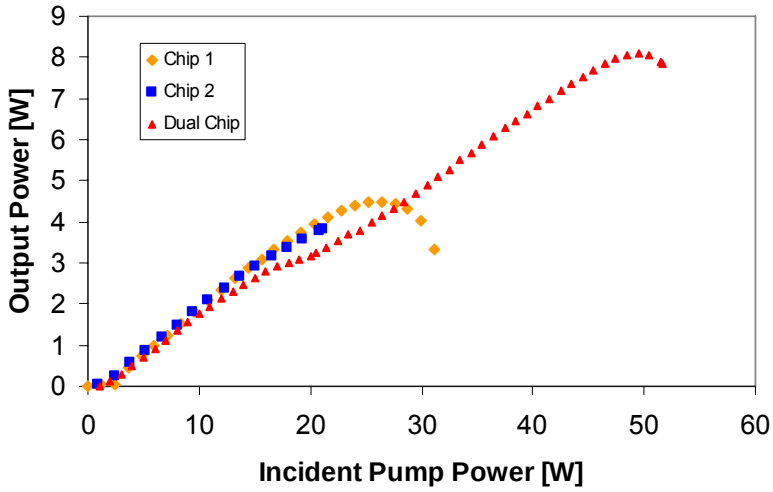

Fig. 3.11: Output power transfer characteristics for the dual chip setup for cooled (-5°C) operation, Chip 1: Pout = 4.2W, Chip 2: Pout = 3.8W, Maximum slope 20%, Dual Chip: Pout = 8.1W.

Tuning performance

By inserting a simple, angle-tuned, quartz birefringent filter in the external cavity, the lasers could be readily tuned over 100nm. By varying the heatsink temperatures and output coupler reflectivities the tuning ranges could be extended to 150-170nm. Figure 3.12 below shows the tuning performance of a selection of the best 1.9, 2.02, 2.25 and 2.3 µm samples fabricated, typically with R=99% output coupling mirrors.

The best performing sample so far in terms of output power has been the 2.0µm sample (6W). This sample could be tuned from 1.89 to 2.06µm (a total of over 170nm) for different mount temperatures and output coupling values. For 15°C and a 1% output coupling mirror the laser operated above 1W output over the range 1.959 to 2.023µm (64nm). The total tuning range for 15°C for this sample was 154.4nm. For the 1.9µm sample the high power performance was similar to the 2.0µm sample with output powers (over 4W for cooled operation, 3W at 15°C) and tuning range at 15°C of 125nm from 1.864 to 1.989µm.

At the slightly longer wavelengths around 2.2µm quaternary GaInAsSb quantum wells are used and the efficiency of the structures are reduced slightly due to a combination of thermal and chemical limitations such as a slightly reduced carrier confinement in the wells. Nevertheless, the performance of these samples is still impressive covering many atmospherically significant molecules in this wavelength range, thereby opening up a wide range of potential environmental remote sensing and pollution monitoring applications.

Also plotted, is the initial demonstration of the longest GaSb-based OPSDL performance of 100mW output power at 2.8µm generated within the project from a non-optimized sample (no tuning experiments have yet been performed with this sample). Hence figure 3.12 shows the entire wavelength range covered by the VERTIGO OPSDLs.

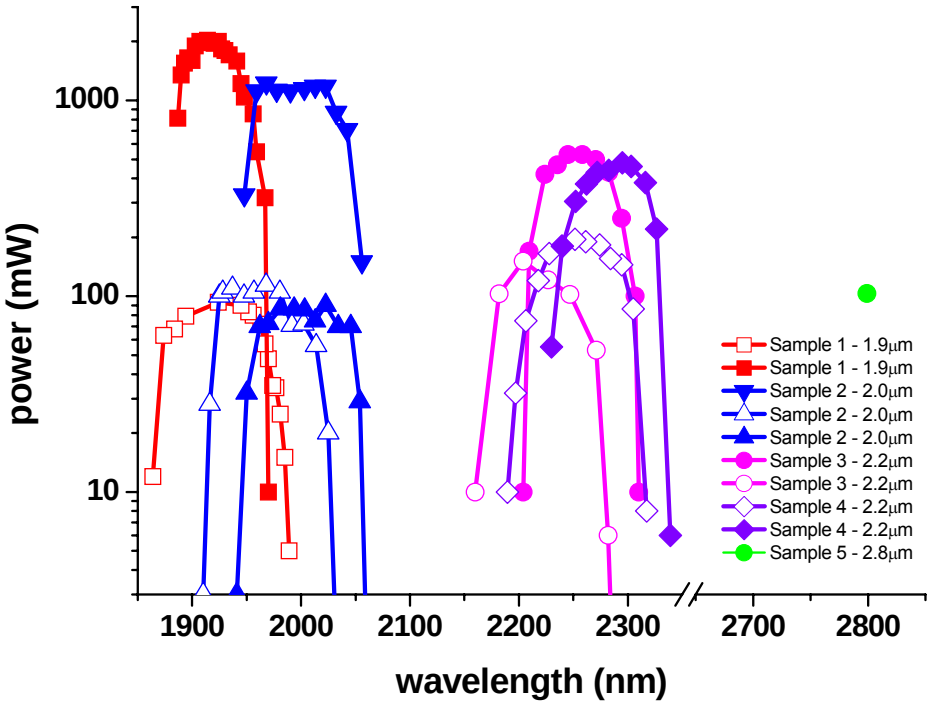

Fig. 3.12: Tuning characteristic (with rotation of BRF) of various samples ranging from 1.9 to 2.3µm for different operating temperatures and output coupling values showing the complete tuning range of the samples to date. Also included is the free-running emission wavelength of the very first OPSDL emitting at 2.8µm (no tuning experiments have been performed on this sample yet). Hence this figure shows the entire wavelength range covered by the VERTIGO project.

Lifetime measurements

The lifetime of the mounted GaSb-based OPSDL chip is a critical value for all real world applications of this new technology. Therefore, a separate experimental setup was built at the IAF, solely reserved for continuous operation and data logging of the 2.Xµm OPSDL under various conditions.

In Fig. 3.13, the output power of the OPSDL is shown versus elapsed time together with the power transfer characteristic before and after the aging experiments. Apart from the first 100-200 h, the decrease is almost linear. Therefore, the lifetime of the OPSDL chip was determined by extrapolating this linear part of the measurement (see Fig. 3.13, left side). By using the common definition of 20 % loss as “end of life”, the extrapolated lifetime was in the range of 4000 – 8000 hours, which is an encouraging, result for this very first tests. This lifetime is well above the common requirement for medical laser (>1000 h).

In Fig. 3.13, right side, the power transfer characteristic of the OPSDL sample are compared before and after the aging experiments. The threshold pump power as well as the power level of thermal rollover is almost unchanged, the slope efficiency is slightly lower after aging. These findings suggest a change in the internal losses that might be due to a damage of the heatspreader or the semiconductor surface, although no damage was visible by optical inspection. But as this is only the very first sample, further tests are necessary to clarify this point.

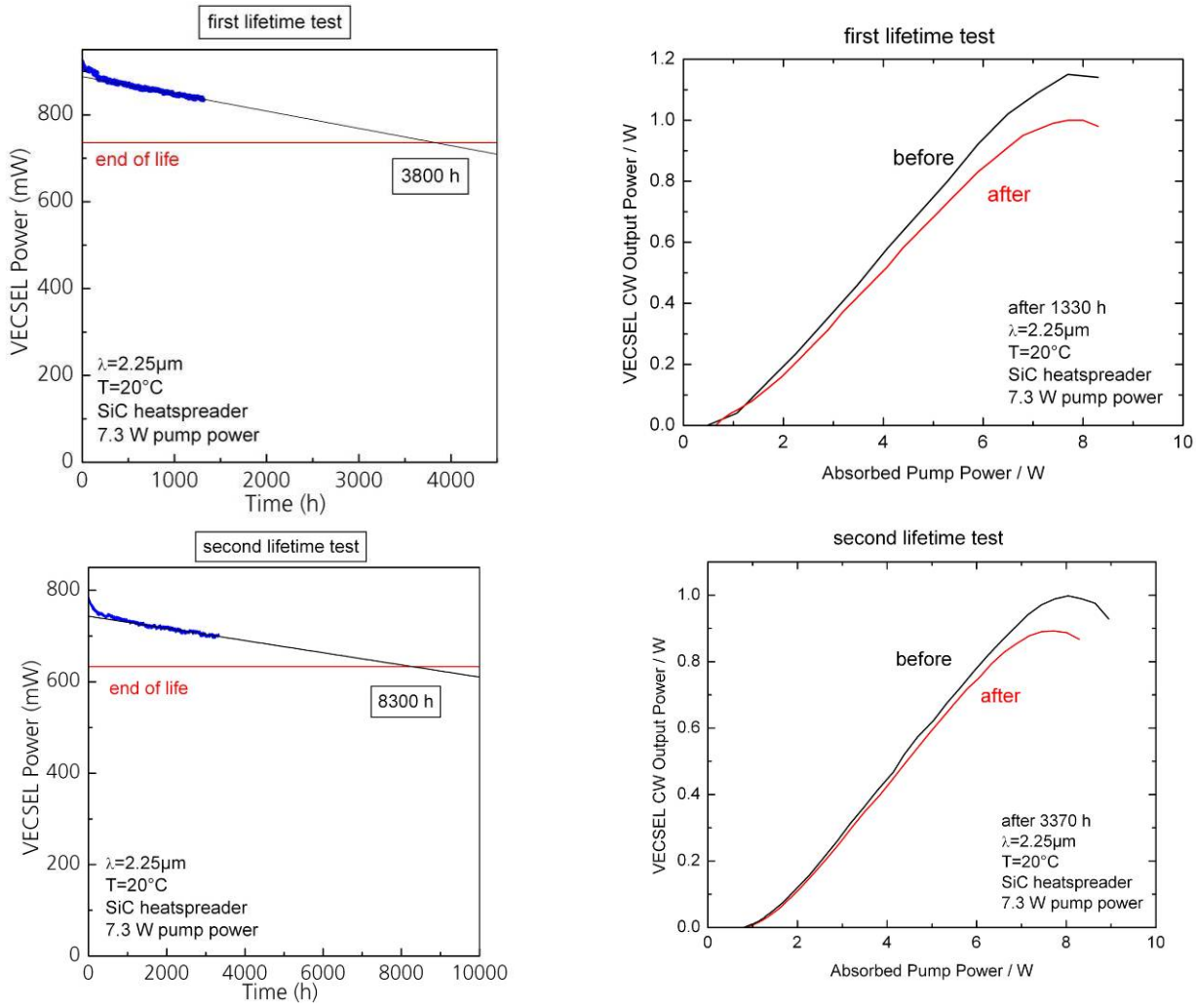

Fig. 3.13: Output power vs. time (left) and power transfer characteristics before and after the aging experiments (right) for different 2.25µm OPSDL samples, bonded to SiC heatspeaders.

Pulse pumping

In addition to using high-power CW pumps, investigations were carried out with a number of OPSDL samples using new high peak or 'on-time' power pump sources that have been developed for collision avoidance LIDAR in the automotive industry. These compact sources emit high power (up to 75W) pulses for 100s of ns while costing 100 times less than the cw fibre coupled pump sources. This provides the prospect of very cheap and compact OPSDL sources for applications where cw outputs are not required. These laser sources represent a new approach to practical light sources and were very relevant to the advanced concepts and the modulation work packages of VERTIGO.

Typically, the pulsed-pumped investigations used two polarisation coupled 75W OSRAM SPL-PL90_3 pump lasers (see figure 3.14 below). These were used to pump both 2.0µm and 1.9µm samples which performed similarly with pulse pumping while displaying markedly different output performance when pumped with cw light.

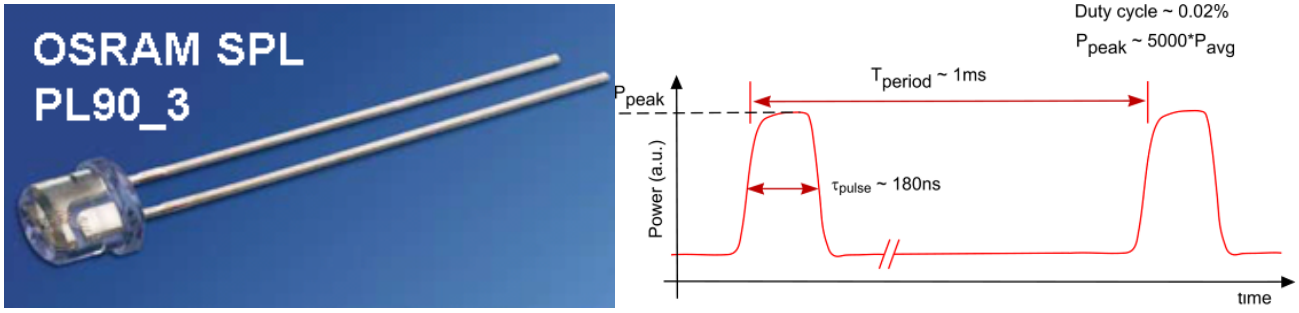

Fig. 3.14: left: photograph showing the 75W OSRAM SPL-PL90_3 in plastic package and right: a schematic of the typical output from this source when driven with an avalanche transistor pulse circuit. Specifications Wavelength – 905nm, Bandwidth ~ 7nm, Peak current – 40A, Peak power – 75W, Pulse duration - <200ns, Pulse frequency - <10kHz (0.1%), Operating temp - -40 – 85°C.

Figure 3.15-left below shows a photograph of the polarisation-coupled pump setup. After two aspheric f=8mm collimating lenses and a polarisation beam combining cube an f=11mm aspheric focussing lens was employed to direct the pump pulses onto the OPSDL. In this configuration the combined on-time pump power was approximately 120W (fig. 3.15-right).

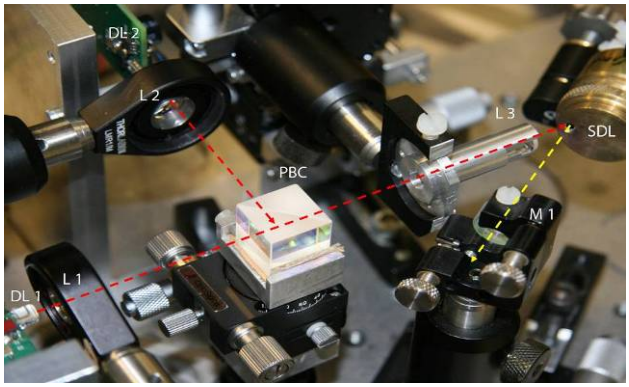

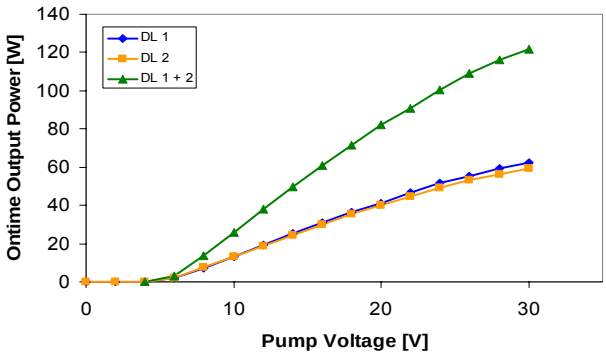

Fig. 3.15: left: Photograph showing the directly coupled pulse-pump diodes (D1 & D2) showing the polarising cube and the collimation (L1 & L2) and coupling lens (L3) and right: the output power transfer characteristic with pump voltage to the driver circuit of each of the diodes and the combined on-time power at the system focus. The maximum combined on-time power (incident on chip) from the pump unit was 120W.

The 1.9µm and 2.0µm samples were compared directly in a 2-mirror cw and pulse-pumped cavity at room temperature. Figure 3.16 below shows the directly compared power transfer characteristics of each, where the corresponding maximum output powers from the OPSDLs at 1.9 and 2.0µm were 20W and 18W respectively (for comparison the maximum cw output power obtained from these samples at room temperature under similar conditions was 1.8 and 2.6W respectively). As described previously for the cw case the M^2 beam quality factor could be significantly optimised to around 1 for a 2 mirror oscillator by carefully managing the resonator/pump waist ratio by adjusting the cavity length. In the case of the pulse-pumped laser however it was found that the beam quality factor could not be improved below 4.5 using this procedure. Figure 3.17 below compares the M^2 measurements with the resonator/pump waist ratio of a pulse-pumped and cw OPSDL It is therefore assumed that the

transient heating is supporting higher transverse mode behaviour during the pump pulse envelope in some way.

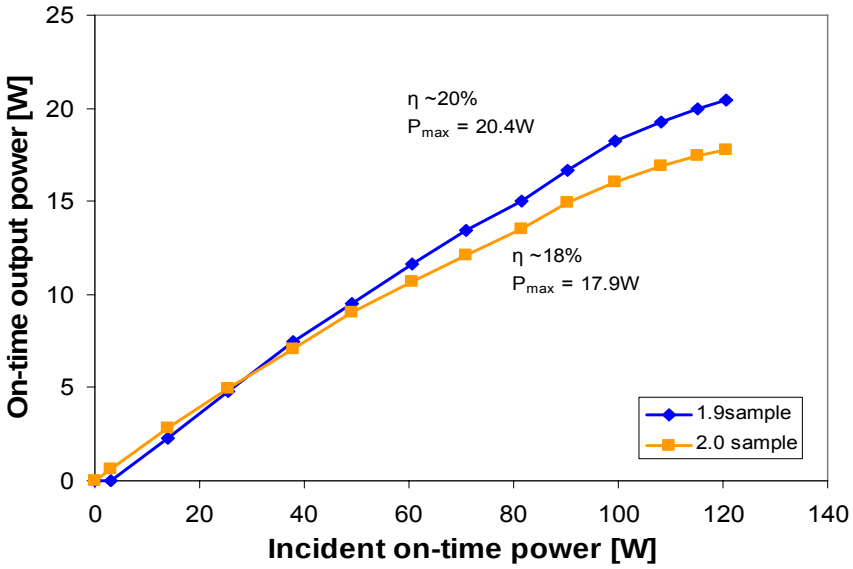

Fig. 3.16: the on-time output power characteristic of the directly pumped 1.9 and 2.0µm OPSDL samples giving 20W maximum power in a square pulse from the 1.9um OPSDL (18W for 2µm).

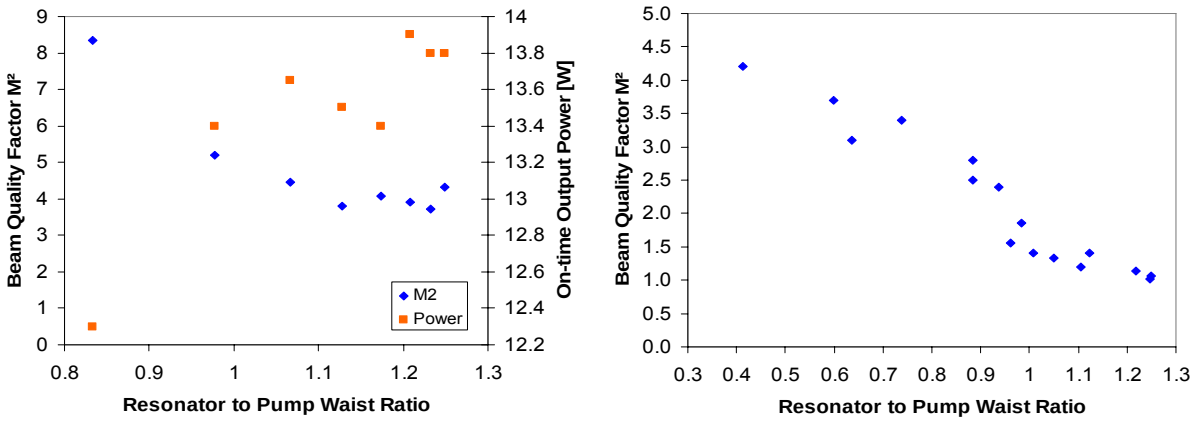

Fig. 3.17: Beam-quality factor of the pulsed pumped OPSDL (left) and a 2.0 cw operated OPSDL (right) in a 2-mirror resonator for comparison. While the cw laser is capable of running at M² values of close to 1 the pulsed system has a minimum M² of 4.5.

To further investigate the potential for the pulse-pumped format for a number of applications which require or desire higher pump pulse energies or longer duration pulses the pulse durations were increased by adapting the driving circuitry. In this way the current pulses were increased to approximately ~1µs by reducing the duty cycle to ~100Hz to avoid heating in the electronic components and catastrophic thermal failure of the OSRAM laser diodes. It was found that the on-time power stays roughly constant (with slight fade) and therefore the pulse energy increases fairly linearly.

From the behaviour of the drive circuit and pump it was possible to interpolate a maximum pulse duration of around 8µs for the current system. Figure 3.18-left below shows the pump and OPSDL output pulses recorded when the pump pulse duration was increased to 1.3µs. This follows the typically observed temporal behaviour of the pulsed pumped OPSDL showing a short turn-on delay due to the required heating to align the emission and reflectivity features of the OPSDL chip. After an initial time delay (in this case ~25ns) the output OPSDL pulse closely tracks the pumping pulse with no relaxation oscillations due to the short carrier lifetime.

To investigate the spectral behaviour of the pulse-pumped OPSDL (and effectively the differential temperature rise of the OPSDLs) the pulsed output was passed through a grating monochromator and the temporal response measured. By tuning the monochromator to each of the diamond heatspreader etalon modes and recording the resultant pulse shape in turn (example in figure 3.18-right below) the instantaneous spectrum at different times during the duration of the pulse could be reconstructed (figure 3.19-left) and the corresponding temperature rise derived (figure 3.19-right).

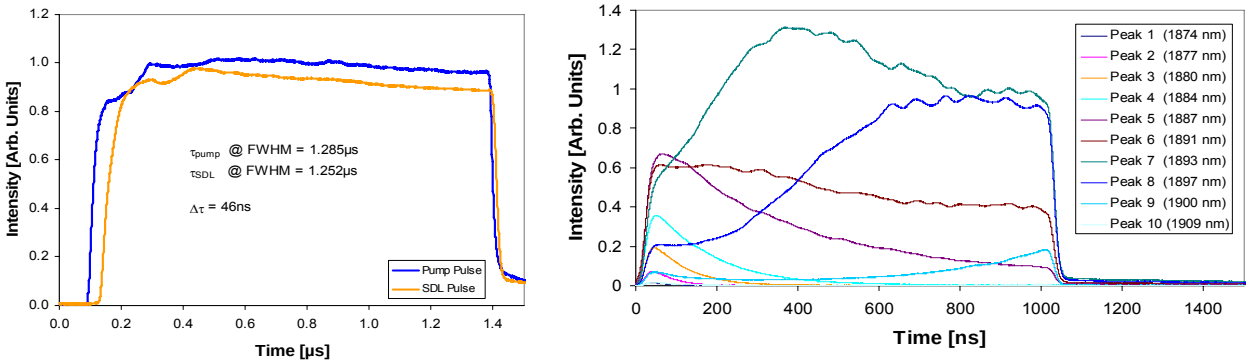

Fig. 3.18: left: output temporal behaviour of the OSRAM pulsed laser pump arrangement and the OPSDL when the pump pulse was extended to 1.3µs – the OPSDL closely follows the pump with a turn-on delay of 46ns – due to heating of the pump laser there is an 11% drop in output power with heating of pump laser (pump duty cycle 1:10000). Right: Temporal behaviour of the 9 diamond etalon modes able to oscillate during the pump pulse window measured using the monochromator in front of the fast photodiode as a highly selective spectral filter.

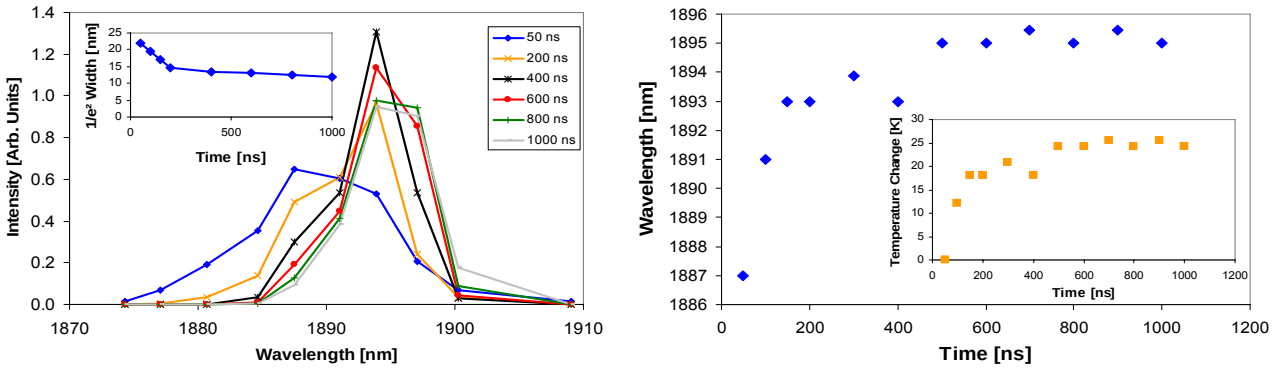

Fig. 3.19: left: reconstructed instantaneous spectra of the 1.9µm pulse-pumped OPSDL at 6 points during the pump pulse showing a clear slowing of thermally induced chirp with the longer (~1µs) pump pulses. Right: Plot of the centre wavelength with time (blue) for the 1.9µm pulse-pumped OPSDL showing a 9nm wavelength shift and corresponding

temperature rise (inset) in the device (orange) showing a 25°C temperature change associated with the 0.33nm/K drift rate of the OPSDL.

In-well pumped OPSDL

The in-well pumped structure was designed for an emission wavelength close to 2.25 µm and a pump wavelength of 1.96 µm. A 3 × 3 mm^2 OPSDL chip was cleaved from the wafer and bonded to a 380 µm thick SiC intra-cavity heatspreader for an efficient heat extraction from the active region. A Thulium-doped fiber laser emitting at 1.96 µm was used as pump source. For maximum pump absorption, the pump angle was adjusted to approximately 10° to the OPSDL chip's surface normal in order to match the pump resonance of the OPSDL structure to the pump wavelength. This pump angle is close to the value calculated based on the target layer thicknesses of the structure (18°) and thus documents that the grown structure agrees well with the original design. Focusing the pump radiation on the chip surface resulted in a pump spot diameter of approximately 200 µm. All laser experiments were carried out in continuous-wave operation at a heat sink temperature of 20°C; the transmission of the output coupling mirror was varied in several steps between 1.6% and 13%.

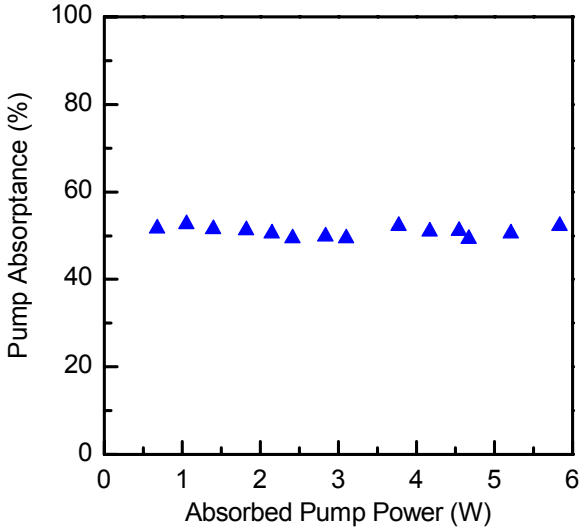

Fig. 3.20: Pump absorptance in dependence of the absorbed pump power fort the in-well-pumped OPSDL realized within this work

Without any external pump recycling optics, a pump absorptance above the oscillating threshold of more than 50% was achieved (see Fig. 3.20). This result proves that sufficiently high pump absorption can readily be achieved within the in-well pumping scheme although the gain medium incorporates less absorbing material compared to barrier-pumped OPSDLs. Using a single external mirror for pump recycling, re-directing the pump light reflected off the OPSDL chip back onto the pump spot, the total pump absorption can be increased to ~75%.

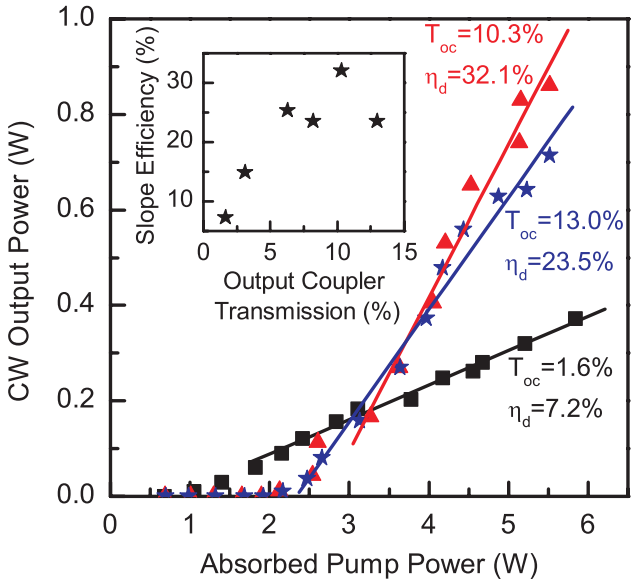

Fig. 3.21: CW output power of the present in-well pumped VECSEL for output coupling mirror transmissions T_{oc} of 1.6% (black squares); 10.3% (red triangles); and 13% (blue asterisks), respectively at a heat sink temperature of 20°C. The full lines indicate the linear fit functions used to obtain the respective slope efficiencies, η_d. The values for η_d and T_{oc} are displayed at the side of each power curve. In the inset, the measured slope efficiency is displayed as a function of the output coupling mirror transmission.

Figure 3.21 shows for the present in-well pumped OPSDL, the CW output power as a function of the absorbed pump power for several transmission values of the output coupling mirror. The maximum slope efficiency amounts to 32.1% at a heatsink temperature of 20°C, being approximately two times higher than slope effieicency measured with barrier-pumped OPSDLs at the same emission wavelength. To the best of our knowledge, this value represents the highest reported slope efficiency of a OPSDL emitting at a wavelength above 1.3 µm. The maximum slope efficiency was achieved at an output coupling mirror transmission higher than 10%. Increasing the transmission to 13% leads only to a slight decrease in the efficiency (see inset in Fig. 3.1.3). Higher transmissions could not be tested due to the lack of appropriate output coupling mirrors. The capability of this laser to tolerate such high cavity losses despite of the short optical path length within the gain medium (accumulated thickness of the QWs: 130 nm) implies that the modal gain is relatively high.

Thus we have demonstrated the successful implementation of the in-well pumping approach to OPSDLs emitting in the wavelength range above 2 µm. A power slope efficiency higher than 32% with respect to the absorbed pump power has been measured for continuous-wave laser operation at room temperature (20°C). This result documents the increased conversion efficiency due to the reduced quantum defect. Although gain media in in-well pumped OPSDLs feature a more complex structural layout, direct pumping of the QWs is a promising concept especially when targeting longer emission wavelengths. When heading towards the wavelength range above 3 µm, using standard near-infrared diode lasers would lead to a very large quantum defect and therefore to a reduced conversion efficiency and an exceedingly large thermal load.

For practical purposes, the Thulium-doped fiber laser used in the experiments can be replaced by a more compact and cost-efficient pump source such as fiber-coupled GaSb-based diode laser arrays emitting at 2 µm. Performance of such diode laser has advanced over the last couple of years and should continue to improve further in the near future.

Temperature mapping of OPSDL laser

Experimental setup

In order to study the temperature distribution of the OPSDL chip under operating conditions, a new thermoreflectance (TR) setup was built around the setup used for optical pumping. To model the thermal phenomena properly, one has to take into account the possible ways of converting the energy that is delivered to the system. The total energy coming from the pump beam, is converted to heat, emitted as laser output and also emitted by spontaneous emission process. The heating power can be calculated as follows:

$$P_{heat} = P_{pump} - P_{pump,refl} - P_{laser} - P_{spont} = (1 - R_{pump})P_{pump} - P_{laser} - \eta_{rad}\eta_{QD}(1 - R_{pump})P_{pump,threshold}$$

The last term is the power which is radiated by spontaneous emission. Assuming that the gain (and consequently the inversion) is clamped to a constant level above threshold, this spontaneous emission power is equal to the absorbed threshold pump power multiplied with the radiative efficiency η_{rad} of the QWs and an efficiency $\eta_{QD} = \lambda_{pump}/\lambda_{laser}$ which accounts for the quantum defect (the ratio of the laser photon energy to the pump photon energy). The above reasoning, provides the basis on which the lowering of temperature can be expected for oscillating device. The fraction of pump power, is converted to useful output radiation, decreasing the heat generation in the structure.

In the WP2 the temperature mapping of OPSDL chips was performed in the normal incidence TR setup. That implied certain restrictions on the OPSDL thermal investigation, namely, investigation of running OPSDLs was impossible. To overcome this obstacle, the apparatus for thermal mapping of OPSDL was reconfigured and built from the scratch in new geometry. The scheme and photos of the new TR experimental setup is shown in figure 3.22.

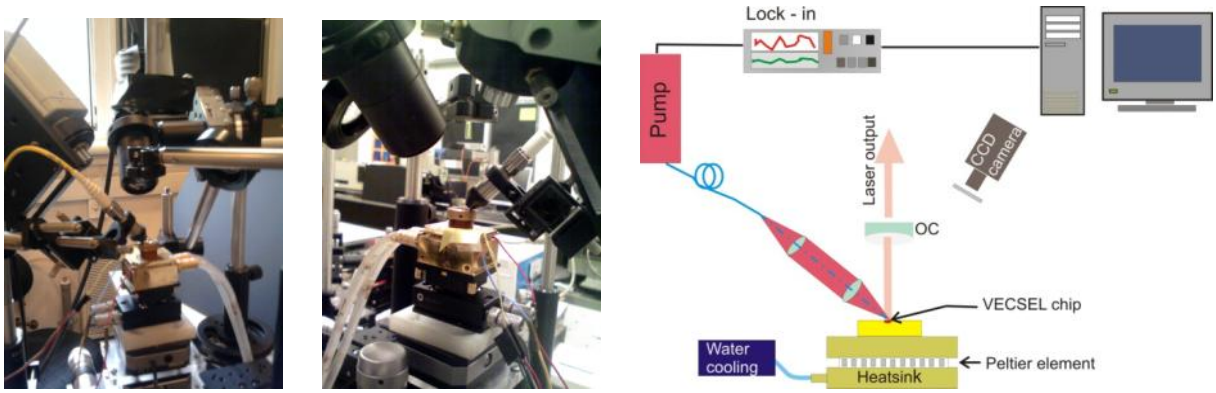

Fig. 3.22: Photographs and scheme of the experimental thermoreflectance setup in the angled configuration.

The specifics of the measurement, required the OPSDL sample together with output coupler and pump optics to be placed on positioning x-y-z stages, which are independent of the analysing beam (HeNe laser) and detector, which are fixed in this setup. This allows the precise adjustment of the sample position, and pump beam in respect to the probe beam. Such configuration allows 2D mapping of the temperature distribution on the operating OPSDLs.

The angled TR setup was used to measured the temperature distributions on the surface of OPSDL chips with and without SiC heatspreader. The measurement was performed for operating/oscillating and non operating/non oscillating samples for different pumping conditions.

OPSDL without heatspreader

In the first case, the OPSDL without the heatspreader was optically pumped in pulse mode at 3.6 W with duty cycle dc=5.8 % (pulse width τ_{pulse}= 0.5 ms and cycle width τ_{cycle}= 8.6 ms). The temperature of the heat sink was stabilized at 20°C. The resulting temperature distribution maps are presented in figure 3.23. It can be observed that the temperature increase is lower in case of emitting device. The difference reaches about 3 degrees, and is a consequence of the heat balance of the device. According to the theory, in case of emitting OPSDL, part of the pump power entering the sample is expected to be converted into useful energy of laser pulse instead of becoming a waste heat, as it is the case for non-oscillating OPSDL.

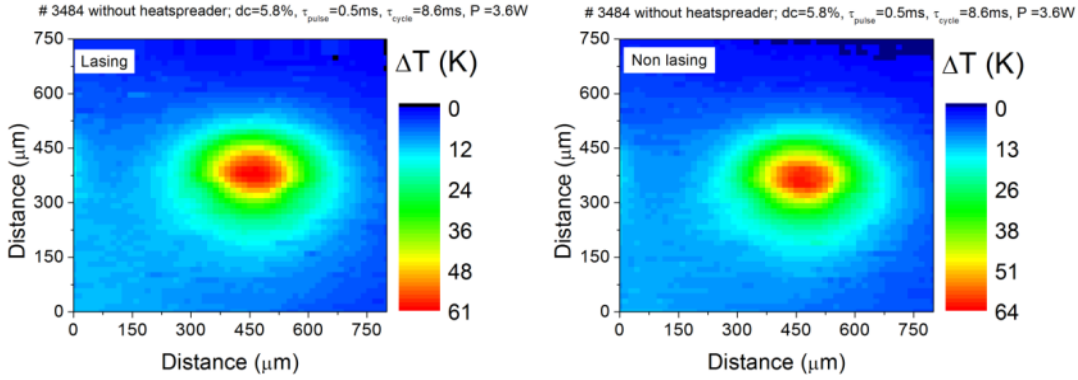

Fig. 3.23: Temperature distribution maps for OPSDL with SiC heatspreader: operating (left) and non-operating (right). OPSDL without heatspreader, duty cycle 5.8%

The temperature profiles taken from the temperature distribution maps are shown in figure 3.24. The comparison of temperature linescans of operating and non operating OPSDL shows that the difference in temperature occurs mainly in the centre of the hot spot.

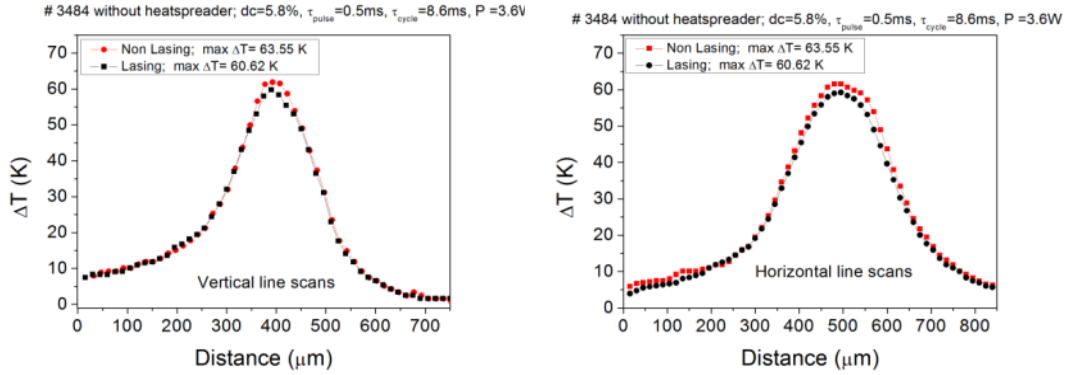

Fig. 3.24: Temperature profiles (horizontal and vertical) taken from the experimental temperature distribution maps for operating (black) and non-operating(red) OPSDL

The next measurement for the OPSDL without the heatspreader was done for the same pump power of 3.6 W with different duty cycle dc=12.5 %, (pulse width τ_{pulse}=0.5 ms and cycle width τ_{cycle}=4 ms). The temperature of the heat sink was stabilized at 20°C. The resulting temperature distribution maps are presented in figure 3.25 The maximal temperature increase is 150 K and is much higher than previously and the difference between operating and non operating reaches 4 degrees.

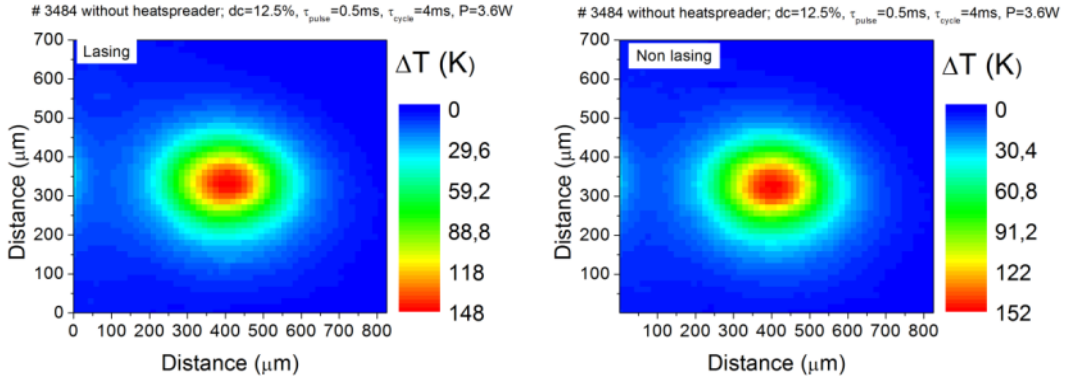

Fig. 3.25: Temperature distribution maps for OPSDL with SiC heatspreader: operating (left) and non-operating (right). OPSDL without heatspreader, duty cycle 12.5%

The duty cycle was extended to dc=25 %, (pulse width τ_{pulse}=0.5 ms and cycle width τ_{cycle}=2 ms). The temperature of the heat sink was stabilized at 20°C. The temperature distribution maps are presented in figure 3.26 Now, the maximal temperature increases are 230K, and the difference between emitting and non emitting OPSDL is only 1K.

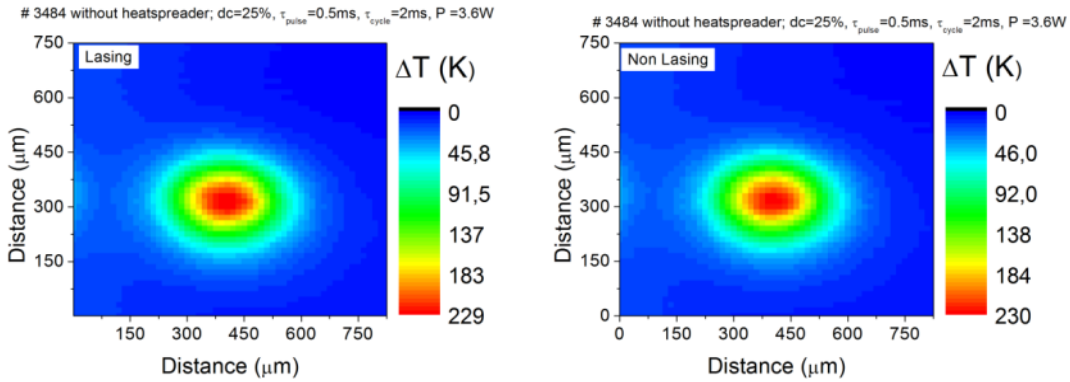

Fig. 3.26: Temperature distribution maps for OPSDL with SiC heatspreader: operating (left) and non-operating (right). OPSDL without heatspreader, duty cycle 25%

The figure 3.27 presents the difference $T_{off} - T_{on}$ for different duty cycles. The lowering of the temperature is observed in case of emitting OPSDL for every duty cycle studied. The difference becomes less significant at higher duty cycle. This is connected with the decrease of the emission time due to the excessive heat load in the active region.

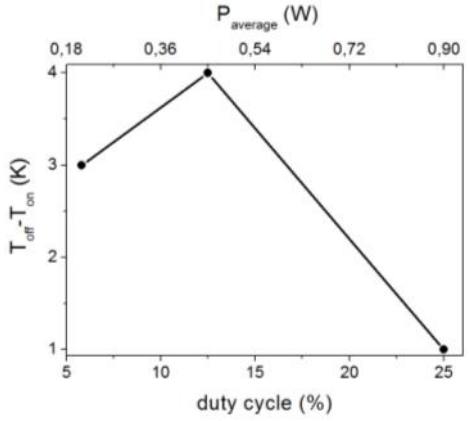

Fig. 3.27: The difference $T_{off} - T_{on}$ for different duty cycles for OPSDL without heatspreader

Figure 3.28 presents maximal temperature increases for oscillating OPSDL (blue line), non oscillating device (red line) and emitted power (black line) versus incident power, for pulse width τ_{pulse}=0.5 ms and cycle width τ_{cycle}=8.6 ms.

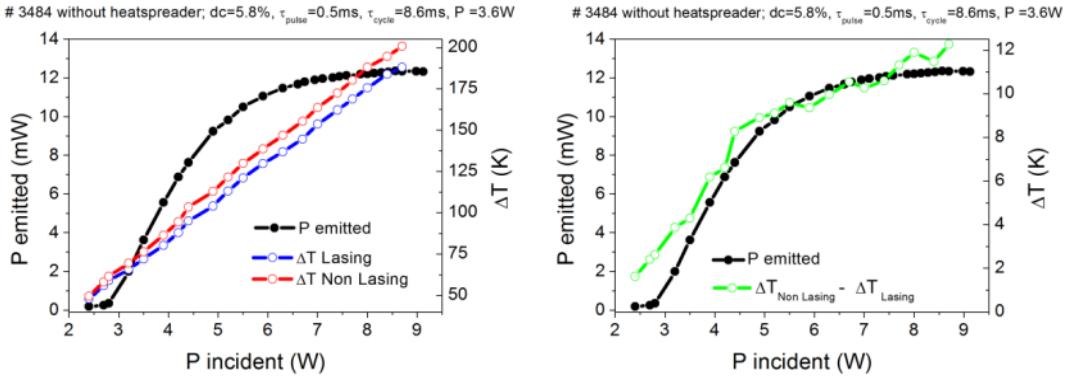

Fig. 3.28: Maximal temperature increases for oscillating OPSDL (blue line), non oscillating device (red line) and emitted power (black line) versus incident power

It can be seen that the difference in maximal temperature increases between oscillating and non oscillating OPSDL becomes more pronounced as the emitted power increases, and reaches 14 degrees at 8.5 W of incident pump power.

OPSDL with SiC heatspreader

The OPSDL with SiC heatspreader was also investigated. The measurement was performed for the same experimental conditions as for the sample without the heatspreader, i.e.:3.6 W at duty cycle dc=5.8 %, (pulse width τ_{pulse}=0.5 ms and cycle width τ_{cycle}=8.6 ms). The temperature of the heat sink was stabilized at 20°C.

The temperature distribution maps are presented in figure 3.29. Now, the maximal temperature increases are 30 K for the non oscillating sample and 25 K in case of the oscillating OPSDL. The difference between emitting and non emitting OPSDL is 5 K. It can also be seen that the temperature increases are lower than in case of the sample without the heatspreader.

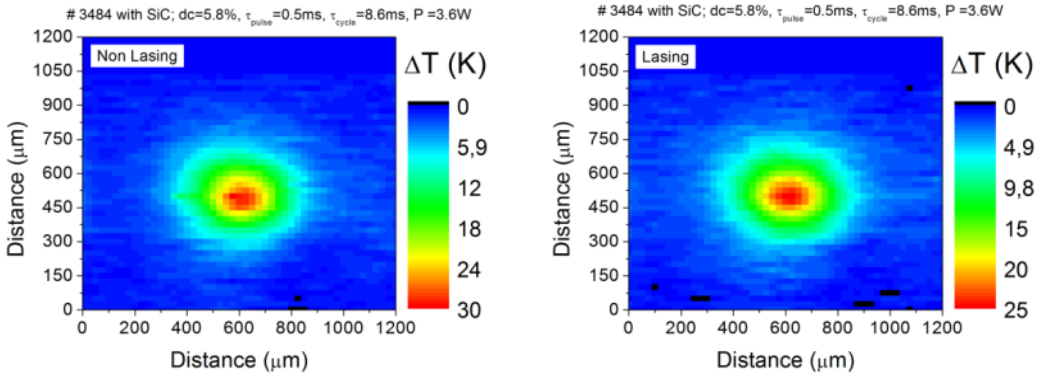

Fig. 3.29: Temperature distribution maps for OPSDL with SiC heatspreader: operating (left) and non-operating (right). OPSDL with SiC heatspreader, duty cycle 5.8%

The temperature profiles taken from experimental maps are presented in figure 3.30. It can be seen that temperature increase takes place not only in the central part of the temperature hot spot, lowering the temperature profile further from the centre.

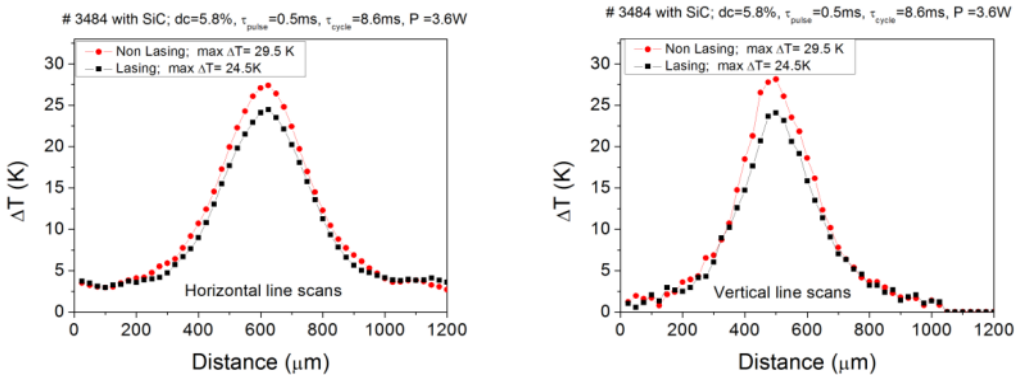

Fig. 3.30: Temperature profiles (horizontal and vertical) taken from the experimental temperature distribution maps for operating (black) and non-operating(red) OPSDL

Next, the OPSDL with SiC heatspreader was optically pumped at 3.6 W with duty cycle dc=50 %, (pulse width τ_{pulse}=4.3 ms and cycle width τ_{cycle}=8.6 ms). The temperature of the heat sink was stabilized at 20°C.

The temperature distribution maps are presented in figure 3.31. Now, the maximal temperature increases are 65 K for the non oscillating sample and 57 K in case of the oscillating OPSDL. The difference between emitting and non emitting OPSDL is 8 K. It can also be seen that the temperature increases are lower than in case of the sample without the heatspreader.

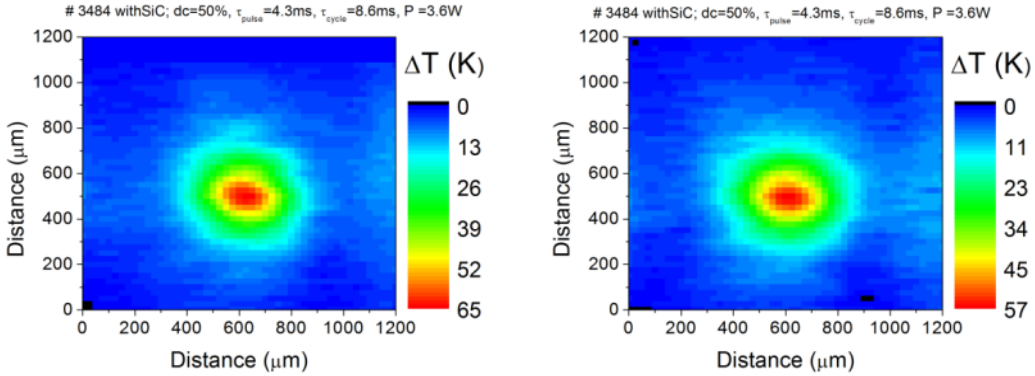

Fig. 3.31: Temperature distribution maps for OPSDL with SiC heatspreader: operating (left) and non-operating (right). OPSDL with SiC heatspreader, duty cycle 50%

The temperature profiles taken from experimental maps are presented in figure 3.32. Again, it can be seen that temperature increase takes place not only in the central part of the temperature hot spot, lowering the temperature profile further from the centre.

Figure 3.33 presents maximal temperature increases for oscillating OPSDL (blue line) and for non oscillating device (red line) and emitted power (black line) versus incident power, for pulse width τ_{pulse}=4.3 ms and cycle width τ_{cycle}=8.6 ms. The difference T_{off}-T_{on} increases as the emitted power increases, reaching almost 40 degrees at 12 W of incident pump power.

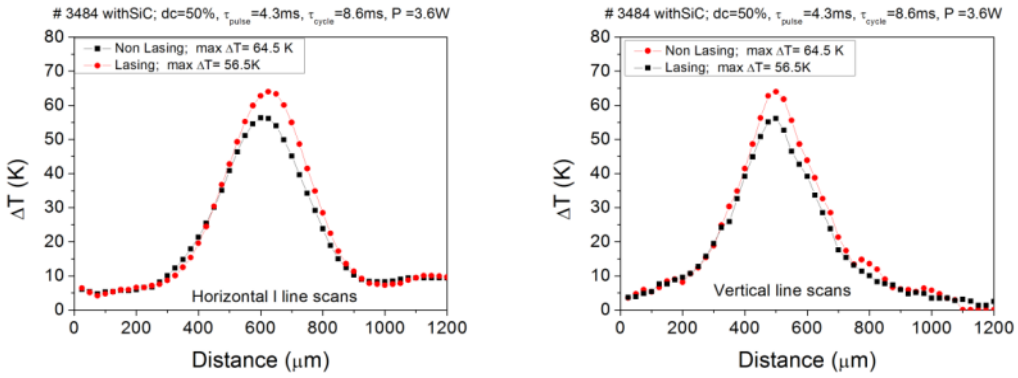

Fig. 3.32: Temperature profiles (horizontal and vertical) taken from the experimental temperature distribution maps for operating (black) and non-operating(red) OPSDL

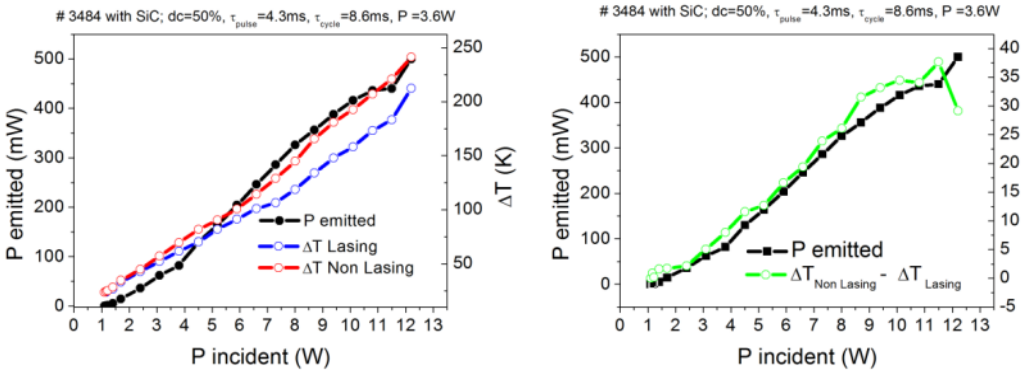

Fig. 3.33: Maximal temperature increases for oscillating OPSDL (blue line), non oscillating device (red line) and emitted power (black line) versus incident power

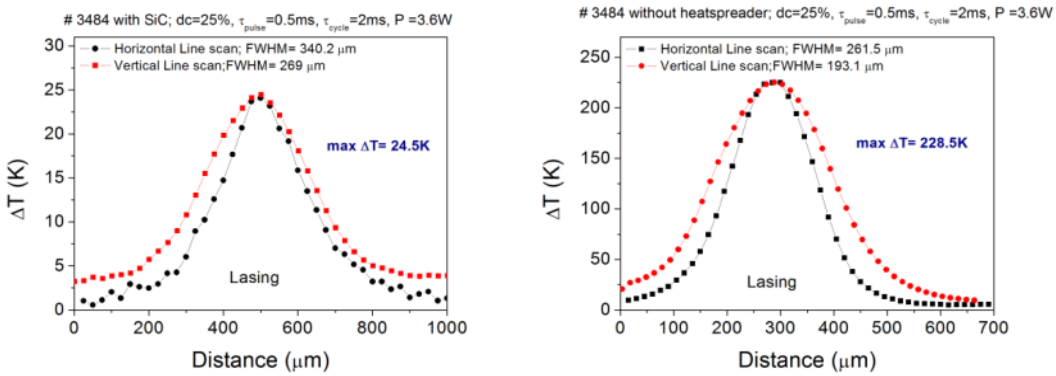

VECSEL w/o HS	
Max ΔT (K)	228.5 K
FWHM_H	261.5μm
FWHM_V	193.1μm

VECSEL SiC HS	
Max ΔT (K)	24.5 K
FWHM_H	340.2 μm
FWHM_V	269 μm

Fig. 3.34: Comparison of temperature profiles (horizontal and vertical) taken from the experimental temperature distribution maps for operating OPSDL with and without the heatspreader

Figure 3.34 presents comparison of temperature profiles between oscillating OPSDL sample with SiC heatspreader and without heatspreader registered for the same experimental conditions. The temperature increase in case of the OPSDL with SiC heatspreader is reduced by the factor of almost 10 in comparison to the OPSDL without the heatspreader.

In this task the use of thermoreflectance technique has been reported for the first time, to investigate thermal properties of the oscillating optically pumped surface emitting lasers. The original achievements of this task include design and construction of experimental setups allowing the measurement of the temperature distributions on the surface of the OPSDL chips with and without heatspreader. For the first time, the lowering of the temperature of emitting OPSDLs was observed experimentally, in an original experimental setup.

Development of the VERTIGO Common Gain and Basic Laser Module

Once successful high power OPSDLs had been demonstrated then work began on the key modular photonics component concept within VERTIGO. Here the idea for a compact and versatile source technology was centred around an SDL chip mounted in a standardized sub-mount that could be used in any laser characterization or deployment configuration. This sub-mount would then be incorporated on a platform for the thermal management and pumping of the semiconductor chip, the so-called 'common gain module' (CGM) which would then be incorporated withinin a simple resonator geometry to form a 'basic laser module' or BLM. It was decided that the CGM would take the form of a machined half-cube shape that could hold the SDL sub-mount and pump optics at the required angle and then be easily adapted to form the BLM. Figure 3.35 below shows the format of the first BLM fabricated.

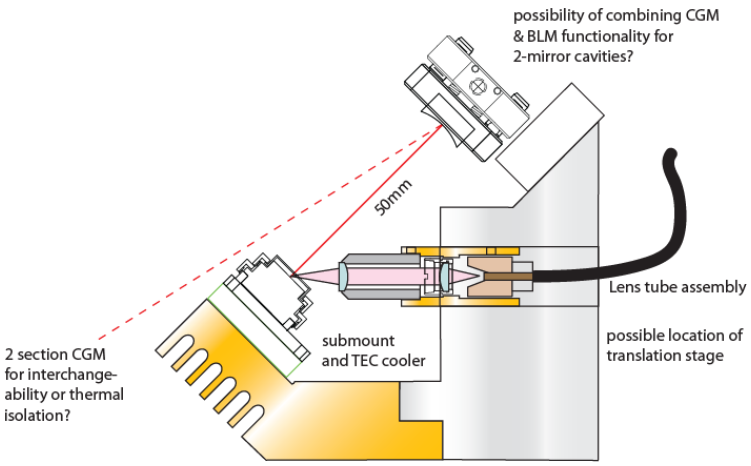

Figure 3.35: Design schematic of the rigid bracket CGM design showing the lens tube assembly and basic laser module (BLM) functionality.

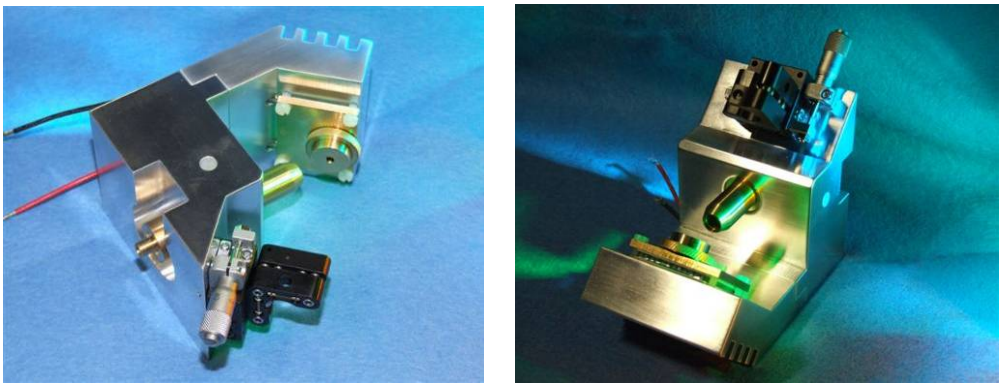

Figure 3.36: Photographs of the first version pre-prototype CGM fabricated at the IOP.

The sub-mount, cooler plate, pump optics and output coupler were mounted in the CGM frame shown schematically and pictorially above, to form the BLM. This CGM/BLM was configured with all the optical components in a simple 2-mirror configuration and a 2.0µm OPSDL sample shown in figure 3.37 below. With the TEC cooled plate held at 12°C the module yielded 3W output power and at room temperature 2.4W was achieved.

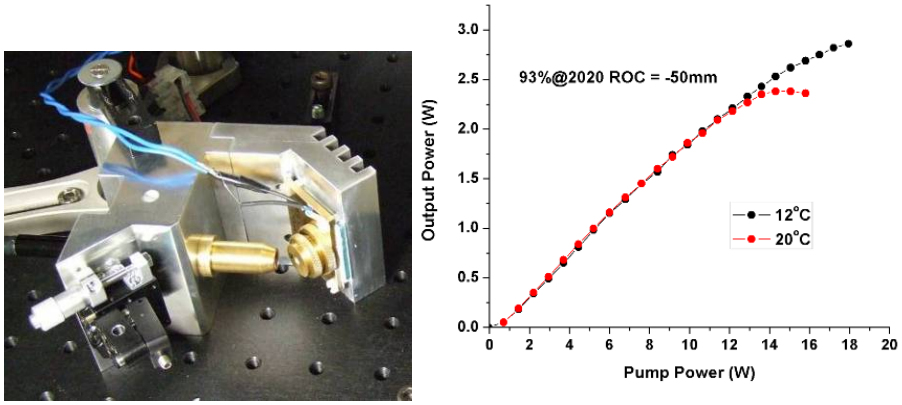

Figure 3.37: Photograph showing the CGM/BLM mounted on an optical breadboard and pumped with a 25W 980nm pump unit (left) and an output power transfer showing 3W operation with the plate held at 12°C and 2.4W with the plate at 20°C (right).

The beam quality factor of the BLM was also assessed for a number of different output powers and cavity lengths. Here greater than 2W cw output was achieved at 20°C with greater than 1W achieved in TEM_{00} operation, with M^2 measured to be less than 1.5 at 20°C. Figure 3.38 shows a typical beam waist measurement (dots) used to gather the data plotted in subsequent figures and includes a theoretical comparison (line) for the calculated M-squared value. Figure 3.39 shows the behaviour of the M-squared parameter for the BLM with varying cavity length (with output power fixed just above 1W) and output power (with cavity length fixed at 5.5cm) respectively, it can be seen that M-squared values below 1.5 were possible for cavity lengths up to ~7cm and output powers up to 2W. The M-squared parameter measured at 1W output power was 1.18.

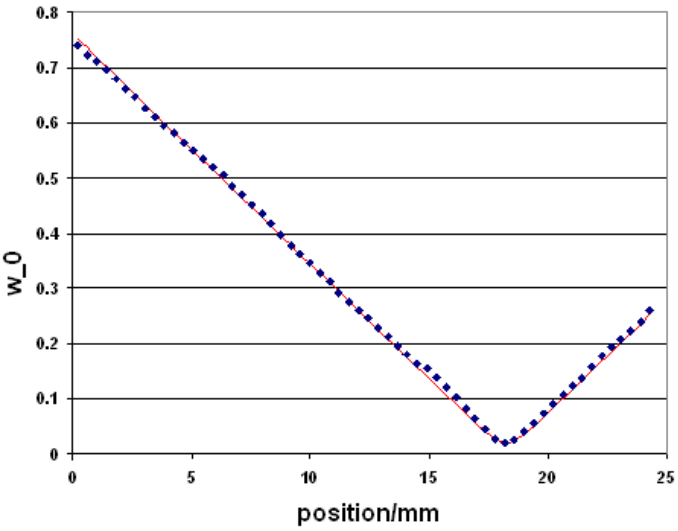

Fig. 3.38: Typical sequence beam profile measurements (dots) taken through a focus to measure the M-squared beam quality parameter using the InGaAs Dataray Beamscope P8 measuring system (output power ~1W, M^2 ~ 1.18). The theoretical beam waist profile necessary to obtain the measured m-squared value is plotted on top of the data (red line).

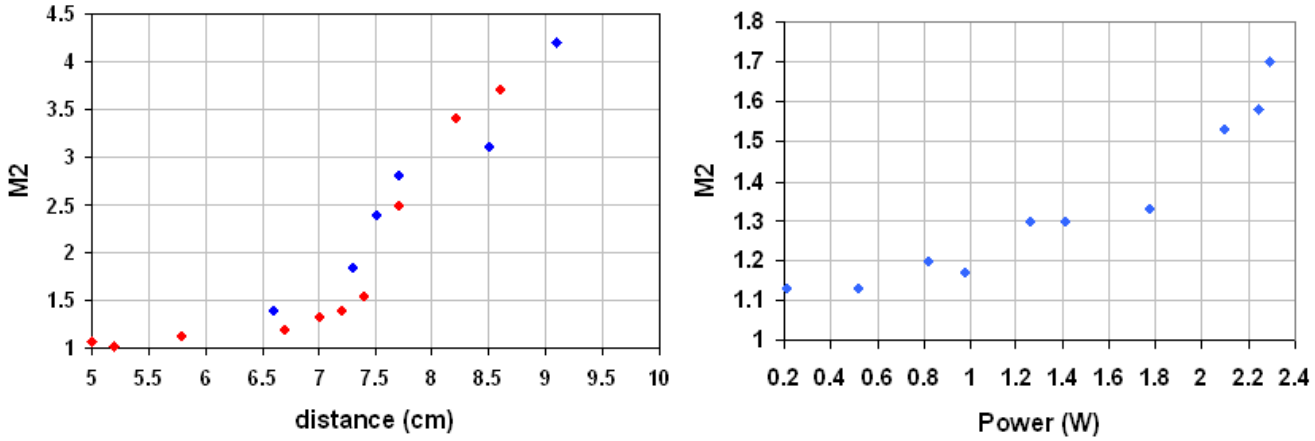

Fig. 3.39: Left: M-squared parameter plotted against cavity length of the BLM with output power ~1W (red and blue points represent different measurement runs) and right: the M-squared parameter plotted against output power with the cavity length fixed at 5.5cm.

Engineering module

The VERTIGO Common Gain Module, described above, is designed to offer all the necessary flexibility for different operation conditions; it allows a wide range of temperature of the OPSDL chip, different pump spot sizes (thus optimized efficiencies for different levels of output power), and can be easily incorporated into different resonator setups.

In order to test and demonstrate the ability of the OPSDL concept to be realized, in a compact geometry, a second module was developed in cooperation between the IAF and IOP, where the flexibility of the first design was exchanged for a miniaturized setup. As can be seen in Fig.3.40, the module is much smaller than the one described above, with a total outer dimensions of 7x5x3 cm^3.

In Fig. 3.41, the power transfer characteristic of an OPSDL chip, incorporated in the engineering module is shown. The OPSDL sample was bonded to a SiC heatspreader and is emitting at 2.0 µm. The laser module was stabilized by a TEC element, mounted on a water cooled base plate to 20°C temperature. A fiber coupled 980 nm laser diode was used as pump source. A maximum output power of 2.8 W was achieved with a mirror reflectivity of 95.2 %.

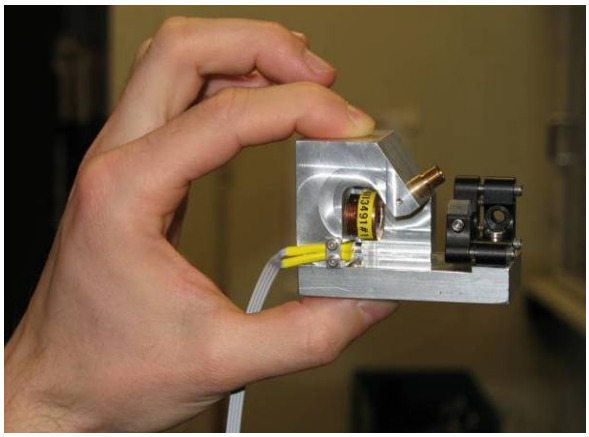

Figure.3.40: Photograph of the engineering OPSDL module, where the flexibility of the first design was exchanged for a miniaturized setup.

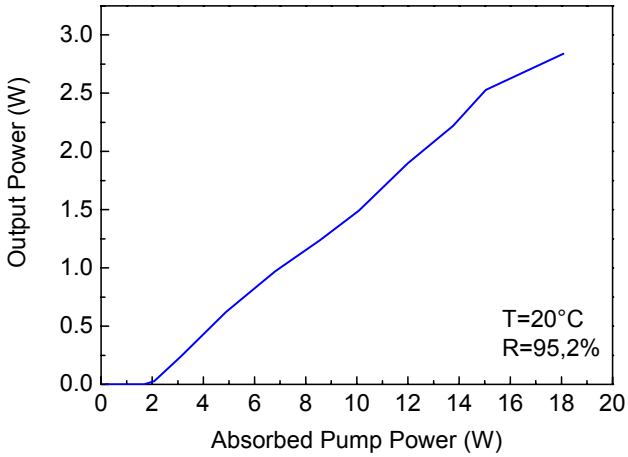

Fig.3.41: Power transfer characteristic of the laser module with a 2.0 µm OPSDL chip with SiC heatspreader, stabilized to 20°C temperature, using 980nm fiber coupled pump diodes. The maximum output power is 2.8W in CW-operation.

Also with the compact engineering module shown in Fig. 3.40, a high-power (>1W CW) TEM_{00} mode (M^2<1.5) operation could be successfully demonstrated (one of the VERTIGO milestones): In order to achieve pure single-mode operation, the ratio of pump spot diameter vs. mode spot diameter was decreased in order to suppress higher order modes. As this module does not have the flexibility to change the cavity length, this was achieved by using a pump laser with a smaller fibre diameter and by adjusting the pump optics. An OPSDL chip with SiC heatspreader and 2.0µm emission wavelength was used and the heatsink temperature was set to 20°C. After careful alignment, the output power was 1.3W and the beam profile showed a very good agreement with a Gaussian shape, both in horizontal and in vertical direction (see Fig. 3.42 c and d). The actual beam quality measurement was done by strictly following the ISO 11146 Standard, i.e. the second moment beam diameter definition was used (instead of the popular $1/e^2$ definition) and for every position 5 scans were averaged before the beam

diameter was determined. The results, shown in Fig.3.42 a and b, clearly reveal that the beam quality parameter M^2 is well below 1.5 with a value of 1.28 in the horizontal and 1.30 in the vertical direction.

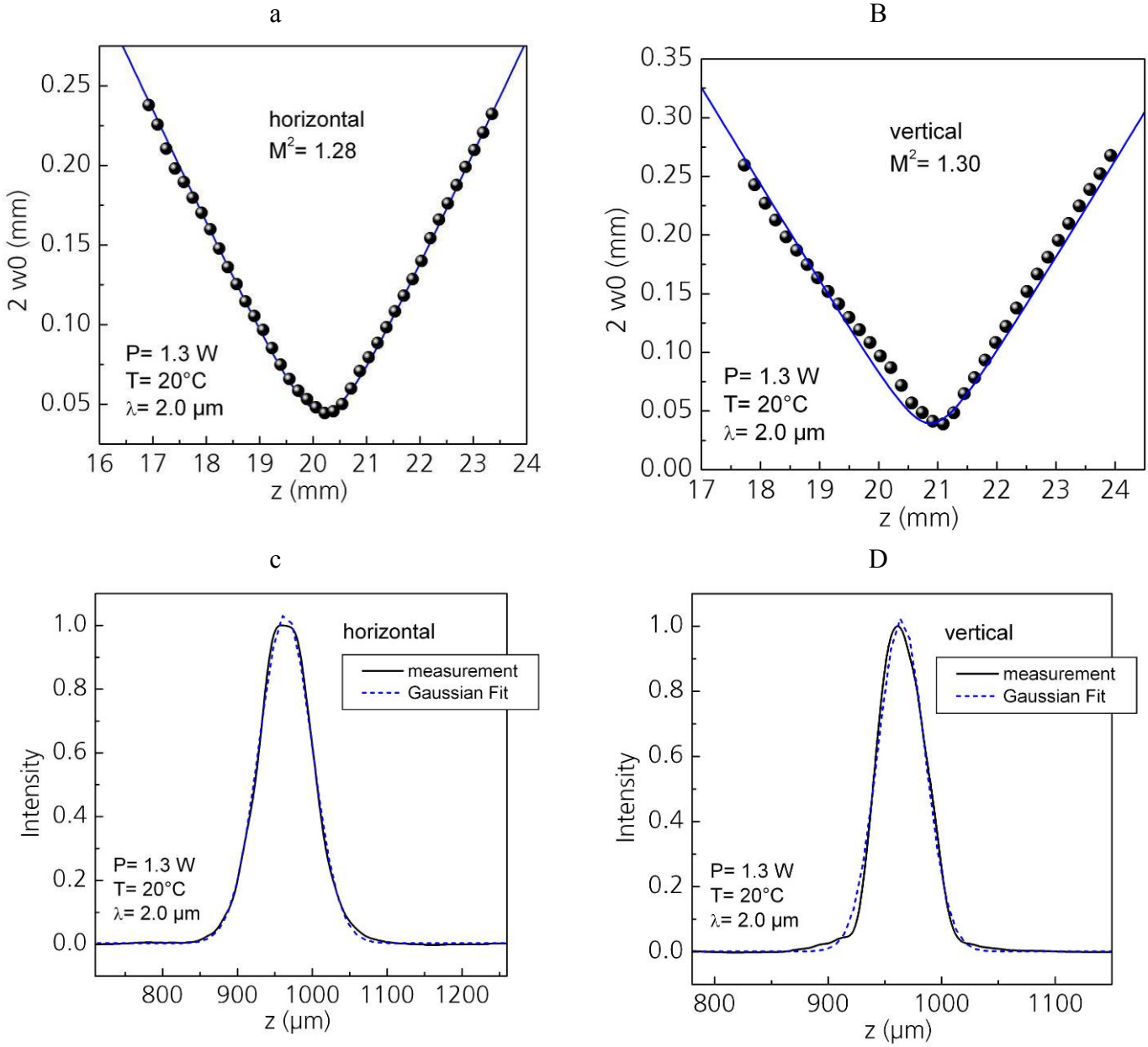

Fig. 3.42: Results of the beam quality measurements at 1.3W output power: The M2 values are well below 1.5 in both directions (1.28 horizontally, 1.30 vertically). Typical pictures of the beam profile are shown in c) and d) together with a Gaussian fit to the measured curve, revealing the very good agreement between the two.

Complete OPSDL laser system

The IAF has developed a complete laser system, based on the VERTIGO Basic Laser Module (Compact Engineering Module) and incorporates besides this 2.X µm OPSDL the fiber-coupled pump laser (commercial 980 nm diode laser, 10 W pump power), a red pilot laser and a monitor diode, all in a compact package with a 12.5 x 14 cm^2 footprint and a high of 5 cm (see Fig. 3.43 below)

This laser system was on display, actively running for three days at the VERTIGO project exhibition at the European ICT event in Lyon. No readjustment of the laser cavity or pump setup was necessary after the OPSDL system was moved from Freiburg to Lyon demonstrating the robustness of the developed setup. Additionally, this three day exhibit acted as a further lifetime/stress test of the OPSDL unit: The laser system described above was operated within a larger sealed box, for laser safety reasons, which was illuminated by four strong halogen lamps on the exhibit booth raising the temperature inside the box to values close to 40°C. Despite this, no change in laser performance was measured and no readjustment of the module was necessary throughout the whole exhibition.

With a SiC-bonded 2.25µm OPSDL chip inside, the module is delivering over 500mW of output power. This is limited by the rather small pump laser inside the module and not by the OPSDL chip itself. With new, compact 980nm pump laser module, it should be possible to realize laser systems with 1-2W output power in the same compact housing shown in Fig. 3.43.

Fig. 3.43: Hermetically sealed OPSDL laser system, including pump laser, monitor photodiode and red pilot laser.

1.4.5. WP4 Applications

VERTIGO Narrow Linewidth Module

Within the framework of WP4 LISA designed, constructed and characterized a Narrow Linewith Module (NLM) with OPS samples from the IAF and tested this module for seed applications. Taking into account the results achieved in WP2 and WP3 a v-shape resonator was chosen for the NLM. The OPS chip is mounted on the VERTIGO sub-mount and pumped at 976 nm with a fibre coupled laser diode. A schematic of the resonator and the pump set-up used in the NLM is shown in Fig. 4.1. For wavelength selection in the NLM a Volume Bragg Grating (VBG) is used. A VBG was chosen as this element can be used for wavelength selection and output coupling at the same time. In a standard 3-mirror configuration the OPS chip is placed roughly at the focal position of a curved cavity mirror ensuring a relatively collimated beam in the longer arm of the resonator and a tight intracavity focus on the chip. The pump optics utilized a collimating and focusing optic similar to that of the BLM providing a 1:1 image of the pump fibre facet at the OPS chip.

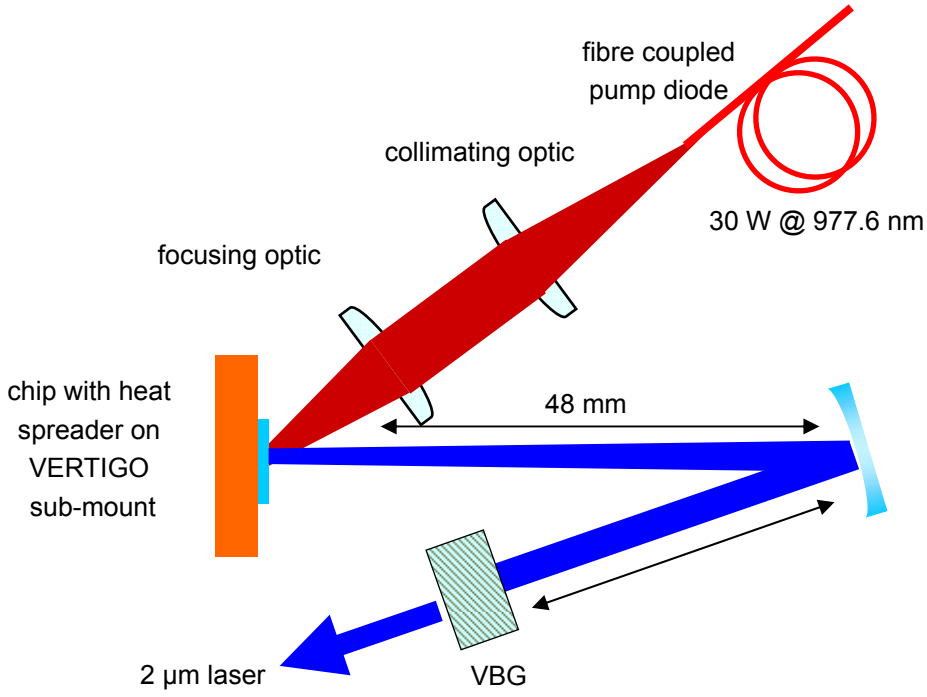

Fig. 4.1: Schematic set-up of the OPSDL resonator used in the Narrow Linewidth Module

To achieve optimal mechanical stability of the laser resonator, the resonator housing is machined from a single aluminium block – a standard technique for single-frequency lasers. The OPS chip is cooled with a TEC and external passive cooler assembly. The folding mirror and the VBG can be adjusted from outside the module with micrometer screws. A standard SMA connector is integrated in the wall of the housing to couple in the pump light. To keep the housing airtight all holes in the walls were sealed and an anti reflection coated window used to couple the 2 µm laser beam out of the housing.

This window is mounted under a small angle to avoid back reflections into the laser cavity. The total size of the NLM is 100 x 75 x 75 mm³ (without the passive cooler). This size was chosen to have a compact module which is still easy to build up and where some components can still be exchanged for experiments. For a future product the size of the NLM could be further reduced. A picture of a complete NLM is shown in Fig. 4.2.

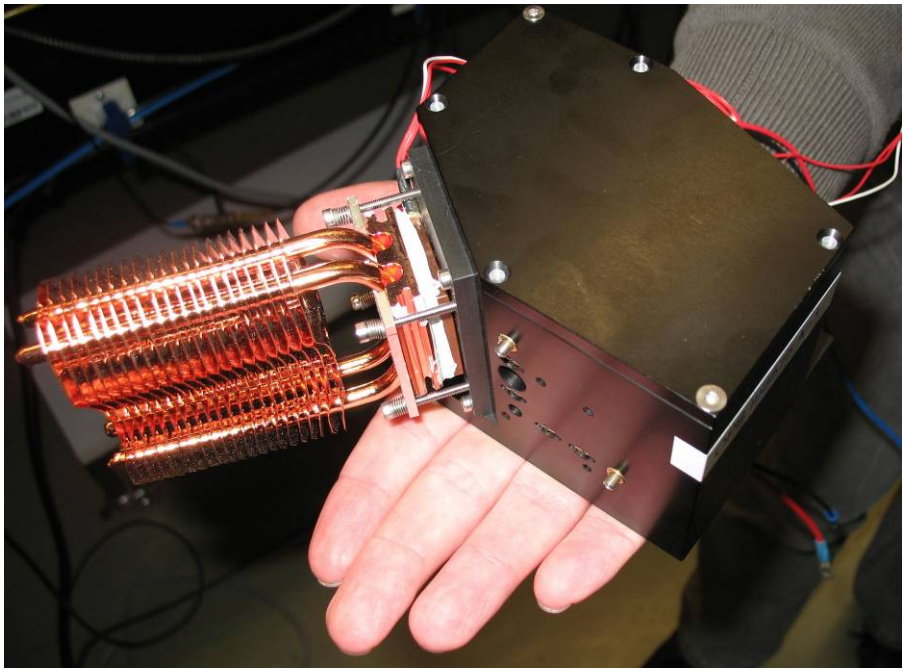

Fig. 4.2: NLM used for the linewidth measurements at the IAF with external passive cooler for the 'hot-side' of the OPS TEC.

During the project different NLMs with various VBGs and plane output coupling mirrors were realised. Fig. 4.3 shows typical output power transfer curves of a NLM with OPS sample (3575) with a SiC heatspreader. With a 2.2% transmitting plane output coupler a maximum cw output power at room temperature of 900 mW was achieved. The output power of the module is highly stable. The power fluctuations during continuous operation over several minutes are in the order of only 1 %. With OPS sample III3575 and VBGs designed for 2013 nm and 2021.3 nm about 350 mW of output power could be realised at both wavelengths. The lower maximum output power achieved compared to the plane output coupling mirrors results mainly from the lower VBG output coupling - in the order of 1 %. Therefore the slope efficiency for the laser operation with the VBG is only about 3.5 % with respect to the incident pump power and the overall efficiency is about 2.2 %. This is comparable to results achieved in the laboratory using a birefringent filter for wavelength selection.

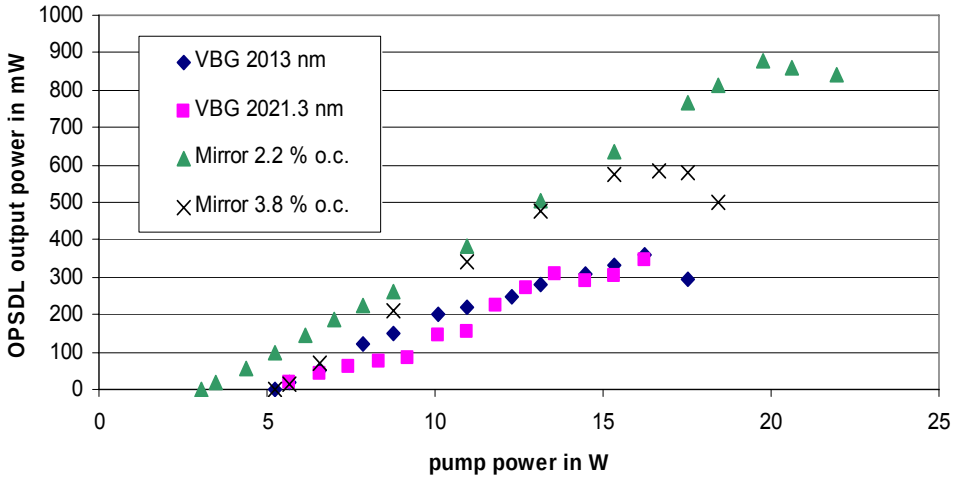

Fig. 4.3: NLM output curves for cw laser operation using OPS sample III3575 A-1 and plane output coupling mirrors or different VBGs as output couplers

The output of the OPSDL with the VBGs was measured to be single-longitudinal-mode up to an output power of about 250 mW at 2021.3 nm and up to 220 mW at 2013 nm. At higher output powers multi mode operation was observed. This multi mode operation results mainly from the low output coupling. When using VBGs with higher output coupling rates, even higher single-longitudinal-mode output powers should be achieveable. The multimode operation at high output powers also causes large output power variations. During single-mode operation the output power is stable. To prove the single-mode character of the NLM laser emission the emission spectra of the module were measured with a Fourier transform (FT) spectrometer and a scanning fabry-perot interferometer (SFPI). With the FT spectrometer it could be verified that the OPSDL operates at the design wavelength of the grating and with the SFPI the linewidth could be measured. The linewidth of the NLM was measured at the IAF was a commercial confocal SFPI with a free spectral range of 1 GHz and a finesse of about 400 in the 2 µm wavelength range. Output spectra of the NLM using the 2021.3 nm VBG for wavelength selection measured with this SFPI are shown in Fig. 4.4. The spectra were measured at 220 mW of NLM output power; the right side shows the free spectral range of the SFPI and the left side shows the laser mode in high resolution to measure the linewidth.

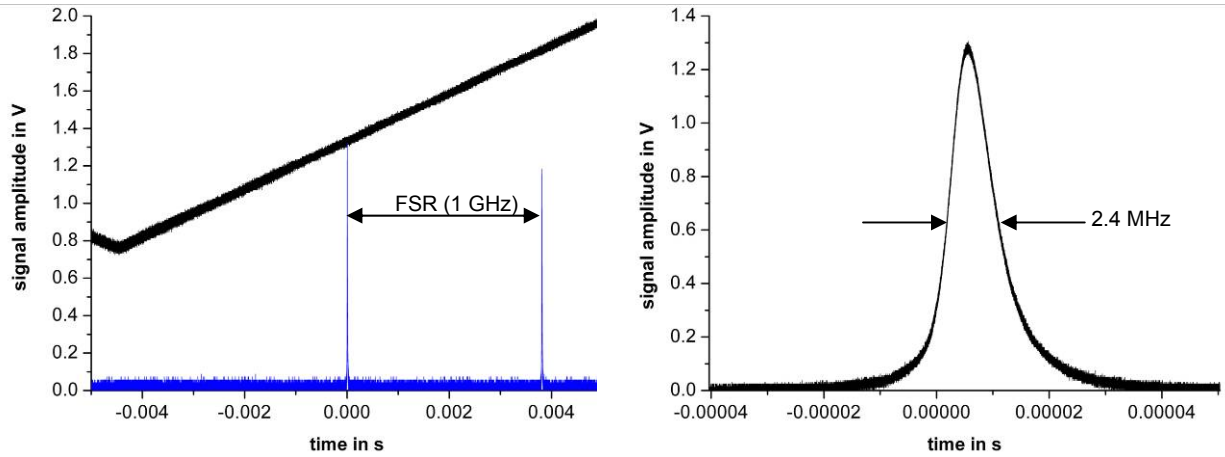

Fig. 4.4: Output spectrum of the NLM at 220 mW of output power measured with the SFPI. Right side full spectrum and left side zoom in.

The full linewidth of the laser emission measured at half maximum was 2.4 MHz for 220 mW of output power. This linewidth was also measured for other output powers. This is in the same region as

the calculated resolution of the SFPI. Taking into account the complex alignment of the SFPI and the adjustment of the laser beam path with respect to the SFPI axis it becomes apparent, that the measured linewidths were limited by the resolution of the SFPI. Therefore the actual laser linewidth can be even much smaller than the measured ones. The long term wavelength stability over several minutes of the NLM observed in the laboratory was clearly below 1 GHz when the module was operated at a fixed output power level. Thus the developed NLM and even exceeds all specifications made for the module.

Narrow linewidth 2µm OPSDL as seed source

During the project two different seed experiments were successfuly carried out at LISA, which demonstrate that the NLM can be used as seed source. The high output power of > 100 mW and the narrow linewidth make the NLM an ideal seed source for many high-power, narrow-line lasers. In the first experiment a Tm:YAG ring laser was seeded with the NLM. The ring laser could be operated either cw or q-switched, using an AOM. In the experiments the seed beam of the OPSDL was coupled into the ring resonator through the output coupling mirror. To protect the OPSDL from the ring laser beam an optical isolator was used between both resonators. With the laboratory set-up it could be demonstrated that the available seed power from the NLM is sufficient to seed the ring laser. 50 mW of seed power at 2021.3 nm were sufficient to achieve ring laser emission at this wavelength, where an atmospheric transmission window exists. Up to 3 W of seeded output power in cw operation were achieved at this wavelength and up to 2 mJ of pulse energy for a repetition rate of 500 Hz. So far without an active stabilization of the ring laser cavity seeding could only be observed for short terms.

In a second experiment a thulium fibre laser was seeded with the OPSDL. In this experiment an OPSDL with a birefringent filter for linewidth narrowing and tuning was used. The seed beam was coupled into a commercial multi-mode Tm-doped double clad fibre through the same optic as the pump beam (see Fig. 4.5). Due to the high-brightness OPSDL beam, by using an additional lens the seed beam could be coupled almost completely into the fibre core.

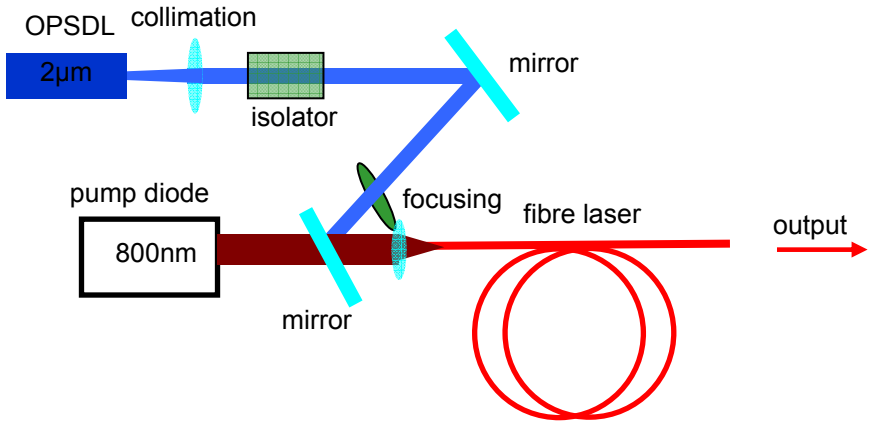

Fig. 4.5: Setup for the seed experiments with the thulium fibre laser

With about 30 mW of launched seed power into the fibre core an amplification of the seed power to 3 W could be achieved. The fibre amplifier adopted the wavelength and the linewidth of the OPSDL. An output spectrum of the fibre laser with and without seeding is shown in Fig. 4.6. The maximum amplification was limited due to parasitic laser operation that started at higher pump powers. This laser oscillation could be suppressed by changes in the fibre amplifier design, therefore much higher output powers should be achievable.

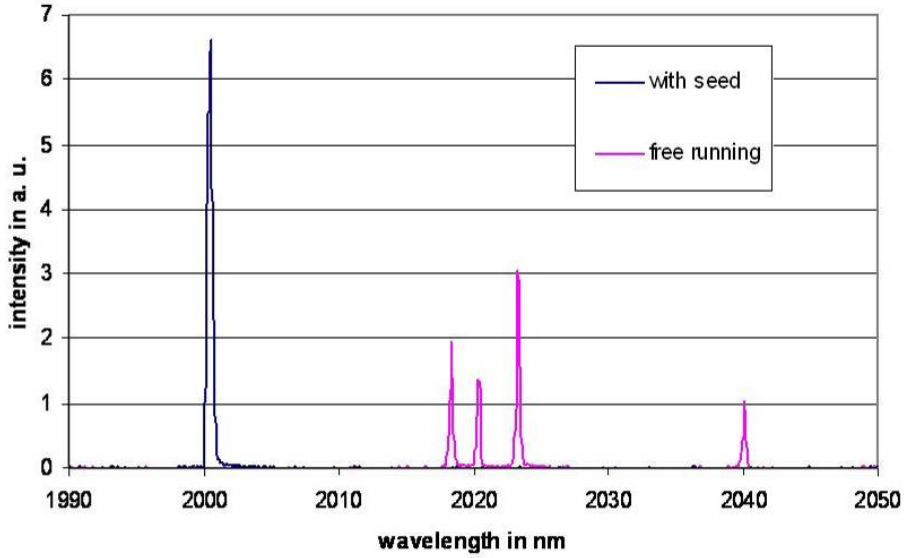

Fig. 4.6: Output spectra of the seeded and the free running thulium fibre laser

The 2 µm wavelength range is called "eye safe", since laser radiation of this wavelength is absorbed in the cornea and vitreous body of the eye and does not reach the retina. Therefore the threshold for untreatable eye damage is much higher than for shorter wavelengths. Laser systems that operate in the "eye safe" wavelength range have great market potential especially in free space applications where eye safety is very important. So these laser systems are ideal for the usage in LIDAR (Light Detection And Ranging) systems. The 2 µm laser systems are also of interest for medical applications. There are several aspects which make 2 µm lasers a promising candidate for highly precise surgical applications for both soft and hard tissue. The most important property is the high absorption in water combined with minimal penetration depth within human tissue. The second important aspect is the coagulation effect caused by the 2 µm laser radiation, which suppresses the bleeding during operations.

The strongest requirements for 2 µm laser system regarding special wavelength, linewidth, long term stability and output power have to be fulfilled for sensing applications. For medical applications the requirements are weaker. Especially for Doppler-LIDAR systems very narrow linewidths and high output powers are required. Most of these requirements could already be fulfilled by the NLM developed during this project and the successful seeding of two different potential high-power 2 µm laser sources was demonstrated.

Modulated OPSDL for free space optical communication (FSO)

As indicated previously, the FSO telecommunications market has declined considerably since the inception of the VERTIGO project concept. At the time, FSO was chosen as one of the two focus applications from among the many potential applications for a compact, high-power 2.Xµm laser source as the industry was still buoyant and enterprise level players such as CFS were confident that given the right technology FSO systems could be implemented at a network level. While there is still every confidence that the technology developed during the VERTIGO programme would go a long way to addressing the FSO source technology shortfalls that were present at the time, the metro communications market focus has moved entirely away from optical solutions to the 'last mile' problem and network level solutions. Most industry insiders currently agree that in the short to medium term there is little or no prospect in optical communications in the medium range 1-10km

markets. This is primarily and predominantly due to the very significant technological and cost advances in microwave and THz RF wireless technologies in the last four years, which have, to a large extent, negated the advantages once offered by optical systems over RF. Indeed, the major emphasis for FSO technology research and exploitation has diverged to very long range applications of data (and even power) transfer between satellites and between satellites and the earth and in the parallel free-space distribution of information on the very short range such as high speed optical wireless communications in an office environment or 'smart entertainment' systems in aircraft cabins. While VERTIGO technology could be used in both these fields to implement eye-safe laser transmission systems, both would require significant technology steps in terms of power scaling and miniaturisation respectively and therefore significant technical and financial investment. For many of the reasons that it was hoped would drive 2.Xμm FSO systems to the network infrastructure level, this technology however remains an attractive prospect for important niche markets such as covert communications where speed and range are not as crucial as guaranteed anonymity and message security. Despite the above argument, the various component tasks of the project that were focussed towards the modulation of 2.Xμm OPSDLs and the final demonstration of a free-space optical link were, and still remain very relevant for a variety of emerging and important applications and were therefore pursued with no less verve.

For the demonstration of high speed free-space optical (FSO) links as the second applications strand of the Vertigo project a number of potential methods of modulation for OPSDL devices were discussed. The decision was taken to investigate the use of intracavity electro-absorption modulators (EAMs). A design discussion document was drafted and distributed between partners. The resultant EAM design was grown at the IAF and processed at TL. An optical test rig was constructed to asses the modulation performance (extracavity) of the EAMs. Here the OPSDL output and co-incident pilot beam were reflected onto the surface of the modulator mounted in an XYZ jig. A pair of contact probes were used to supply a bias to the modulator structure while the assembly can be viewed by a microscope or camera from above.

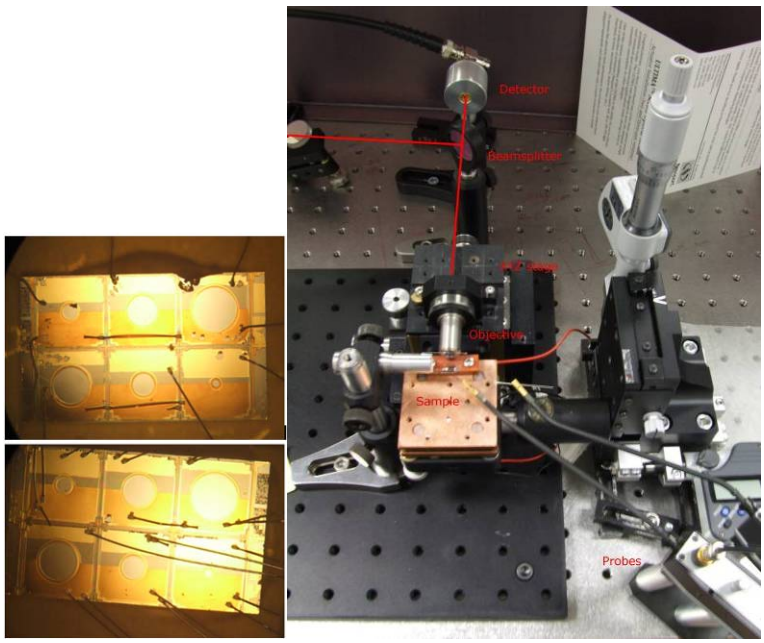

Fig. 4.7: Microscope images of the wire bonded modulator samples (left) and the optical test rig to investigate the modulation performance of the intracavity modulators

The first batch of EAM modulators were wire bonded to suitable chip mounts (figure 4.7-left) and the electrical characteristics tested. Unfortunately the tests revealed that all the modulator structures were electrically shorted. Further samples where processed but were not finalized by the end of the project.

Mach-Zehnder waveguide modulators

The major risk posed to the successful demonstration of an FSO link was the outcome of the modulation studies and EAM development strand so backup modulation strategy was also pursued. The high output beam qualities associated with OPSDL sources meant that the use of Mach-Zehnder (MZ), Lithium niobate ($LiNbO_3$), extracavity waveguide modulators represented the best alternative route to GHz modulation at 2.2µm. Photline technologies (www.photline.com) - a manufacturer of high speed 1-40GHz telecoms modulators - in Besancon, France, agreed to develop a MZ modulator at a minimal development cost. Initial waveguides were grown and tested using a setup as shown schematically in figure 4.8 and information fed back to Photline who were able to fabricate the M-Z modulator shown below in figure 4.10.

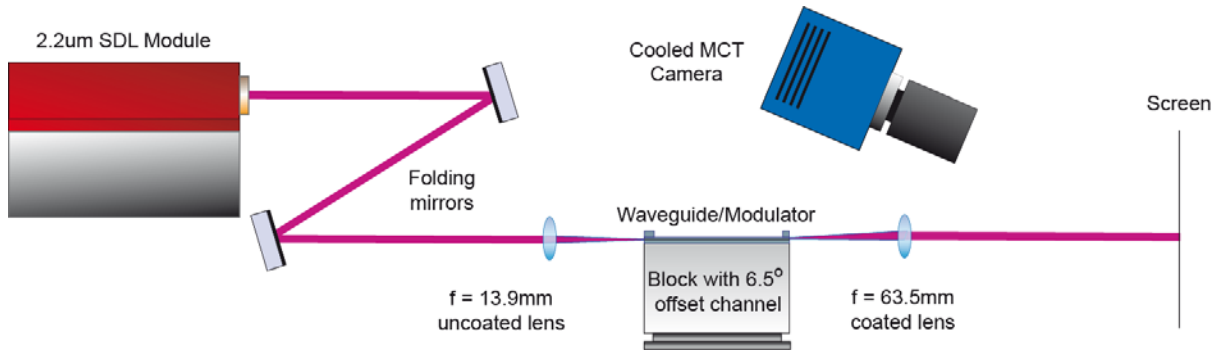

Fig. 4.8: Schematic of the waveguide assessment setup.

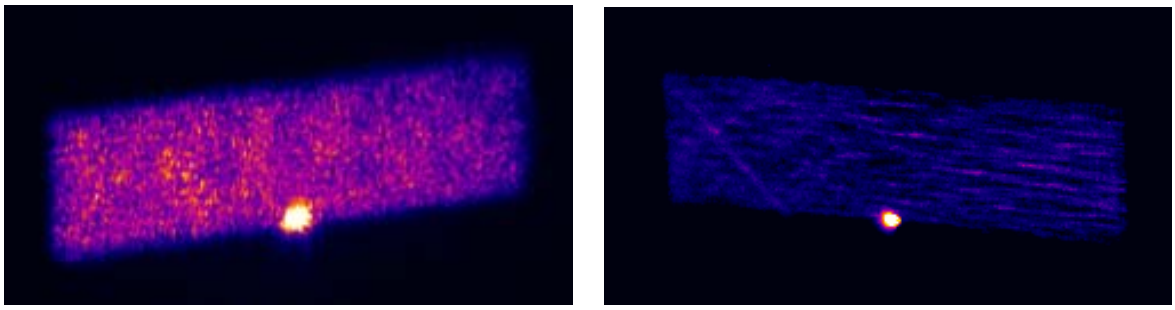

Fig. 4.9: Examples of the waveguide coupling showing light leaking into the slab modes.

The packaged Photline modulator (MZ-2.2-LN-01) arrived at the end of October 2009 and was immediately assessed in a similar manner to the waveguide samples shown above. Table 3 below shows the characteristic parameters and the factory test performance of the modulator when assessed with a 1.6µm telecoms laser source.

Fig. 4.10: Close-up of the modulator showing the bare guide ends – circled.

Vπ DC @ 100Hz @ 1660nm	7.9V
Vπ RF @ 50kHz @ 1660nm	3.4V
Electrical return loss 0.04-1GHz	-9.2 dB
Electro-optic bandwidth S21@-3dB from 0.04GHz	>1GHz
DC extinction ratio with PM in/out fibres @ 1660nm	– 27dB
Insertion loss with PM in/out fibres @ 1660nm	-4.1dB
Optical return loss	<-45dB

Table 3: Characteristic parameters and the factory test performance of the 2.2µm MZ modulator.

In order to asses the mid-IR performance of the modulator the test-bed shown schematically and photographically in figure 4.11 below was used. Here, due to the current lack of MCT Mid-IR camera at the IOP, a red pilot beam, co-linear with the 2.2µm light from the OPSDL, is used to perform rudimentary coupling into the waveguide using the image formed at the indicated aperture. This coupling is then enhanced by applying a lower frequency (1-40MHz) RF signal to the modulator and the modulated 2.2µm signal optimised via careful alignment of the lenses. This approach has been shown to be an effective and repeatable method of coupling for this modulator. Figure 4.12 shows a typical alignment signal from the modulator.

Initial experiments using a VIGO systems PVI-2TE-10.6[2] detector showed modulation up to ~200MHz which was limited by the bandwidth of an internal amplifier. Alternative detectors should permit the full bandwidth of the photline modulator to be demonstrated.

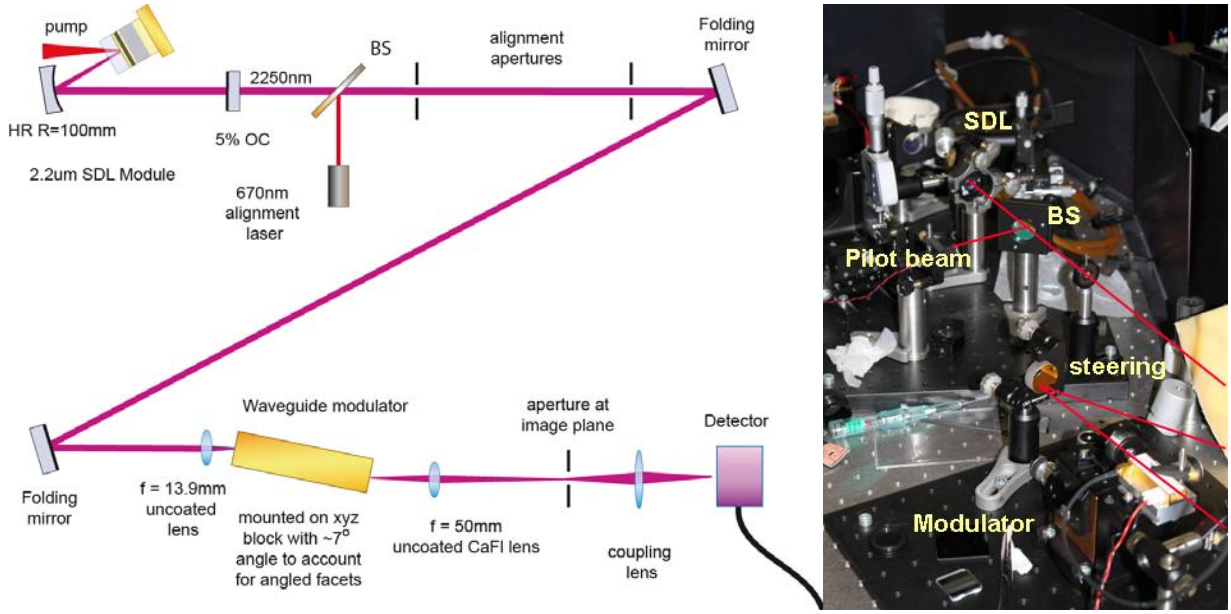

Fig. 4.11: Left: Schematic of the test setup for the MZ waveguide modulator showing the alignment laser and beamsplitter (BS) used to locate the waveguide. Right: Lab setup of the modulator test rig at the IOP.

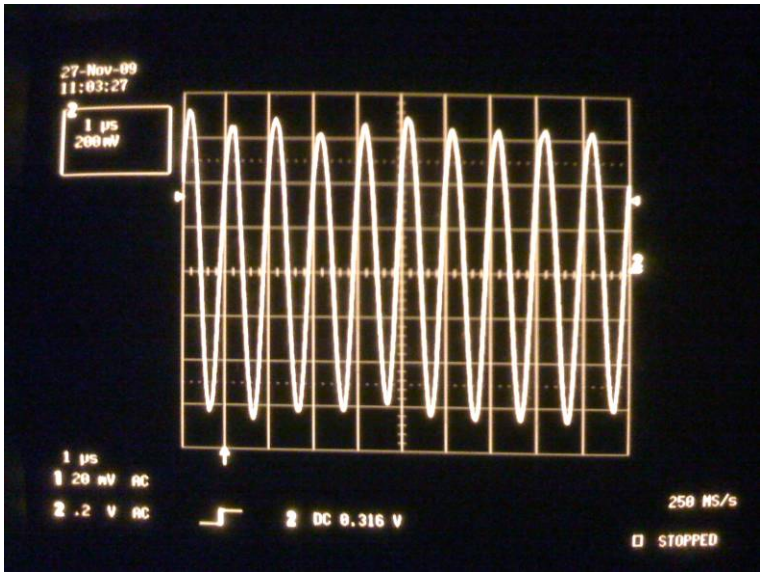

Fig. 4.12 Example of a lower frequency (~1MHz) modulation signal used to align the waveguide modulator.

Modulated Laser Module development

Given the successful modulation (albeit less than 1GHz) the modulated laser module (MLM) for the FSO demonstration task shown schematically in figure 4.13-top was constructed. Figure 4.13-bottom below shows the module on the bench out of its housing. Here the basic laser module (BLM) and pump unit (Lumics 10W 980nm laser) were mounted on a single cooled block which could be liquid or air cooled. This module used a simple optical system to couple light into the waveguide modulator as

the output from the BLM was allowed to freely propagate from the output coupler diverging to fill a single f=13.6mm aspheric coupling optic (shown in the centre of fig. 4.13).

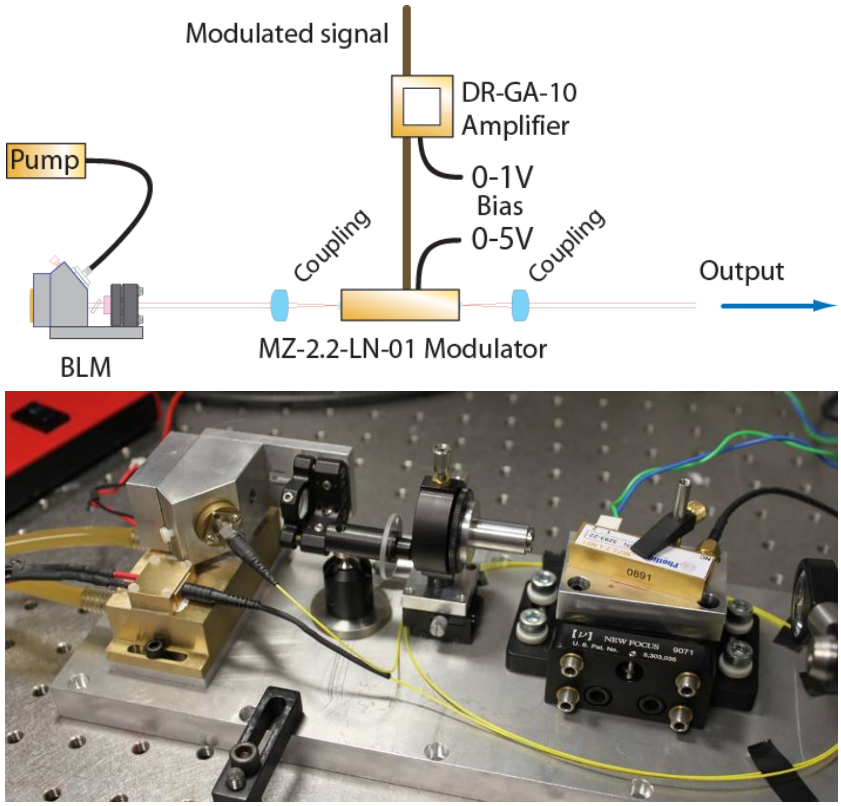

Fig. 4.13: Top: Schematic of the 2.2µm modulated laser module, Bottom: Photographs of the 2.2µm modulated laser module layout showing the BLM coupling optics, amplifier and mounted modulator with ~7° offset angle.

The output from the MLM was collected using a simple telescope arrangement and allowed to propagate along the bench to a detector. A free-space signal transmission link was demonstrated at 15Mb/s and previously longer links at 200Mb/s were realised. When faster more sensetive detectors are aquired longer links up to 1.25Gb/s with the full transmit electronics described below (PECL signal and Gb ethernet switch) will be demonstrated as there is no inherent bandwidth limit below this in the module architecture.

OPSDL based test setup for free-space optical communication

The requirements of the optical modulation required and the format of a transmitter test rig were discussed in detail with CFS. For the purposes of an FSO demonstration the idle signal from an Ethernet switch was used. This was converted to an appropriate RF drive signal for the modulator using custom electronics and then amplified and supplied to modulator (see figure 4.14).

Cablefree supplied the IOP with a standard A1000 FSO housing unit (see figure 4.15) for future demonstration development. The housing was customised by adding an in-house baseplate to act as a breadboard for the optical components shown schematically in figure 4.15 below.

The delay in delivery and subsequent delay in modulation testing until the project end meant there was a delay in the commencement of the modulated module development and FSO demonstration activities

however, this work will be very relevant to some of the long range sensing activities planned to be investigated by the project partners.

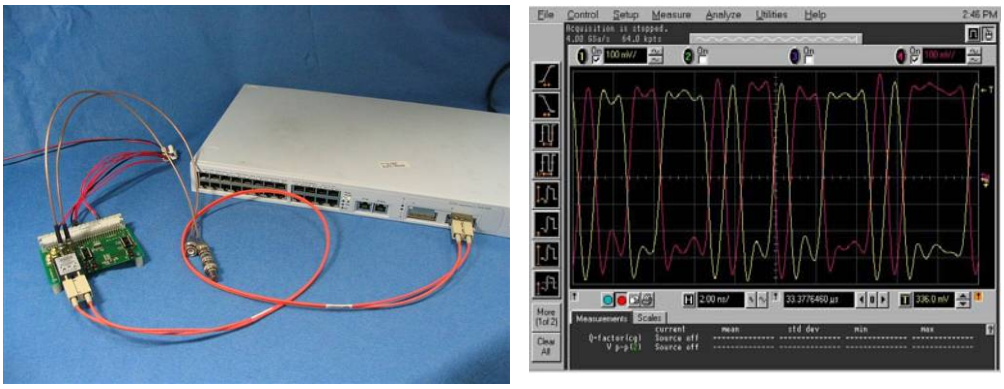

Figure 4.14: Photograph of the 3C17304 Superstack3 4228|G Ethernet switch and Cablefree Gb GIGAFBRM ISS.A Ethernet board incorporating a Finisar V23826-K305-C63 850nm, 1.25Gbps Fibre transceiver unit (left), oscilloscope trace of the 1.25Gbps differential PECL idle signal from the Ethernet switch (right).

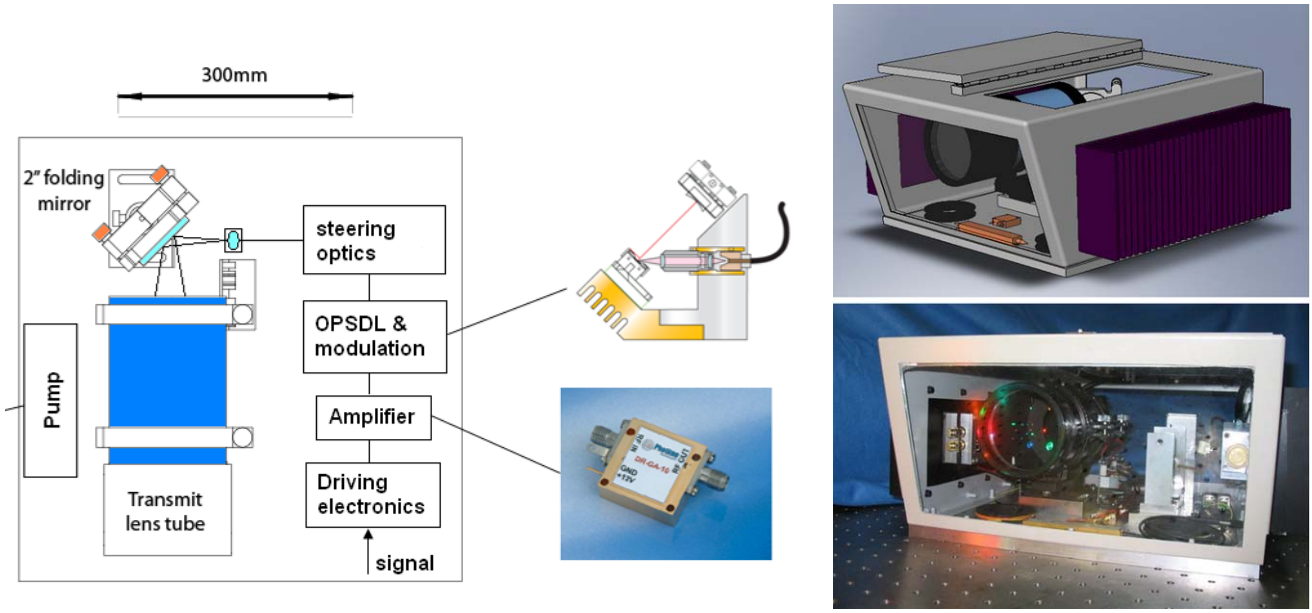

Figure 4.15: Block diagram of the electro-optic setup of the FSO demonstrator (left) and visualization and photograph of the test set up mounted in the FSO housing (right).

Solid-state laser pumping

An area that has become a significant and interesting area of study during the course of the VERTIGO programme has been the use of OPSDLs to pump further crystalline solid-state laser stages. This work has been possible due to the concurrent study of mid-IR solid-state lasers at the IOP and due to the

unprecedented power levels achieved within the project to date. Figure 4.16 below shows a good number of solid-state crystalline gain materials in the 1-8µm wavelength region in which laser action has been observed in either pulsed or cw mode. While some of these offer many interesting and significant laser material and output properties such as high gain (>50% efficiency), durability, wide wavelength coverage (supporting µm's of tunability and fs pulses) and high energy storage, exploitation of these materials is often hampered by lack of appropriate pump lasers. Available pump lasers are often very expensive (Tm/Ho fibre lasers), of poor beam quality (broad area long wavelength diode lasers) or unstable and prone to noise or feedback instabilities (Tm-based solid-state lasers). The multiwatt output powers observed from the Sb-based OPSDLs developed in VERTIGO, has permitted the prospects of low-cost, compact and efficient pumping of these materials. The high brightness of these sources can be used to promote low threshold laser performance from the mid-IR materials and allow resonator design flexibility. The properties of each laser system can be used to compliment each other for example the very short carrier lifetime of the OPSDL may be used to provide a low-noise, feedback-insensitive pump source while the long upper-state lifetimes and fine energy-band structure of the solid-state materials (Cr^{2+}:ZnSe for example) may be used to provide energy storage and large wavelength flexibility (1.9-3.3µm) traditionally difficult for an OPSDL to achieve on its own. Another significant advantage of the OPSDL format over many of the other pump laser formats is that the OPSDL is wavelength flexible or engineerable, allowing the precise control and therefore absorption optimisation of the pump wavelength.

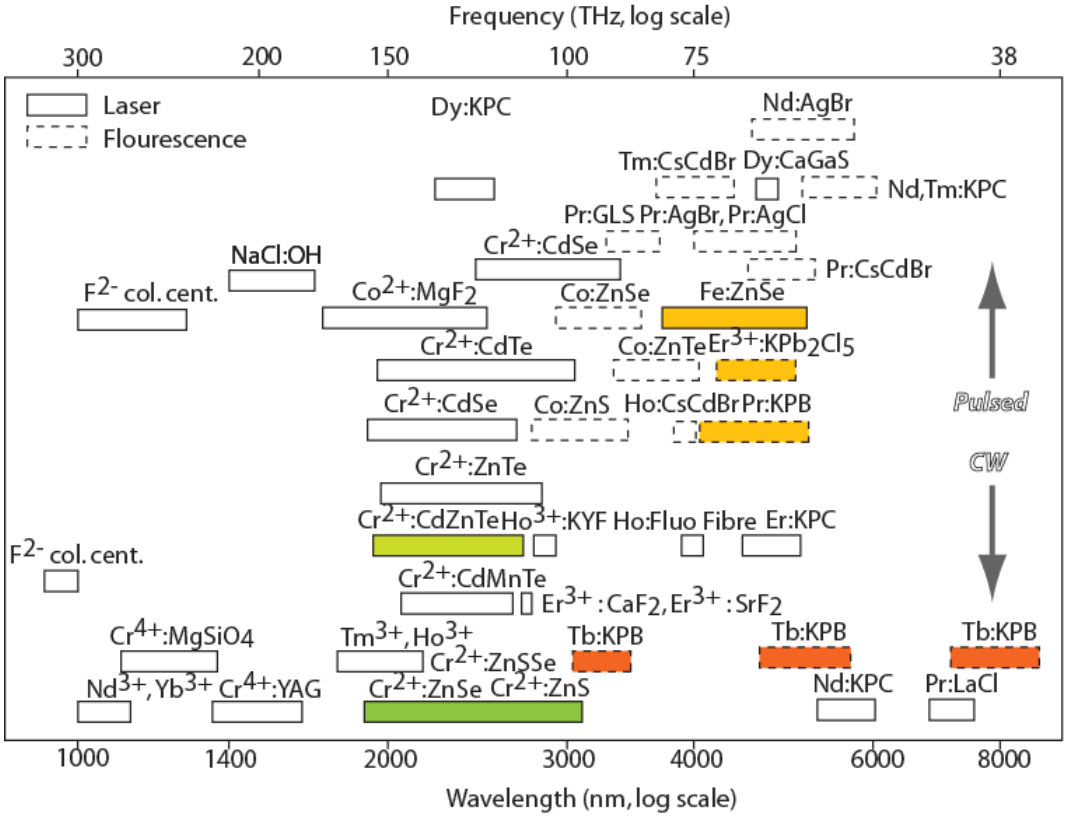

Fig. 4.16: Graphical representation of the tuning range in laser oscillation and fluorescence in pulsed and cw operation of a wide variety of near-IR and mid-IR optical gain materials.

In order to investigate many aspects of the OPSDL pumping of solid-state laser materials, a number of different resonators and materials (namely Cr^{2+}:ZnSe and Cr^{2+} doped CZT) were tried with the 1.9 and

2.0µm OPSDLs under the umbrella of the VERTIGO advanced concepts work. The highlights of this work are now detailed below.

Figure 4.17 below shows the typical layout for the OPSDL pumping work, where the OPSDL output was typically focussed into a 3-mirror 'V' cavity or 4-mirror 'Z-fold' resonator, constructed around a short Cr^{2+}:ZnSe crystal. No optical isolation was required between the pump and laser, showing the robustness of the OPS gain medium, however, often a simple Brewster-angled quartz plate was included in the OPSDL to remove any polarisation instabilities that could be induced by feedback. The noise of the overall laser system was measured showing very low noise <0.14% RMS [0.1Hz – 100MHz] operation for an unstabilised laser. Figure 4.18 shows some typical output power characteristics for different arrangements, each showing high slope efficiencies (up to ~50%) and moderate power (1-2W) operation of the solid-state laser. In order to investigate the tuning behaviour of these lasers, a single prism would be included in one of the resonator arms and tuning affected by changing the angle of the end–mirror in the plane of the prism (horizontal or tangential plane). In this manner cavity mirror limited tuning of around 300nm was typically possible for these materials (~2250 to 2550nm is shown in figure 4.18 inset below for a 2µm OPSDL-pumped Cr:ZnSe laser).

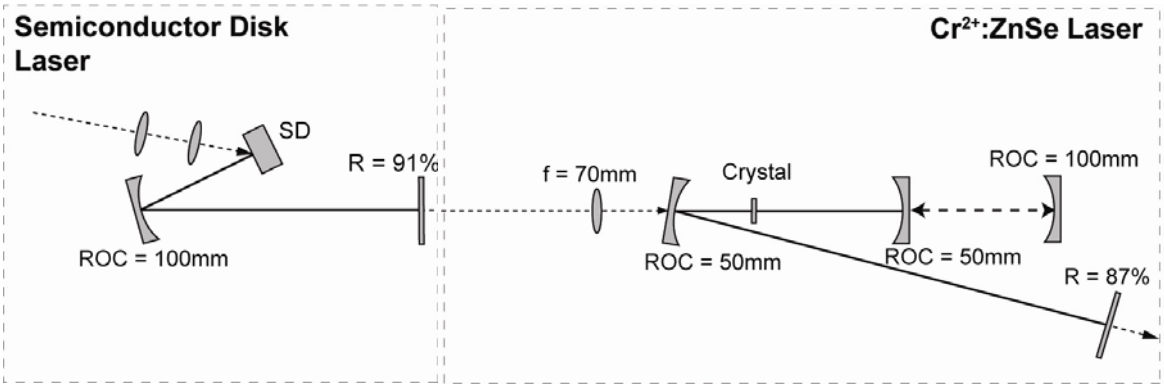

Figure 4.17: Schematic of the typicall resonator arrangement used to asses OPSDL pumping of mid-IR laser materials. The output from the high-power 2.02µm or 1.9 µm OPSDL was focussed into the doped dielectric gain media in a 3-mirror cavity, often due to the non-optimised lengths of the crystals some pump retro-reflection was used to increase efficiency.

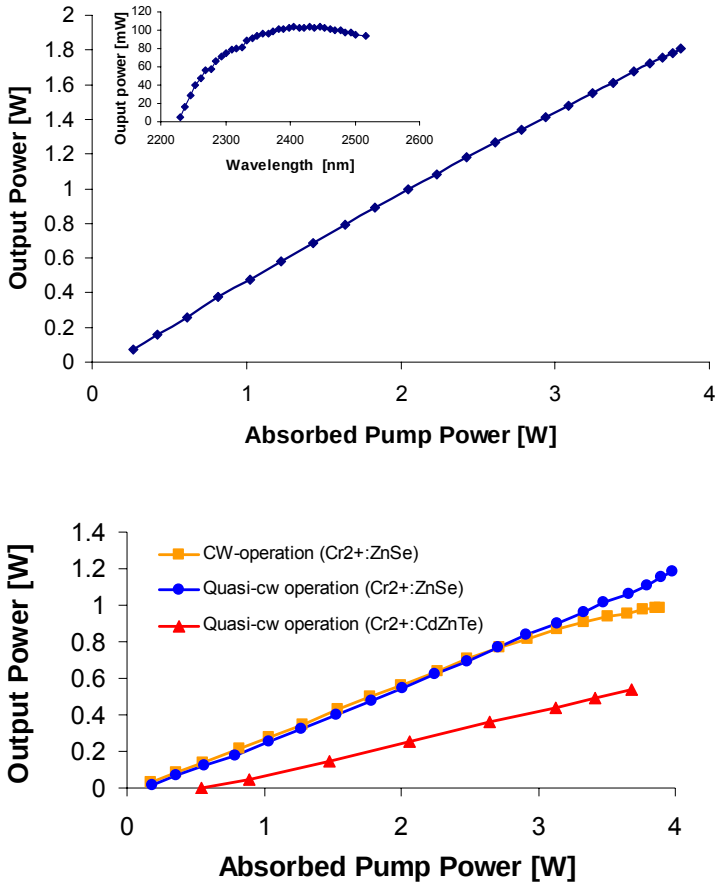

Figure 4.18: Top: Pump-power-limited output power transfer characteristic of an OPSDL pumped Cr:ZnSe laser showing over 1.8W output and a mirror-limited tuning range of 300nm (inset). Bottom: output power transfer characteristic of CW and Quasi CW operation of a Cr:ZnSe and Cr:CZT pumped in a similar manner.

In a further experiment, a second OPSDL sample was placed as the end-mirror of the Cr:ZnSe laser resonator and the OPSDL pumped by a second 980nm fibre-coupled pump diode (see figure 4.19 below). In this arrangement the OPSDL acted as an intracavity saturable absorber mirror that could dynamically effect the output performance of the laser and whose response could be tuned either by temperature or by optical pumping.

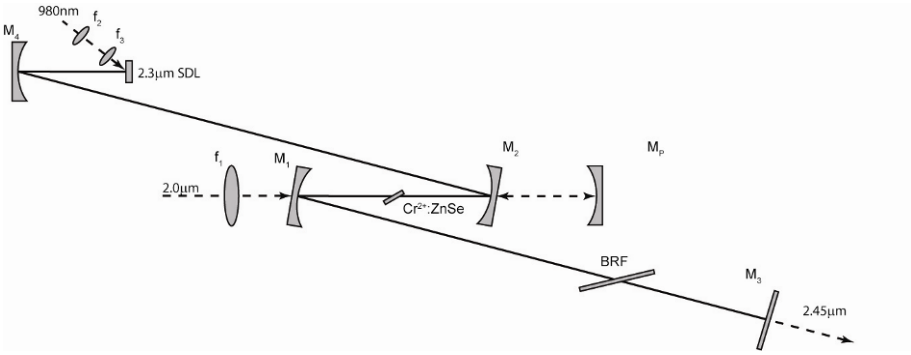

Fig. 4.19: Schematic of the Cr:ZnSe laser with intracavity 2.3µm OPSDL pumped with a 25W, 100µm fibre-coupled laser and mounted on a TEC for temperature

tuning.

The laser was tuned to 2.3µm using the BRF plate promoting q-switched operation with 90ns pulses at 1MHz repetition rate. Averaging consecutive pulses 4000 times revealed pulse to pulse jitter ~120ns (see figure 4.20)

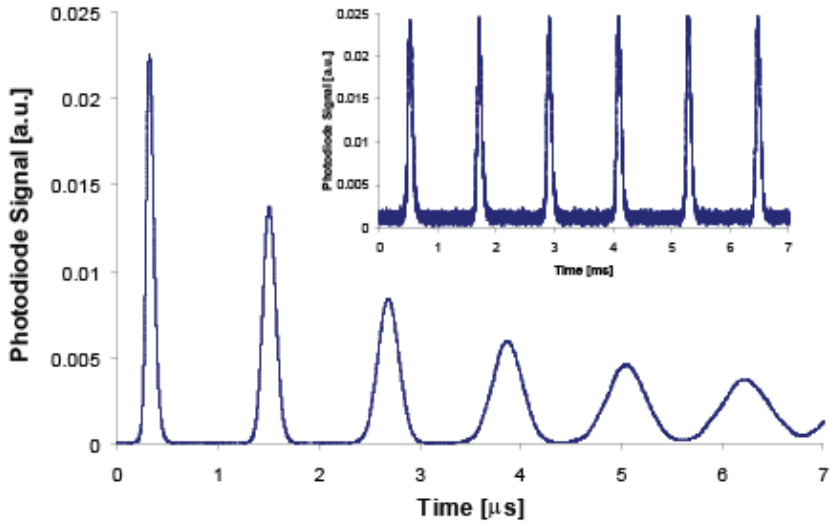

Fig. 4.20: Inset: Output of the Q-switched Cr:ZnSe laser and the time averaged results (main) showing the effect of pulse timing jitter repetition rate ~1MHz, average output power of ~500mW.

By either varying the temperature of the intra-cavity OPSDL to shift the absorption band of the quantum wells or by varying the incident pump power on the 2nd chip the q-switching could be switched on or off in the order of ~0.05ms (figure 4.21). In this way, the same semiconductor disk laser structure was used to concurrently pump and control the temporal behaviour of the laser.

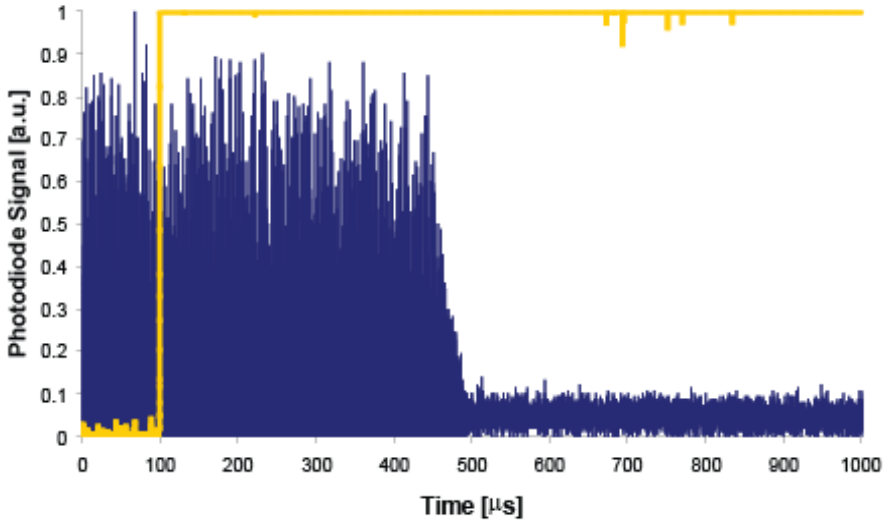

Fig. 4.21: Switching of the laser behaviour from q-switched to cw (left to right) using

optical pumping of the intracavity OPSDL.

Finally, to investigate the limits of flexibility, compactness and cost effectiveness the two strands of pulse pumping and solid-state laser pumping outlined above were combined in a number of pulse-pumped OPSDL-pumped Cr:ZnSe lasers. The fibre-coupled pulse-pumped OPSDL setup described in the section above was used to pump a Cr^{2+}:ZnSe laser in the setup shown schematically in figure 4.22 below.

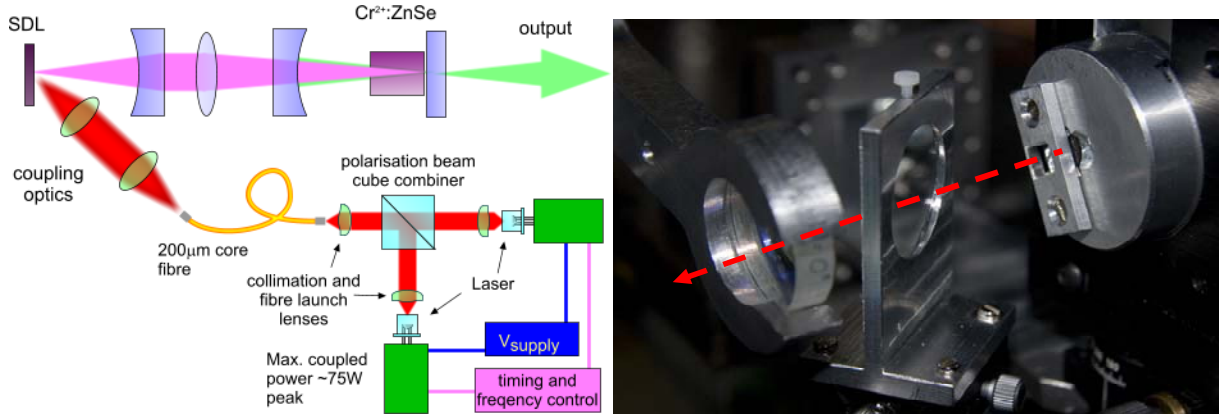

Fig. 4.22: left: Schematic of the compact pulse-pumped Cr2+:ZnSe laser: 905nm pump set up - 2x 75W polarisation combined and fibre coupled diodes, 180ns pulses at 10kHz (65W out of fibre) focussed using two f=11mm aspheric lenses onto 1.9/2um OPSDL resonator with an R = 96% 50mm ROC output -coupling mirror focussed using a f=50mm CaFl lens onto the 3mm thick Cr2+:ZnSe in a near-hemispherical resonator consisting of HR plane mirror and an R = 92%, 50mm ROC output coupler – an optional 1mm thick quartz BRF was employed for tuning. Right: Photograph of the Cr:ZnSe laser stage showing the short resonator with IC BRF tuning element.

Here, a very simple linear resonator arrangement (details below figure) was used for the Cr:ZnSe laser was used to reduce the threshold and crucially, the cavity lifetime to enable oscillation. The temporal behaviour of the pump, OPSDL and the Cr:ZnSe laser outputs were measured on a fast photodiode. As shown in figure 4.23, the OPSDL output pulse mirrors the pump pulse due to the short carrier lifetime, with duration of 160ns and a turn on delay of 50ns. The Cr:ZnSe laser responds with a typical gain switched pulse response (due to the long upper state lifetime in the order of μs), with an output pulse duration of ~21ns and a 145ns turn on delay (due to the cavity lifetime). The recorded pulse energy from the Cr:ZnSe laser was ~200nJ.

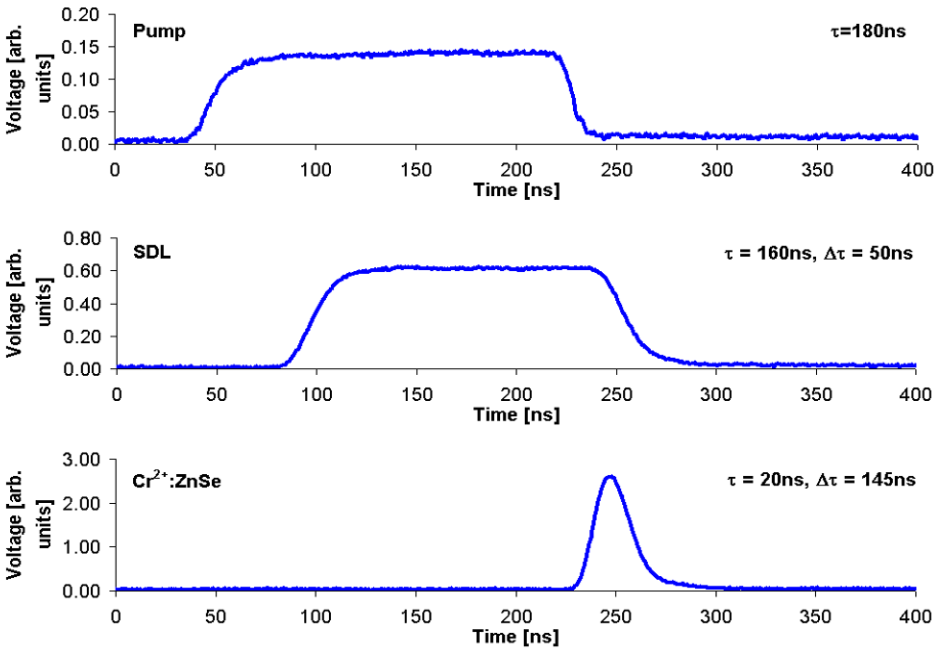

Fig. 4.23: Output of the pump (top), OPSDL (middle) and the Cr:ZnSe (bottom) laser referenced to the pump pulse.

The Cr2+:ZnSe laser delivered up to 9.5W peak power which in a 21ns pulse at a repetition frequency of 10kHz corresponds to a 200nJ pulse energy (see figure 4.24 below). The pulsed-pumped output was tuned over 80nm with a BRF shown in the inset below.

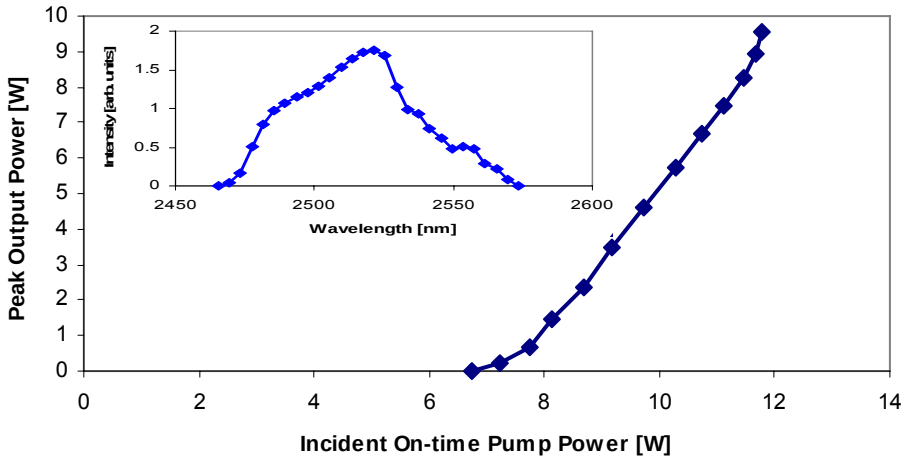

Fig. 4.24: Output power performance and BRF tuning (inset) of the pulse-pumped Cr^{2+}:ZnSe laser.

1.5.Project Logo

1.6.Project Website

Information about the project and the achievements can be found on the project website at
http://www.2micron-laser.eu

Newsletters about the project achievements and information about the VERTIGO OEM laser modules can be found at the News & Events section of the homepage:
http://www.2micron-laser.eu/area-public/news-events.htm

2. Dissemination and use

2.1.Section 1 – Exploitable knowledge and its use

Exploitation knowledge (description)	**Exploitable product(s) or measure(s)**	**Sector(s)** of application	Timetable for commercial use	Patents or other IPR protection	**Owner** and Other partners involved
Epitaxy of high-quality GaSb-based OPSDL structures for the 2.0 – 2.8 µm wavelength range	high-power 2.Xµm OPSDL	communication, sensing, medical applications, research	intermediate	in progress	IAF
bonding of SiC intracavity heatspreaders to the OPSDL chips	high-power 2.Xµm OPSDL	communication, sensing, medical applications, research	intermediate	propriety process know-how	IAF
bonding of diamond intracavity heatspreaders to the OPSDL chips	high-power 2.Xµm OPSDL	communication, sensing, medical applications, research	intermediate	propriety process know-how	IOP
Use of heatspreader to have second function	General to all SDLs	communication, sensing, medical applications, research	intermediate	patent application	IOP
Pulsed pumped SDLs	New sensor lasers and for material diagnostics	sensing, applications, research	intermediate		IOP
Development of experimental setup for thermal characterization of OPSDL lasers	high-power OPSDL	applications, research	intermediate	propriety process know-how	IET
Experimental	high-power	applications,	intermediate	propriety	IET

temperature determination of OPSDL lasers	OPSDL	research		process know-how	
Wavelength stabilization and narrowing with VBG	Single frequency 2.x µm laser	communication, sensing, medical applications, research	Soon	propriety process know-how	LISA
Seeding of thulium doped fibres	high-power narrow linewidth 2.x µm sources	medical, sensing applications	intermediate	propriety process know-how	LISA
SiC heatspreader fabrication	specific heatspreader	SC laser	Immediate	Process know how	TL
GaSb substrate removing	Laser fabrication	SC laser manufacture	Intermediate	Process know how	TL

Exploitable knowledge

Robust and flexible source technology – VERTIGO laser modules

The VERTIGO programme has generated the next generation of high-power, high-brightness, eye-safe, 2.Xµm laser sources with many modes of operation and application.

In addition to world leading power and tuning performances, single-frequency operation and modulated outputs of up to 200MHz, as well as compact, high-power pulsed OPSDL embodiments have also been realised with direct relevance to many applications areas. All this has been achieved using potentially low-cost components due to the flexibility of the OPSDL format. Within the project programme, engineering prototypes were developed in a robust, modular and reconfigurable geometry leading to commercial prototypes which will permit new approaches to address important existing and emerging challenges in areas such as:

- Airport sensing and security
- Resource assessment and management in the renewable energy industry
- Sensitive detection for environmental monitoring at range for applications health and security

The Basic laser module (BLM) represents the simplest form of engineered OEM OPSDL in a robust and modular unit applicable to a wide variety of resonator configurations and housings. The IAF have demonstrated the 2nd stage engineering BLM in a compact housing with a number of incorporated diagnostic and alignment features (Fig. 5.1)

Consortium partner LISA laser OHG designed and constructed a compact, Narrow Linewidth Module (NLM, see Fig. 5.2) which provides a very high mechanical and thermal stability of the laser resonator and the pump optics. The NLM can deliver over 200 mW of single-longitudinal-mode laser power at room temperature when using a Volume Bragg Grating (VBG) as output coupler and wavelength selective element. The linewidth of the single-mode NLM was measured to be below < 2.4 MHz, which was the resolution limit of the available Scanning Fabry-Perot Interferometer. This laser module is ideally suited as master oscillator or seed laser for sensing applications (e.g. LIDAR).

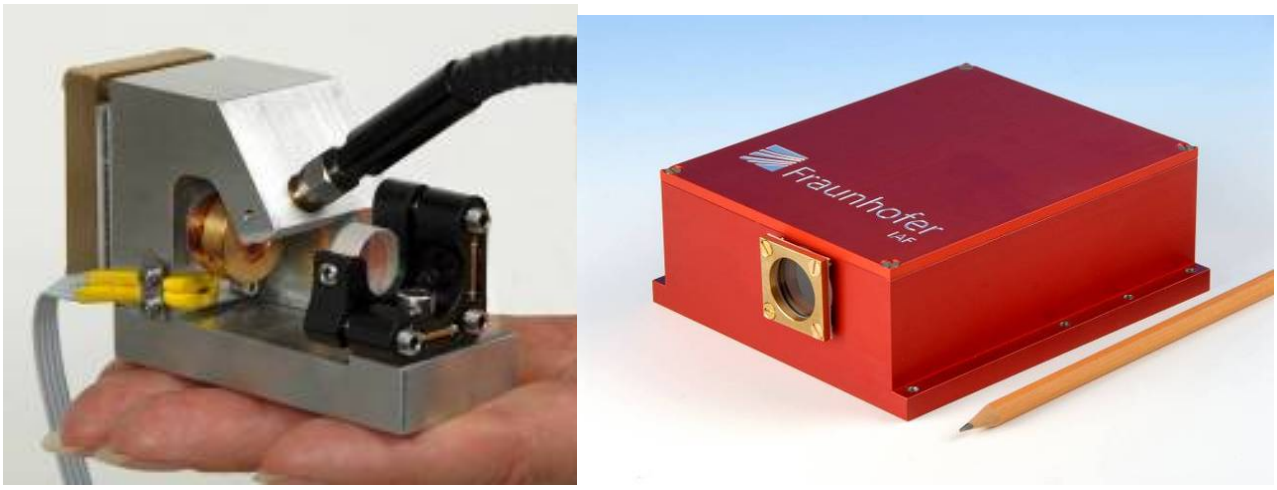

Fig. 5.1: Top: Basic laser module (BLM) – engineering version, bottom: housed engineering BLM

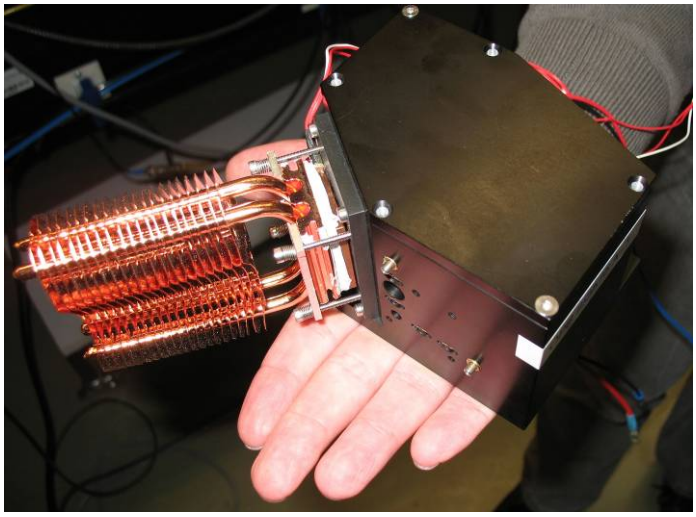

Fig. 5.2: NLM used for the linewidth measurements at the IAF with heat sink for the OPS TEC cooler

Pulse- pumped laser modules novel and low-cost high-power laser source

The ability to produce up to 20W on-time power in a highly compact and low-cost package is a significant step to unlocking further applications potential of the VERTIGO 2.Xµm technology. This format has received considerable interest

Pump for low cost tunable systems

The cw and pulsed-pumped 2.Xµm OPSDLs have unique properties which make them ideal sources with which to pump 2nd stage solid-state lasers. This in itself is a highly exploitable technology

Swept Wavelength sensors for remote spectroscopy

By exploiting the thermal properties of the pulsed-pumped 2.Xμm OPSDLs a constantly sweeping mid-IR source could be realised which could be employed in a number of scanning spectroscopy and metrology applications at range due to the favourable beam quality of the OPSDL and also with a considerable cost advantage over existing technologies.

Intracavity pumping of lasers and OPOs to allow compact, efficient, tunable sources further into the mid-IR for many applications

The placing of solid-state laser gain media and non-linear parametric generation crystals within the OPSDL resonator has been recently shown by the IOP to further enhance the potential performance and has a number of advantages for the generation of longer wavelengths especially when coupled with materials whose spectroscopic, optical and thermo-mechanical properties are not optimised for efficient output.

External Mach-Zhender waveguide modulator technology

One of the other areas of exploitable technology to emerge from the programme is the development of mid-IR MZ waveguide modulators through the company Photline Technologies. While this was viewed as a backup technology to the IC semiconductor modulators it was hoped would be developed within the consortium the enquiries that were made to Photline about developing this telecoms technology have provoked them to investigate this area and use it in recent technology announcements/advertising as well as develop a test modulator for the VERTIGO project. It is clear that within this 3rd party with extensive knowledge of the relevant markets this is viewed as a valid technology for exploitation.

Temperature mapping of OPSDL lasers

The method to measure temperature distribution on the surface of OPSDL chips and working lasers, based on thermoreflectance, has been developed. The measurement technique provides temperature distribution map with high spatial and temperature resolution. The method can be used for OPSDLs as well as for solid-state disk lasers. The experimental setup was developed and tested with various project samples.

Application areas and exploitation routes

At the outset of the VERTIGO programme it was stated clearly that there were many and varied applications for stable and versatile 2.Xμm OPSDL technology, in fact the 2-3μm region has been described by many as ‘applications rich’ and ‘source poor’. The two applications areas of FSO and wind-LIDAR that were chosen were viewed as demonstrator areas for the technology with the most interest and immediate routes to real-world deployment. As VERTIGO developed the consortium partners have become more aware of the shortcomings of the FSO industry as a whole, and which of the other sectors are currently most promising. During the course of the VERTIGO programme a large number of further opportunities have emerged with potential commercial interest.

The VERTIGO technology forms the potential basis for a solid, economic sensor laser technology able to set new standards in the local and global monitoring of the environment, industrial process, airport and aircraft safety and renewable wind energy production. Also, augmented VERTIGO OPSDL technology may be employed in the security sectors - in the detection of chemical and IEDs and in covert communications amongst others. These sectors are addressable either by directly adapting the

lasers to these roles or by using the OPSDLs as a stable pump or seed platform for secondary stage laser systems where the attractive and unique properties developed may be used to their full potential.

Fig. 5.3: A collection of illustrations depicting the many applications and potential applications areas addressed by VERTIGO 2.Xμm OPSDL technology.

FSO

As indicated previously the FSO telecommunications market has declined considerably since the inception of the VERTIGO project concept. At the time FSO was chosen as one of the two focus applications from among the many potential applications for a compact high-power 2.Xμm laser source as the industry was still buoyant and enterprise level players such as CFS were confident that given the right technology FSO systems could be implemented at a network level. While there is still every confidence that the technology developed during the VERTIGO programme would go a long way to addressing the FSO source technology shortfalls that were present at the time the metro communications market focus has moved entirely away from optical solutions to the 'last mile' problem and network level solutions. Most industry insiders currently agree that in the short to medium term there is little or no prospect in optical communications in the medium range 1-10km markets. This is primarily and predominantly due to the very significant technological and cost advances in microwave and THz RF wireless technologies in the last four years which have to a large

extent negated the advantages once offered by optical systems over RF. Indeed, the major emphasis for FSO technology research and exploitation has diverged to very long range applications of data (and even power) transfer between satellites and between satellites and the earth and in the parallel free-space distribution of information on the very short range such as high speed optical wireless communications in an office environment or 'smart entertainment' systems in aircraft cabins. While VERTIGO technology could be used in both these fields to implement eye-safe laser transmission systems, both would require significant technology steps in terms of power scaling and miniaturisation respectively and therefore significant technical and financial investment. For many of the reasons that it was hoped would drive 2.Xμm FSO systems to the network infrastructure level, this technology however remains an attractive prospect for important niche markets such as covert communications where speed and range are not as crucial as guaranteed anonymity and message security. These emerging security and military are becoming increasingly important for critical advantage to be maintained in the high-tech battlefield arena. In these arenas industry standardisation is not a necessity, rather a flexible source technology such has been developed in VERTIGO is required to be able to meet a particular customers system needs. Here, speed of systems takes less precedence than the other properties of a source technology for an extreme example would be submarine systems that transmit at a few bits per second.

Sensing

A huge potential market exists in the further development of single-frequency and high-power OPSDLs for sensitive multi gas and chemical sensing in a number of industrial safety, process control and legislation enforcement and in long and short range environmental monitoring.

Here the benefit to the economic growth, health and safety of the EU community is clearly evident, if industrial processes can be done more efficiently and safely, reducing waste and risk or if previously undetectable trace amounts of pollutants or pathogens can be detected and emission rules enforced then there are not only potentially commercial benefits but significant societal ones as well. Coupled with the environmental LIDAR applications for airport and aircraft security and safety already under investigation in VERTIGO the potential benefits in the sensing sector and for a safer, cleaner more planet friendly Europe are evident. In addition, the ability to sensitively detect and distinguish different gaseous oxide isotopes of carbon and sulphur and other elements are becoming key in the efficient prospecting and extraction of oil and gas in the energy industry, a major employer across Europe and the world. Further more specific sensing exploitation exists in the direct application of the 2.Xμm OPSDL technology in wind farm assessment and management of wind resource which represents a current and key requirement in the renewable energy industry.

Medical therapy

There are several aspects which make 2 μm lasers a promising candidate for highly precise surgical applications for both soft and hard tissue. The most important property is the high absorption in water combined with minimal penetration depth within human tissue. The second important aspect is the coagulation effect caused by the 2 μm laser radiation, which suppresses the bleeding during operations. Consortium partner LISA laser OHG will use the developed semiconductor disk laser to provide innovative solutions in the area medical therapy (precise laser scalpel).

Potential barriers

The novel aspect of this technology may serve to isolate it from some potential markets however as is being proved in the high power visible markets for medical, mainframe laser replacement and large

scale display lasers by the Coherent Inc. - the worlds largest scientific and solid-state laser manufacturer by volume - the OPSDL technology is proving a robust and disruptive technology able to compete with more traditional laser technologies in terms of output power, performance, reliability and crucially cost. For these reasons, the OPSDL is displacing many legacy OEM laser technologies in Coherent's own laser systems and is providing new previously unobtainable wavelength sources which are opening up new markets and unlocking applications for these sources.

Further technical barriers that were identified at the outset of VERTIGO have been the reliability of the heatspreader bonding process and the reliable supply of low birefringent polished diamond samples for the highest power operation. Three factors have reduced the efficacy of this potential technology barrier: over many subsequent demonstrations the bond quality of a well attached heatspreader has shown to be very robust; the supply of high quality, low-birefringence diamond has been shown to be now reliable and reproducible (after internal discussions and collaborations with Element Six, the worlds leading supplier and processor) and that the use of relatively low cost SiC heatspreaders have been shown to greatly reduce the cost of the final OPSDL sample while only marginally reducing the maximum output performance

Alternative sources

The following sections detail some of the potential alternative or rival sources to the VERTIGO OPSDL developed and also further details on some application areas and exploitation routes for this technology.

There are a number of significant optical sources in the 2-5μm wavelength range however as indicated previously many have significant disadvantages which has hampered either their realisation at specific required wavelengths or power levels or their deployment in specific applications. The figure 5.4 below shows the range of sources schematically and the primary alternative or potentially alternative technologies are outlined in table 4 below, with the specific advantages and disadvantages of each technology. The specific advantages of the OPSDL technology over these alternatives is then outlined and in some cases, where appropriate, the advantages of the hybridisation of the discussed technology with an OPSDL are stated.

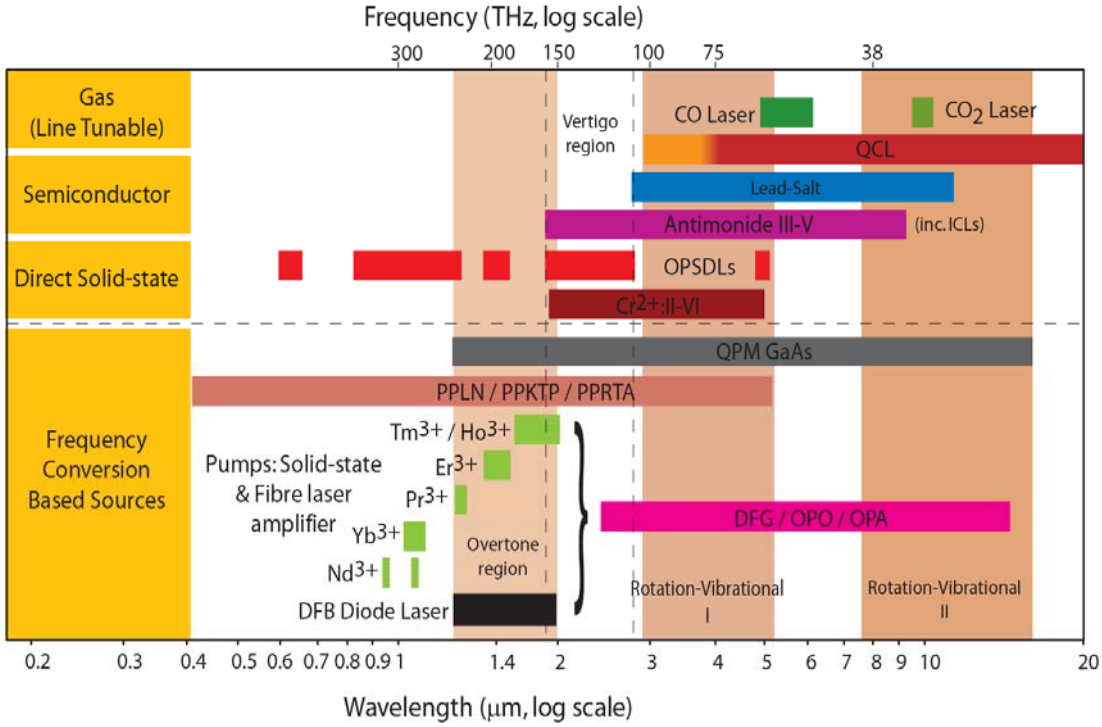

Fig. 5.4: Laser and coherent optical sources in the 0.2 to 20µm wavelength region

Alternative technology	**Pros**	**Cons**	**OPSDL advantages or advantages of hybrid Alternative/OPSDL technology**
Antimonide direct injection (diode) lasers & optically-pumped edge emitters	Electrically pumped Broad wavelength range type I: 2-3µm type II: 3-9µm Optically pumped versions Unstable resonator versions	More complex structure Non-insulating structure higher losses – non radiative processes Decreasing efficiency Low brightness (in general) Low power above 2.3µm Cryo cooling above 3µm for high powers (W)	High brightness Insulating structure More simple design λ coverage? Cavity flexibility
Mid-IR solid-state Lasers	Wide λ coverage High E pulses	Pump sources Purging required Extended cavity layout	Simplicity Gain region engineering

	fs pulses Narrow linewidth High brightness Low threshold Efficiency (>50%)	3 stage optical system Material quality	Direct low-brightness diode pumping Possible as good pump sources
Quantum cascade and interband lasers	V. simple format – compact, 1 stage Electrically pumped Multiwatt at longer λ Broad wavelength range Slow but steady progress towards 2μm ~MHz linewidths without stab. & locking Potentially cheap!?	Complex structure (incr. with shorter λ) Long growth times Poor beam quality Not in 2-3μm Low power below 3.9μm Cryo cooling below 3.5μm Significant thermal load	High brightness λ coverage
OPOs and parametric sources	Very wide potential λ coverage Good pulsed performance External cavity flexibility	Complex configurations CW – very high thresholds Limited pumps – limits potential tuning ranges No energy storage? 3 & 4 stage optical systems Stability – sophisticated electronics – for best low thresh performance Intensity effect - needs high power	Simplicity Cost Possible simple OPO pump source when we have to use 2nd stage – good route to λ expansion Tunable pump – further λ tuning enhancement
Lead Salt laser	Access to λ Low noise N2 cooling	Poor output quality Cryo cooling Low power mW Temp cycling – mechanical misalignment variation in linewidth	Virtually all aspects of OPSDL technology is better if the specific wavelength ranges can be accessed

		Need temp (mK) and current (mA) stability F-P not constant which causes tuning	

Table 4: Potentially alternative technologies to 2.Xμm OPSDLs with specific advantages and disadvantages and the potential advantages of the OPSDL technology (or a hybrid solution involving the OPSDL) over these technologies.

2.2.Section 2 – Dissemination of knowledge

Planned / actual dates	Type	Type of audience	Countries addressed	Site of audience	Partner responsible / involved
18.6.07	conference, invited talk	scientific, marketing, sales	international	CLEO Europe 2007, Munich, Germany	IAF / IOP
18.6. – 22.6.07	exhibition	scientific, marketing, sales	international	LASER 2007 Exhibiton, Munich, Germany	IAF
6.6.07	seminar talk	scientists, students	Germany	Phillips University, Marburg	IAF
since Jan. 07	Project website	www	international	www.2micron-laser.eu	IAF
15/05/07	Conference – invited talk	Scientific	worldwide	MIOMD VIII, 14th - 16th May 2007, Bad Ischl, Austria	IOP/IAF
March 2007	Publication – pulsed pumping	Scientific	worldwide	Optics Express OSA Online journal	IOP/IAF
July 2007	Publication - thermal analysis	Scientific	worldwide	JQE	IOP/IAF
Date(s): 7 - 11 April 2008	Conference SPIE Photonics Europe	research community/ industrial partners/	EU	Strasbourg, France	IET/IAF,IOP
18.6.07	conference, invited talk	scientific, marketing, sales	international	CLEO Europe 2007, Munich, Germany	IAF / IOP
18.6. – 22.6.07	exhibition	scientific, marketing, sales	international	LASER 2007 Exhibiton, Munich, Germany	IAF
8.07	conference, invited talk	scientific	international	Narrow Gap Semiconductors, University of	IAF

				Surrey, Guildford, England	
Nov. 2007	workshop	scientific	international	Workshop on Semiconductor Lasers, IET 26-27 November 2007	IET
2007	PhD thesis	scientific	international	Dorota Pierścinska, Warsaw 2007 PhD thesis (in English)	IET
Jan. 2008	conference, invited talk	scientific, marketing, sales	international	Photonics West 2008, San Jose, USA	IAF / IOP
Jan. 2008	seminar talk	scientists, students	USA	University of Arizona, Tucson, USA	IAF
Jan. 2008	Publication - High-power, (AlGaIn)(AsSb) semiconductor disk laser at 2.0µm	Research community	international	Optics Lett., 33, 201 (2008). OSA Journal	IOP, IAF
Feb. 2008	Publication	general audience	international	second project newsletter (www.2-micron-laser.eu)	IAF, VERTIGO consortium
Feb. 2008	DB/NS to US Arizona – mid-IR material workshop, invited talk	scientific,	USA	University of Arizona, Tucson, USA	IAF / IOP
Feb. 2008	Publication - Thermal Management in 2.3µm Semiconductor Disk Lasers	Research community	Worldwide	IEEE Journal of Quantum Electronics 44, 125 (2008)	IOP, IAF
March 2008	publication	general audience with technical	international	Laser Fokus World	IOP

		background			
April 2008	conference, invited talk	scientific, marketing, sales	international	Photonics Europe 2008, Strasbourg, France	IAF
April 2008	paper: high-power 2.25 µm OPSDL	scientific	international	IEEE Photon. Technol. Lett 20, 502 (2008)	IAF
April 2008	conference	scientific	international	Workshop on Recent Advances of Low Dimensional Structures and Devices , Nottingham, UK	IET, IAF
May 2008	conference	Research community	Worldwide	Conference lasers and Optoelectronics CLEO2008	IOP, IAF
May 2008	publication	general audience with technical background	international	www.Optics.org	IOP
May 2008	Networking event – EU projects V(E)CSEL day in Copenhagen	scientific	international	Copenhagen, Denmark	IAF, IOP, IET
2008	publication	general audience with technical background	international	SPIE Newsroom (spie.org)	IAF / IOP
Sept. 2008	workshop	scientific, marketing, sales	international	OPSDL workshop within the MIOMD IX conference, Freiburg, Germany (www.MIOMD-9.de)	IAF, VERTIGO consortium
Nov. 2008	conference	scientific,	international	LEOS 2008	IAF

		marketing, sales			
2008	Publication - High-brightness long-wavelength semiconductor disk lasers	Research community	international	LASER & PHOTONICS REVIEWS, 1-22 (2008).	IAF, IOP
June 2008	conference, Measurement and simulation of thermal properties of GaSb-based OPSDL	scientific	international	15th International Conference Mixed Design of Integrated Circuits and Systems Poznań, 19-21 June 2008	IET, IAF
4-9/05/2008	Conference presentation at lasers and Optoelectronics CLEO2008 (2 papers)	Research community	Worldwide	Worldwide	IAF,IOP
26-29/08/2008	Conference presentation at 18th UK Quantum Electronics and Photonics conference QEP-18 (2 papers)	Research community	UK	UK	IAF,IOP
7-11/09/08	Conference presentation – Two invited talks in the special OPSDL session and two posters presented at MIOMD IX	Research community	Worldwide	Freiburg, Germany	IOP/IAF/IET
6-8/10/08	Invited Presentation at 2nd international	Industrial users	Worldwide	Doubletree Hotel San Diego-Mission Valley in San	IOP/All

	Applications of High-Power Semiconductor Lasers conference			Diego, California	
25-27/11/2008	Networking event – ICT Event	Research community and Industrial users	Europe wide	Lyon, France	IOP/IAF/All
24-29/01/2009	Conference presentation – Invited talk at Photonics West 2009	Research community and Industrial users	Worldwide	San Hose, California, USA	IOP/All
21/05/08	Networking event – EU projects VCSEL day in Göteborg	Research community	Europe wide	Chalmers University of Technology in Göteborg, Sweden	IET,IAF,IOP
14-19/06/2009	Conference presentation – three oral presentations at European Conference on Lasers and Electro-Optics (CLEO-Europe 2009)	Research community and Industrial users	Worldwide	Munich, Germany	IOP,IAF, LISA
14-19/06/2009	exhibition	scientific, marketing, sales	international	LASER 2009 Exhibiton, Munich, Germany	IAF
08-12/06/2009	Conference presentation – oral paper presented at the conference for Middle Infrared Coherent Sources	Research community	Worldwide	Trouville, France (2009).	IOP/IAF

	(MICS2009)				
28/09/2009	Publication - Semiconductor disk laser pumped Cr^{2+}:Znse lasers	Research community	Worldwide	Optics Express, Vol. 17, Issue 20, 18136-18141, (2009) OSA Journal	IOP/IAF
Dec 2009	Meeting in Stuttgart	Research comunity	UK and Germany	Stuttgart, Germany	IOP,IAF
31/01/2010-03/02/2010	Advanced Solid-State Photonics conference (ASSP)	Research community and Industrial users	Worldwide	San Diego, CA, USA	IOP/IAF
March 2010	Publication – book chapter, Long wavelength GaSb disk lasers, in Semiconductor Disk Lasers	Worldwide	Worldwide	O. G. Okhotnikov (ed.), Wiley-VCH	IAF/ IOP
02/2010	Publication – PhD Thesis, Nils Hempler				IOP
Jan 2010	Conference presentation – invited talk at Photonics West 2010	Research community	Worldwide	Worldwide	IAF
Aug. 2008	Publication – in-well pumped OPSDLs	Research community	Worldwide	Appl. Phys. Lett. 93, 181113 (2008)	IAF
Okt. 2008	Publication – double-chip OPSDL	Research community	Worldwide	IEEE Photon. Technol. Lett. 21, 848 (2009)	IAF
March 2010	article in SPIE Newsroom	general technical audience	Worldwide	www.spie.org	IAF,IOP, LISA
March 2010	IEEE Photonics Society. Poland	Members of IEEE Photonics Society	Poland	Warsaw	IET

	Chapter Meeting	Poland Chapter			
June 2010	Publication in ELEKTRONIKA (monthly journal of Polish EEE Society)	General	Poland		IET
28.06 - 2.07.2010	Invited presentation at National Nanotechnology Conference	General	Poland	Poznań	IET

IAF

An invited talk was given at the CLEO Europe conference in Munich (June 2007), presenting the VERTIGO project and consortium and the latest results from the project partners (IAF/IOP) on GaSb-based OPSDLs. It was a very good opportunity to present the high power results for these 2.Xµm OPSDL to the wider laser community. Further on, the IAF presented their products at the LASER 2007 exhibition, which took place at the same time in the exhibition halls of the Munich conference center. The IAF used this opportunity to present the results on GaSb-based 2.Xµm OPSDLs to the wider technical community, present at this trade fair.

Another invited talk was given by the IAF in July 2007 at the Narrow Gap Semiconductors conference at the University of Surrey, Guildford, England, presenting the newest results from the GaSb-based OPSDLs.

A seminar talk was given at the University of Marburg, Germany, presenting the VERTIGO results to a broad audience of students and members of the group of Prof. Koch, who are working on theoretical semiconductor physics.

A project homepage was created with the address “www.2micron-laser.eu”, which is active since January 2007. This page includes a public section and two password protected sections for the EU and the consortium members.

In the second project year (June 2007 – May 2008) the IAF presented VERTIGO results at the CLEO Europe conference in Munich, Germany (invited talk, together with IOP); at the Narrow Gap Semiconductor Conference (invited talk) at the University of Surrey, UK; at the Photonics West (invited talk, together with IOP) in San Jose, USA and at the Photonics Europe (invited talk) in Strasbourg, France.

Further on, seminar talks have been given at the at the University of Arizona in Tucson, USA, also in the framework of the results achieved within VERTIGO

In order to reach a more general audience, IAF has initiated an article at the SPIE newsroom platform. This article has been written in close cooperation with the IOP and is currently in the process of editing.

In order to spread the VERTIGO results in the long-wavelength infrared community, the IAF has organized a topical workshop on long wavelength OPSDL and VCSEL within the framework of the MIOMD-IX conference, which will take place in Freiburg, Germany in September 2008. As this conference addresses scientists as well as people from industrial companies active in the Mid-IR regime, this will be an excellent opportunity to share results and discuss potential new applications and projects.

Photonics West 2010:

another invited talk highlighted the VERTIGO results at the Photonics West 2010:

→ GaSb-based optically-pumped semiconductor disk lasers emitting in the 2.0-to-2.8 μm wavelength range
Benno Rösener, Marcel Rattunde, Rüdiger Moser, Sebastian Kaspar, Christian Manz, Klaus Köhler, Joachim Wagner, Fraunhofer IAF

In the last three Photonic West conferences in a row (from 2008 to 2010) there was always a member of the VERTIGO consortium invited to talk about the project results.

Cleo Europe 2009

At the CLEO Europe 2009, three talk by consortium members from IAF, IOP and LISA presented all the different aspects of these 2.Xμm OPSDLs. At the corresponding LASER 2009 exhebition, two OPSDL module were on display at the Fraunhofer IAF booth: a compact 2.Xμm laser based on the VERTIGO Basic laser Module and a running 2.25μm OPSDL, demonstrating the suitability of these laser for intracavity absorption spectroscopy.

in-well pumped OPSDL, APL

the results of the in-well pumped OPSDL where published by the IAF in the following paper:

An improved active region concept for highly efficient GaSb-based optically in-well pumped vertical-external-cavity surface-emitting lasers
Appl. Phys. Lett. 93, 181113 (2008)

double-chip resonator

after some review delay, the results on the two-chip OPSDL characterization where published in:

GaSb-based optically pumped semiconductor disk laser using multiple gain elements
IEEE Photon. Technol. Lett. 21, 848 (2009)

book chapter

The IOP and IAF where invited to submit an article about "Long-wavelength GaSb disk lasers" in the book project "Semiconductor disk laser" from O. Ochotnikov (editor), The book will be published at the beginning of 2010.

SPIE Newsroom article

The IAF was again asked to write an article for the SPIE Newsroom (the second during this project).

IOP

An invited talk was given at the 8th International Conference on Mid-Infrared Optoelectronics: Materials and Devices (MIOMDVIII) in Bad Ischl, Austria 14th-16th May 2007. The talk covered the background technology and motivation for the Vertigo project and the latest 'to-date' results from the project partners (IAF/IOP) on GaSb based OPSDLs. 1.5W Nd:YAG pumped performance at 2.3µm, 1W diode pumped (808nm) performance at 2.3µm, tuning results (>70nm) and single frequency and linewidth narrowed (~4MHz) single frequency performance were discussed. The transcript of this presentation can be found in: "High performance, GaSb-based, optically-pumped semiconductor disk lasers", J.-M. Hopkins, N. Hempler, A.J. Maclean, A.J. Kemp, M.D. Dawson, E. Riis, N. Schulz, M. Rattunde, C. Manz, K. Köhler, J. Wagner and D. Burns, presented at 8th International Conference on Mid-Infrared Optoelectronics: Materials and Devices (MIOMDVIII) in Bad Ischl, Austria 14th-16th May 2007.

A presentation was made at The Conference on Lasers and Electro-Optics CLEO 2007 in Baltimore Maryland USA 2007. This presentation concentrated on the Pulsed pumping performance of OPSDLs and included results of 2.3µm material from the IAF. ~1.7W output power at 2.3µm is demonstrated from a semiconductor disk laser pumped by a 905nm high-power pulsed semiconductor laser. The thermal characteristics and wavelength shift are studied over the 100-200ns pump pulse. - N. Hempler, J.-M. Hopkins, A. J. Kemp, M. D. Dawson and D. Burns, "Pulsed pumping of a 2.3µm InGaAsSb Semiconductor Disk Laser", talk CMFF5, presented at the Conference on Lasers and Electro-Optics, Baltimore 2007.

In March 2007 an Optics express paper was published that contained a detailed analysis of the performance of pulse pumped OPSDLs. High peak power (1.7W) operation was achieved from uncooled OPSDLs pumped with 40W, 120ns, compact, low-cost pulsed pump lasers. Full details are contained in: "Pulsed pumping of semiconductor disk lasers", Nils Hempler, John-Mark Hopkins, Alan J. Kemp, Nico Schulz, Marcel Rattunde, Joachim Wagner, Martin D. Dawson, David Burns,
Optics Express, Vol. 15, Issue 6, pp. 3247-3256 (March 2007).

A paper has been submitted to the IEEE Journal of Quantum Electronics which covers the thermal modeling of OPSDL devices. Finite element analysis is used to study heat flow in a 2.3µm semiconductor disk laser based on GaInAsSb/AlGaAsSb. An intracavity diamond heatspreader is shown to significantly improve thermal management – and hence power scalability – in this laser compared to the substrate thinning approach typically used in semiconductor disk lasers operating around 1µm. The parameters affecting the performance of an intracavity heatspreader are studied in the context of a 2.3µm semiconductor disk laser: the thermal impedance at the interface between the semiconductor gain material and the heatspreader is found to be much more important than the

mounting arrangements for the gain-heatspreader composite; power scaling with pump spot radius – increasing the pump power at constant pump intensity – is found to be intrinsically limited; and the pump wavelength is predicted to have less affect on thermal management than might be expected. Direct pumping of the quantum wells is found to significantly reduce the temperature rise per unit pump power - A. J. Kemp, J.-M. Hopkins, A. J. Maclean, N. Schulz, M. Rattunde, J. Wagner and D. Burns, "Thermal Management in 2.3μm Semiconductor Disk Lasers: a Finite Element Analysis", submitted to IEEE Journal of Quantum Electronics, 2007.

In January 2008 a paper detailing the thermal modelling of GaSb based OPSDLs was published in the IEEE journal of Quantum electronics. The paper concluded that the most appropriate thermal management technique in OPSDLs above 2mm is via the use of intracavity heatspreaders however the power scaling possible with this technique does not scale linearly and as quickly as the threshold increases and therefore power scaling with pumped area is not an indefinite scaling mechanism. Further details may be found in - "Thermal Management in 2.3?m Semiconductor Disk Lasers: a Finite Element Analysis" - A. J. Kemp, J.-M. Hopkins, A. J. Maclean, N. Schulz, M. Rattunde, J. Wagner and D. Burns, IEEE Journal of Quantum Electronics 44, 125 (2008).

In January 2008 a paper was published in Optics Letters which detailed the performance achieved at 2.0mm from the VERTIGO OPSDL. The high output powers of 3.7W at 10°C and >5W°C and a wide tuning range ~70nm. Full details can be found in - "High-power, (AlGaIn)(AsSb) semiconductor disk laser at 2.0mm" - J.-M. Hopkins, N. Hempler, B. Rösener, N. Schulz, M. Rattunde, C. Manz, K. Köhler, J. Wagner and D. Burns, , Optics Lett., 33, 201 (2008).

The circulation of the above paper led to the publication of a couple of news articles in the photonics press in Laser Focus World - "Tunable 2mm disk laser achieves 5W" (Mar 08) and on Optics.org "Thin-disk lasers set new benchmarks" (Mar 20/08). This coverage has subsequently led to a number of interested parties contacting the consortium for potential collaboration.

Two presentations were made at The Conference on Lasers and Electro-Optics CLEO 2008 in San Hose California USA 2008. The first concerned the high power (5.2W) tuning performance (~170nm) and single frequency performance of 2.02, 2.25 and 2.3mm OPSDLs. The second paper detailed the use of a 5W OPSDL to pump mid-IR chalcogenide Cr2+:ZnSe and Cr2+:CZT lasers. J-M. Hopkins, N. Hempler, B. Rösener, N. Schulz, M. Rattunde, C. Manz, K. Köhler, J, Wagner, and D. Burns, "5W Mid-IR Optically Pumped Semiconductor Disk Laser" - talk CWD4, presented at the Conference on Lasers and Electro-Optics, San Jose, CA 2008. N. Hempler, J.-M. Hopkins, B. Rösener, N. Schulz, M. Rattunde, J. Wagner, U. N. Roy, A. Burger and D. Burns, "Semiconductor Disk Laser Pumped Cr2+:Chalcogenide Lasers" - talk CFW2, presented at the Conference on Lasers and Electro-Optics, San Jose, CA 2008.

On 21st of May 2008 A networking workshop focused on the EU projects concerned with vertical cavity devices "V(E)CSEL day" in Copenhagen was attended. The conclusion of the workshop was that this community should be better connected and that regular networking and wider joint support funding such as a Network Of Excellence should be sought to support future collaborations and encourage cross project linkage. While there was a relatively good turn out on the day It was hoped that in the future more of the EU project consortia working in this field could be encouraged to take part in the future.

On the 20-21st February 2008 The progress in materials development and the thermal management were presented at the international "mid-IR materials workshop" at the Univ. Of Arizona, Tucson, AR, USA by the IOP and IAF. The workshop generated some very fruitful discussions and nature and current limits of the materials technology was discussed at length. It is hoped that some further developments and collaboration will come from this event.

In September 2008 the VERTIGO project and results to date will be presented in two invited talks to be given at the 9th International Conference on Mid-Infrared Optoelectronics: Materials and Devices (MIOMDVIX) in Freiburg, Germany 7th-11th september 2008.

In October 2008 the consortium will be represented in an invited presentation at the 2nd international Applications of High-Power Semiconductor Lasers conference in San Diego, California

4-9/05/2008 CLEO 2008

'5W mid-IR optically-pumped semiconductor disk laser', J.-M.Hopkins, N. Hempler, B. Rösener, N. Schulz, M. Rattunde, C. Manz, K. Köhler, J. Wagner and D. Burns, Oral paper CWD4 Presented at the Conference on Lasers and Electro-Optics (CLEO), San Jose, CA, (2008)

'Semiconductor disk laser pumped Cr2+:Chalcogenide lasers', N. Hempler, J.-M. Hopkins, B. Rosener, N. Schulz, M. Rattunde, J. Wagner, U. N. Roy, A. Burger, D. Burns, Oral paper CWD4 Presented at the Conference on Lasers and Electro-Optics (CLEO), San Jose, CA, (2008)

26-29/08/2008 Photon 08 (inc. QEP18) UK Photonics conference (Sep 08)

'Semiconductor disk laser pumped Cr:chalcogenide lasers', N. Hempler, J.-M.Hopkins, B. Rösener, N. Schulz, M. Rattunde, J. Wagner, A Burger, U. N. Roy and D. Burns, Poster P2.12 presented at the 18th UK Quantum Electronics and Photonics conference QEP-18, Edinburgh August 2008.

'High-brightness Mid-IR optically-pumped semiconductor disk laser', J.-M.Hopkins, N. Hempler, A. Kemp, B. Rösener, N. Schulz, C. Manz, K. Köhler, M. Rattunde, J. Wagner and D. Burns oral presentation presented at the 18th UK Quantum Electronics and Photonics conference QEP-18, Edinburgh August 2008.

7-11/09/2008 MIOMD-IX (Sept 08)

'High-power GaSb-based optically pumped semiconductor disk laser for the 2.Xμm wavelength regime', D. Burns and M. Rattunde, oral presentation (invited) presented at the 9th International Conference on Mid-Infrared Optoelectronics: Materials and Devices (MIOMD-IX), Freiburg, Germany, 7th – 11th September 2008.

'High-power, pulsed-pumped, 2.0μm semiconductor disk laser', J.-M. Hopkins, A.J. Kemp, B. Rösener, N. Schulz, M. Rattunde, J. Wagner and D. Burns, oral presentation presented at the 9th International Conference on Mid-Infrared Optoelectronics: Materials and Devices (MIOMD-IX), Freiburg, Germany, 7th – 11th September 2008.

'Measurement and modelling of temperature in mid-IR semiconductor disk lasers', J.-M. Hopkins, K. Pierscinski, A.J. Kemp, N. Schulz, M. Rattunde, J. Wagner, M. Bugajski, and D. Burns, Poster P11

presented at the 9th International Conference on Mid-Infrared Optoelectronics: Materials and Devices (MIOMD-IX), Freiburg, Germany, 7th – 11th September 2008.

'Semiconductor disk laser pumped Cr2+: Chalcogenide lasers', N. Hempler, J.-M. Hopkins, B. Rösener, N. Schulz, M. Rattunde, J. Wagner, U.N. Roy, A. Burger, and D. Burns, Poster P13 presented at the 9th International Conference on Mid-Infrared Optoelectronics: Materials and Devices (MIOMD-IX), Freiburg, Germany, 7th – 11th September 2008.

6-8/10/2008 AHPSL 2008 (Oct 2008)

In October 08 the IOP was invited to give a presentation on OPSDL technology at the Applications of High power semiconductor lasers conference in San Diego, The conference was attended by many of the leading manufacturers of high-power laser systems and industrial laser users. The talk gave the opertunity to highlight the VERTIGO developments to this audience.

'The Semiconductor Disk Laser: A New Approach to Laser Applications Ready Source Engineering', Oral presentation (invited) at the Applications of High power semiconductor lasers conference (AHPSL2008), San Diego CA, October 2008

24-29/01/2009 Invited talk – Photonics west (Jan 09)

David Burns from the IOP was invited to represent the VERTIGO consortium at Photonics west in San Jose in January 2009. This is one of the largest photonics conferences and is well attended by researchers and industry technologists alike. Again this was an excellent opportunity to sell the VERTIGO 2.Xμm OPSDL technological and scientific advances.

Burns, D.; Hopkins, J.-M.; Kemp, A. J.; Rösener, B.; Schulz, N.; Manz, C.; Köhler, K.; Rattunde, M.; Wagner, J. "Recent developments in high-power short-wave mid-infrared semiconductor disk lasers", Solid-state Lasers XVIII: Technology and Devices. J. Proceedings of the SPIE, Volume 7193, pp. 719311-719311-13 (2009).

14-19/06/2009 CLEO-Europe 2009

CLEO Europe is a large technical and trade conference and covers a large international audience from within and without Europe. The Vertigo project was well represented with the following oral paper presentations in the largest auditorium of the conference.

'Tuning and brightness optimization of high-performance GaSb-based semiconductor disk lasers from 1.86 to 2.80μm,' N. Hempler, J.-M. Hopkins, M. Rattunde, B. Rösener, R. Moser, C. Manz, K. Köhler, J. Wagner and D. Burns, oral paper CB7.3 presented at the European Conference on Lasers and Electro-Optics (CLEO-Europe 2009), Munich, Germany (2009).

'Power scaling of GaSb-based semiconductor disk lasers for the 2.X μm wavelength range', M. Rattunde, B. Rösener, N. Hempler, J.-M. Hopkins, D. Burns, R. Moser, C. Manz, K. Köhler, and J. Wagner, oral paper CB7.5 presented at the European Conference on Lasers and Electro-Optics (CLEO-Europe 2009), Munich, Germany (2009).

08-12/06/2009 MICS2009

The Middle Infrared Coherent Sources conference is a small biennial conference but is attended by some of the worlds key mid-IR laser developers and scientists. The pulsed-pumped and some of the solid-state laser pumped OPSDL work was presented there orally in the following paper.

'Pulsed-pumped 1.9μm and 2.0μm Semiconductor Disk Lasers and their use as pump source for Cr^{2+}:ZnSe', Nils Hempler, John-Mark Hopkins, Benno Rösener, Marcel Rattunde, Joachim Wagner, Vladimir V. Fedorov, Igor S. Moskalev, Sergey B. Mirov and David Burns, oral paper presented at the conference for Middle Infrared Coherent Sources (MICS2009), Trouville, France (2009).

28/09/2009 Optics Express paper

After a significant reviewing delay the following paper on the OPSDL pumped mid-IR lasers was published in Optics Express the photonics publication with the second highest impact ration after Nature Photonics.

'Semiconductor disk laser pumped Cr^{2+}:Znse lasers', N. Hempler, J.-M. Hopkins, B. Rösener, M. Rattunde, J. Wagner, V. V. Fedorov, I. S. Moskalev, S. B. Mirov, and D. Burns, Optics Express, Vol. 17, Issue 20, 18136-18141, (2009).

31/01/2010-03/02/2010 ASSP 2010

ASSP is also a large technical photonics conference in the USA which crucially doesn't have parallel sessions so that exposure can be higher than at the significantly larger multi-parallel session conferences. The following poster has been accepted for presentation.

N. Hempler, J.-M. Hopkins, A. Kemp, B. Rösener, M. Rattunde, J. Wagner and D. Burns, '20W, Quasi-cw GaSb-Based Semiconductor Disk Laser' paper accepted for poster presentation at ASSP 2010 Advanced Solid-State Photonics conference (ASSP), San Diego, CA, USA (2010).

02/2010 Nils Hempler Thesis

One of the researchers at the IOP – Nils Hempler who has spent significant time characterising and exploring many aspects of the VERTIGO OPSDL development is currently writing up his PhD thesis which it is hoped will be ready for submission in February 2010

IET

- PhD thesis Kamil Pierściński "Thermal properties of optically pumped surface emitting lasers. Analysis of heat management in multilayer structures"
- Kamil Pierściński, Investigation of thermal processes in optically pumped 2.X μm lasers Workshop on Semiconductor Lasers, IET 26-27 November 2007
- Dorota Pierścinska, Analysis of thermal processes on the facets of semiconductor lasers, IET Warsaw 2007, PhD thesis (in English)
- Pierściński K., Pierścińska D., Bugajski M., Manz C., Rattunde M.: "Measurements and Simulation of Thermal Properties of Optically Pumped Antimonide VECSELs", *IEEE Proceedings*

*of the 15th International Conference Mixed Design of Integrated Circuits and Systems,*343-347,*2008*

- Pierściński K., Pierścińska D., Bugajski M., Manz C., Rattunde M.: "Investigation of Thermal Management in Optically Pumped, Antimonide VECSELs",Microelectronics Journal, Volume 40, Issue 9 , September 2009, Pages 1373-1378.

- Pierściński K., Pierścińska D., Bugajski M., Manz C., Rattunde M.: "Measurements and Simulation of Thermal Properties of Optically Pumped Antimonide VECSELs", 15th International Conference Mixed Design of Integrated Circuits and Systems (MIXDES15), Poznań 19-21.06.2008

- Pierściński K., Pierścińska D., Bugajski M., Manz C., Rattunde M.: "Investigation of Thermal Management in Optically Pumped, Antimonide VECSELs", Quantum Dot Meeting , Nottingham 07-09.04.2008

- Hopkins J.M., Pierściński K., Pierścińska D., Kemp A.J., Schulz N., Rattunde M., Wagner J., Bugajski M., Burns D.: "Measurement and Modeling of Temperature in Mid-IR Semiconductor Disk Lasers", 9 International Conference on Mid-Infrared Optoelectronics: Materials and Devices (MIOMD9), Freiburg 07-11.09.2008

- Pierściński K., Pierścińska D., Bugajski M., Manz C., Rattunde M., Burns D., Hopkins J.M.: "Temperature Mapping in 2.x um VECSELs", Semiconductor Laser Workshop (SELAWO08), Kazimierz Dolny 01-02.12.2008

- K. Pierściński, D. Pierścińska, M. Bugajski, C. Manz, M. Rattunde, Influence of the Intracavity Heatspreader on the VECSEL Temperature, IEEE Proceedings of the 16th International Conference Mixed Design of Integrated Circuits and Systems – Outstanding Paper Award

- K. Pierściński, D. Pierścińska, M. Bugajski, C. Manz, M. Rattunde, Influence of the Intracavity Heatspreader on the VECSEL Temperature 16th International Conference Mixed Design of Integrated Circuits and Systems, Łódź, 25-27 June 2009